

Enumeration and Representation Theory of Spin Space Groups

Xiaobing Chen^{1,*}, Jun Ren,^{1,*} Yanzhou Zhu^{2,*}, Yutong Yu^{1,*}, Ao Zhang,¹ Pengfei Liu,¹ Jiayu Li,¹ Yuntian Liu,¹ Caiheng Li,² and Qihang Liu^{1,3,4,†}

¹*Department of Physics and Shenzhen Institute for Quantum Science and Engineering,
Southern University of Science and Technology, Shenzhen 518055, China*

²*National Center for Applied Mathematics Shenzhen, and Department of Mathematics,
Southern University of Science and Technology, Shenzhen 518055, China*

³*Guangdong Provincial Key Laboratory of Computational Science and Material Design,
Southern University of Science and Technology, Shenzhen 518055, China*

⁴*Shenzhen Key Laboratory of Advanced Quantum Functional Materials and Devices,
Southern University of Science and Technology, Shenzhen 518055, China*

(Received 31 July 2023; revised 18 April 2024; accepted 16 May 2024; published 28 August 2024)

Fundamental physical properties, such as phase transitions, electronic structures, and spin excitations, in all magnetic ordered materials, were ultimately believed to rely on the symmetry theory of magnetic space groups. Recently, it has come to light that a more comprehensive group, known as the spin space group (SSG), which combines separate spin and spatial operations, is necessary to fully characterize the geometry and underlying properties of magnetic ordered materials. However, the basic theory of SSG has seldom been developed. In this work, we present a systematic study of the enumeration and the representation theory of the SSG. Starting from the 230 crystallographic space groups and finite translation groups with a maximum order of eight, we establish an extensive collection of over 100 000 SSGs under a four-index nomenclature as well as international notation. We then identify inequivalent SSGs specifically applicable to collinear, coplanar, and noncoplanar magnetic configurations. To facilitate the identification of the SSG, we develop an online program that can determine the SSG symmetries of any magnetic ordered crystal. Moreover, we derive the irreducible corepresentations of the little group in momentum space within the SSG framework. Finally, we illustrate the SSG symmetries and physical effects beyond the framework of magnetic space groups through several representative material examples, including a candidate altermagnet RuO₂, spiral spin polarization in the coplanar antiferromagnet CeAuAl₃, and geometric Hall effect in the noncoplanar antiferromagnet CoNb₃S₆. Our work advances the field of group theory in describing magnetic ordered materials, opening up avenues for deeper comprehension and further exploration of emergent phenomena in magnetic materials.

DOI: 10.1103/PhysRevX.14.031038

Subject Areas: Condensed Matter Physics, Magnetism,
Materials Science

I. INTRODUCTION

Symmetry has always been one of the core aspects of physics and materials science. The crystallographic group theory, which Fedorov and Schönflies refined at the end of the 19th century, provides a fundamental framework for understanding and predicting the properties and behavior of crystal solids, facilitating advancements in fields ranging from solid-state physics and chemistry to materials

engineering [1]. The complete set of symmetry elements exhibited by three-dimensional (3D) nonmagnetic or paramagnetic solids are depicted by 32 point groups (PGs) and 230 space groups (SGs), the latter of which include rotations, reflections, inversion (*P*), translations, and their combinations. The wave-function properties of such crystals, like phase transition, selection rules, and band degeneracy, are successfully described by the representations (reps) of 230 SGs.

The crystallographic group theory was further explored in the early 20th century when Shubnikov and others realized that magnetic materials exhibit additional symmetries beyond the purely geometric symmetries found in nonmagnetic crystals. By introducing antiunitary time-reversal operation *T* that flips the direction of spin, the 32 PGs and 230 SGs are extended to 122 magnetic point groups (MPGs) and 1651 magnetic space groups (MSGs), respectively [2]. With the development of x-ray-diffraction

*These authors contributed equally to this work.

†Contact author: liuqh@sustech.edu.cn

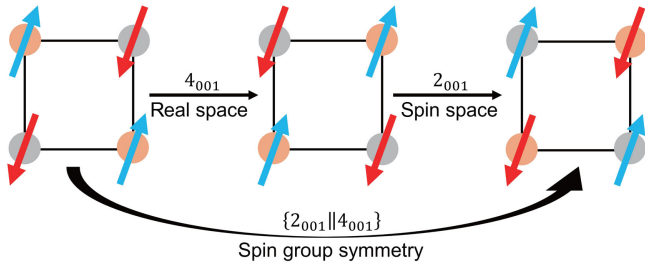


FIG. 1. Schematic plot of a spin group symmetry of an antiferromagnetic structure. It takes a fourfold rotation (4_{001}) in real space followed by a twofold rotation (2_{001}) in spin space, constituting a spin group symmetry $\{2_{001}\parallel 4_{001}\}$. Such a symmetry operation contains separated lattice and spin rotations and is thus beyond the framework of magnetic groups.

and neutron-diffraction techniques, the structure of a given magnetic crystal and the orientation of its spins can be determined and assigned a specific MSG. Since then, the theory of MSGs has been believed to be the ultimate theory in understanding the exotic properties such as ordering phenomena, phase transitions, spin excitation, and band topology in all magnetic ordered materials [3–9]. However, as an axial vector, spin symmetry contains not only T that reverses its direction (like an inversion operator in spin space), but also spin rotation operations. The underlying concept of MPG and MSG is based on the assumption that a rotation operator acts simultaneously on spatial and spin coordinates. Exemplified by a simple collinear antiferromagnetic order shown in Fig. 1, the system does not exhibit any fourfold rotations within the regime of magnetic groups. However, if we consider the spatial coordinate and spin coordinate separately, the system thus has a spatial fourfold operation followed by a twofold spin rotation. Therefore, from a geometric perspective, separating rotational operations from real space and spin space is necessary to fully describe the symmetry of a system with a vector field [10]. Such an extended magnetic group, first proposed in the 1960s, is referred to as a spin group [11–18], which includes both spin point groups (SPGs) and spin space groups (SSGs).

From a physical perspective, the spin group also constitutes the symmetry-operator group of magnetic Hamiltonians capturing the behavior of corresponding quasiparticles. Examples include single-particle Hamiltonians for electrons and the Heisenberg Hamiltonian for spin waves when spin-orbit coupling (SOC) is not considered [15,19,20]. Even in the presence of SOC with certain forms, the system can manifest some hidden symmetries associated with a particular spin group [21–23]. With the recent prosperity of antiferromagnetic spintronics [24–26], it has been recognized that antiferromagnetic order can generate various spintronic effects that typically emerge in systems with strong SOC, such as spin splitting, spin current, and spin torque [27–44]. Consequently, spin group symmetries

naturally serve as a starting point for investigating these Hamiltonians and related effects. For example, the recently discovered “altermagnetic phase” in collinear antiferromagnets is defined in the SOC-free limit, and thus is delimited by spin groups [45–48]. In addition, the spin group also helps us understand the band structures, topology, and transport phenomena in systems with negligible SOC [49–52], and provides descriptions of complex magnetic orderings (e.g., helical, spiral, quasi-one-dimensional helimagnets) [53–55] and fruitful applications to magnetically ordered quasicrystals [56–58].

The development of crystallographic group theory includes the enumeration and classification of groups, as well as the rep theory. While the theories of crystallographic groups and magnetic groups have been firmly established in textbooks [1,2], the theory of spin groups is still in its nascent stage, with only the enumeration of 598 SPGs completed so far [18]. The enumeration of SSGs and the related rep theory describing band degeneracies and wave-function properties are still lacking. This is because including degrees of freedom in both real space and spin space poses significant challenges in classifying SSGs. For example, the infiniteness of the translation group implies an infinite number of SSGs.

In this work, we present a systematic study of the SSG enumeration and rep theory:

- (i) The entire enumeration procedure starts from the 230 SGs, combining a translational supercell having a maximum order of eight. We traverse all inequivalent normal subgroups and establish their mapping onto a PG in spin space through inequivalent isomorphism relationships. Consequently, using group extension, we establish a comprehensive collection of more than 100 000 SSGs, each labeled with a four index and international notation (Sec. II). The number of SSGs exceeds that of MSGs by 2 orders of magnitude because SSGs involve not only spin-flip operation T but also partially decoupled spin rotation and lattice rotation. In addition, SSGs contain combined symmetry operations of spin rotation and lattice translation corresponding to the propagation vector. Therefore, SSGs offer a more comprehensive symmetry description for magnetic structures in comparison with MSGs. Interesting examples include collinear magnetic structures in cubic crystal systems, spiral magnetic structures with arbitrary angles between nonmagnetic unit cells, cubic magnetic configurations within trigonal or hexagonal lattice systems, etc.
- (ii) We then distinguish inequivalent SSGs for collinear, coplanar, and noncoplanar magnetic configurations, for which the nontrivial operations in spin space play a crucial role. We find that collinear SSGs manifest one-by-one correspondence with the 1421 MSGs, in which the magnetic sublattices with opposite

- directions of local moments can be regarded as black and white. In addition, the number of inequivalent coplanar SSGs is significantly reduced to 16 383 due to the mirror symmetry in spin space. Moreover, in collinear and coplanar magnetic structures, the mirror symmetry in spin space serves as an effective time-reversal operation, thereby preventing the occurrence of the SOC-free anomalous Hall effect.
- (iii) In addition, we derive the irreducible corepresentations (coirreps) of the little group at high-symmetry momenta within the framework of SSG (Sec. III). The band representations of SSGs supporting non-collinear (coplanar and noncoplanar) magnetic configurations are constructed using the projective rep theory and the modified Dimmock and Wheeler sum rule. On the other hand, band representations of collinear SSGs are considered separately due to the presence of infinite symmetry operations in the spin-only group. In particular, the SO(2) spin rotation symmetry provides a simpler perspective in understanding spin degeneracy, where the coirreps can be obtained from the single-valued coirreps of the type-II MSG augmented by some additional degeneracy rules in spin space. From the perspective of SSG, the complete criteria for magnetic-order-induced spin degeneracy and spin splitting can be straightforwardly summarized.
- (iv) We then introduce our online program FIND-SPINGROUP of SSG identification for any given magnetic structure [59], where the SSGs of the 2001 experimentally reported magnetic structures in the MAGNDATA database [60] are also identified (Sec. IV). We also provide several representative material examples to demonstrate their SSG symmetries and physical properties beyond the framework of MSG. The first example is a candidate altermagnet RuO₂, in which extra band degeneracies are observed along Z-R-A high-symmetry lines, while MSG provides only one-dimensional coirrep. These band degeneracies can be attributed to the sticking effect of two conjugated 1D irreps of SO(2) in SSG. The second example is coplanar antiferromagnet CeAuAl₃ with $U\tau$ symmetry, the combination of a twofold spin rotation U and a fractional lattice translation τ . A spiral-order-induced antiferromagnetic spin splitting is found, of which the symmetry requirement differs from that of collinear antiferromagnets, i.e., breaking PT and $U\tau$ [46]. The third example is noncoplanar antiferromagnet CoNb₃S₆. While PT symmetry is broken, it manifests a spin-degenerate band structure within the whole Brillouin zone. Such a spin degeneracy originates from the D_2 double group in spin space at any arbitrary wave vector, providing two-dimensional coirreps and thus prohibiting any

components of spin polarization. Despite its spin-degenerate band structure, CoNb₃S₆ exhibits a geometric Hall effect, i.e., SOC-free anomalous Hall effect originating from magnetic configuration, arising from the nonzero z -direction orbital magnetization. Finally, we provide a summary of the work in Sec. V.

In the appendixes, we begin in Appendix A by defining the SSGs, establishing connections with the more familiar nonmagnetic SGs and MSGs. In Appendix B, we review the international notation for SGs and MSGs. Next, in Appendix C, we introduce the nomenclature for t -type, k -type, and g -type SSGs and show how to obtain all group elements using the international notation of SSGs. These nomenclatures are also integrated in our online platform [59]. In Appendix D, we provide some details regarding the rep theory of SSG, including the projective reps for SSGs, the decomposition of regular projective reps using the CSCO method and the band reps in collinear SSGs. In Appendix E, we provide the specific procedure for identifying the SSG of a given magnetic ordered crystal. Lastly, in Appendix F, we provide the computational methods for the first-principles calculations.

II. ENUMERATION OF SPIN SPACE GROUPS

In this section, we first introduce the construction methodology of SSGs, which is based on the group extension approach of SPGs [17,18]. This approach has also been adopted in constructing the full set of crystallographic PGs, MPG, and MSGs. However, the complexity of SSGs lies in the possible cell expansions to accommodate complicated magnetic orders, leading to an infinite number of SSGs. We thus consider the magnetic supercells with reduced translation symmetry to have a maximum order of eight, obtaining a comprehensive collection of 100 612 SSGs. We then develop the four-index nomenclature for each SSG according to the way of group construction, and the international notation according to the types of Bravais lattices and symmetry operations. Furthermore, we discuss the features of SSGs when considering pure spin operations in collinear and coplanar configurations.

A. Basics and methodology

Compared with MSGs, the critical characteristic of SSGs is that the spatial and spin operations are considered separately (see Appendix A for the types of symmetry operations) [19]. Therefore, the symmetry elements of spin groups can be written as $\{g_s \parallel g_l\}$, where g_l denotes the spatial operation $\{C_n(\theta), PC_n(\theta)|\tau\}$ of the lattice [$C_n(\theta)$, P , and τ are the rotation of the θ angle along the n axes, inversion, and translation, respectively]. To the left of the double bar, $g_s = \{U_m(\phi), TU_m(\phi)\}$ consists of spin rotations $U_m(\phi) \in SU(2)$ and the antiunitary time-reversal

operator T that reverses spin and momentum simultaneously. Similar to that of SPGs, the general form of SSGs, denoted G_{SS} , could be expressed as the direct product of a nontrivial SSG G_{NS} and a spin-only group G_{SO} . The nontrivial SSG is the SSG that has every spin operation combined with a spatial operation (except for the identity element $\{E\|E|0\}$); the spin-only group consists of pure spin operations $\{g_s\|E|0\}$ [17]:

$$G_{\text{SS}} = G_{\text{NS}} \times G_{\text{SO}}. \quad (1)$$

While for noncoplanar magnetic order $G_{\text{SO}}^n = \{E\}$ (identity group), for coplanar magnetic order $G_{\text{SO}}^p = \{E, TU_n(\pi)\} = Z_2^K$, implying the mirror symmetry in spin space (n is perpendicular to the coplanar order). For collinear magnetic order, $G_{\text{SO}}^l = Z_2^K \ltimes \text{SO}(2)$, where $\text{SO}(2) = \{U_z(\phi), \phi \in [0, 2\pi]\}$ contains full spin rotations along a specific axis z [19]. Next, we first focus on the construction of nontrivial SSGs, while the full SSGs directly constructed using Eq. (1) are discussed later.

In analogy to the construction of 598 SPGs, the central idea of constructing nontrivial SSGs is based on the decomposition of normal subgroups of crystallographic SGs and group extension. First, an SG G_0 can be decomposed into cosets with respect to one of its normal subgroups L_0 ,

$$G_0 = L_0 \cup g_1 L_0 \cup \dots \cup g_{n-1} L_0. \quad (2)$$

When the resulting quotient group G_0/L_0 is isomorphic to a PG, one can use such a PG as the operations for spin space, $G^s = \{E, g_{s_1}, \dots, g_{s_{n-1}}\} [g_{s_i} \in \text{SO}(3) \times \{E, T\} \cong O(3)]$, and map G^s to G_0/L_0 through an isomorphism relationship, forming an SSG written as

$$G_{\text{NS}} = \{E\|L_0\} \cup \{g_{s_1}\|g_1 L_0\} \cup \dots \cup \{g_{s_{n-1}}\|g_{n-1} L_0\}. \quad (3)$$

The enumeration of all nontrivial SSGs includes exhaustively enumerating all (G_0, L_0) pairs and inequivalent choices of coset representative elements that lead to inequivalent coset decompositions, finding all G^s isomorphic to G_0/L_0 in spin space, and finding all inequivalent mappings between G^s and G_0/L_0 . However, compared with that of SPGs, the enumeration of SSGs faces more challenges due to the existence of crystallographic translation groups of SGs. To distinguish different cases, three types of subgroups L_0 are categorized:

- (1) A subgroup L_0 of an SG G_0 is referred to as a “*translationengleiche*” subgroup [61] or a t subgroup of G_0 if their translation subgroup $T(G_0)$ is retained, i.e., $T(L_0) = T(G_0)$, while the PG part $P(L_0)$ is a subgroup, i.e., $P(L_0) \leq P(G_0)$. An SSG formed in this way is called a t -type SSG, in which the t index i_t is used to present the reduction of the PG symmetry $i_t = |P(G_0)|/|P(L_0)|$. It is

straightforward that the quotient groups G_0/L_0 of t -type SSGs must be isomorphic to one of the 32 crystallographic PGs. Therefore, the derivation of 598 nontrivial SPGs can be directly extended to obtain t -type SSGs.

- (2) A subgroup L_0 of an SG G_0 is referred to as a “*klassengleiche*” subgroup [61] or a k subgroup of G_0 if the PG part $P(G_0)$ is retained, i.e., $P(L_0) = P(G_0)$, while the translation subgroup $T(L_0)$ is reduced to $T(L_0) < T(G_0)$. An SSG formed in this way is called a k -type SSG, in which the k index i_k is used to present the reduction of the translation symmetry $i_k = |T(G_0)|/|T(L_0)|$. In general, the k subgroup implies cell multiplication to accommodate the magnetic configuration. Therefore, unlike i_t , which can be solely determined by the PG part of G_0 and L_0 , i_k is an independent condition to label an SSG. Importantly, since G_0 and L_0 have the same PG part, the quotient group G_0/L_0 is isomorphic to the quotient group of their translation part $T(G_0)/T(L_0)$, which forms a 3D lattice translation group $Z_{n_1} \times Z_{n_2} \times Z_{n_3}$, where n_i are natural numbers. As a result, the group structures of G_0/L_0 are not limited to 32 crystallographic PGs (they could even be a non-PG) and are countless, leading to infinite numbers of SSGs. In this work, we set a cutoff of $i_k = n_1 n_2 n_3 \leq 8$ to enumerate the SSGs that require cell expansion. For example, an SSG, whose translation quotient group G_0/L_0 has the structure of Z_5 , allows for a fivefold rotation of spins propagating along a specific direction. For the commensurate magnets with $i_k > 8$, their SSGs can still be diagnosed case by case by our procedure.
- (3) The L_0 that have lost PG operations as well as translation operations are called “general” subgroups of G_0 [$P(L_0) < P(G_0)$ and $T(L_0) < T(G_0)$]. An SSG formed in this way is called a g -type SSG, for which the quotient group G_0/L_0 is not necessarily Abelian. For example, G_0/L_0 could be isomorphic to a dihedral group D_n with n being any positive integer. In this case, $T(G_0)/T(L_0)$ is isomorphic to Z_n which contributes a generator r of order n , while $P(G_0)/P(L_0)$ is isomorphic to Z_2 that contributes a generator h of order two. When the coset representative h is chosen as a twofold rotation along an axis perpendicular to the translation vector of r , the two generators satisfy $hrh^{-1} = r^{-1}$, leading to $G_0/L_0 \cong D_n$. Through our construction procedure with a specific i_k cutoff, we find that g -type subgroups constitute most of the total (over 85%).

To mathematically enumerate all group-normal subgroup pairs (G_0, L_0) with a specific i_k index, we adopt an inverse procedure, starting from L_0 and finding all supergroups G_0 whose subgroup contains L_0 . The full list of group-normal subgroup pairs is obtained with the assistance of the

SUPERGROUPS program [62] implemented in the Bilbao Crystallographic Server [63], leading to 10 660 combinations of (G_0, L_0, i_k) . For each combination, there may be multiple possibilities with different coset representative elements, which relates to the symmetry operation between different magnetic sublattices. Furthermore, for a given i_k there are also multiple possibilities fulfilling $i_k = n_1 n_2 n_3$, which correlates the cell expansion along different directions.

After coset decomposition, we next consider the coupled PG in spin space, $G^s \cong G_0/L_0$. The isomorphism relationship implies that given a specific combination of (G_0, L_0, i_k) , G^s could have different choices. For example, if the quotient group G_0/L_0 is isomorphic to a D_8 , G^s could be D_8 , C_{8v} , and D_{4d} . Moreover, for a given G^s , the isomorphic mapping between G^s and G_0/L_0 also have multiple possibilities, leading to different nontrivial SSGs according to Eq. (3). Therefore, by enumerating inequivalent coset decompositions of G_0/L_0 , different G^s and inequivalent mappings between G^s and G_0/L_0 , we are able to identify an SSG by a four-index (L_0, G_0, i_k, m) label. The mathematical procedure of finding inequivalent coset decompositions and inequivalent mappings is provided in Appendix A.

B. Nontrivial SSGs

Through the abovementioned methodology, we can mathematically obtain 122 types of G^s , and 100 612 nontrivial SSGs (G_{NS}) with the cell expansion limited to $i_k \leq 8$. The complete list provided in Supplemental Material [64] includes 8505 t -type, 6738 k -type, and 85369 g -type SSGs. In Table I, we show the statistics of SSGs classified by the crystal systems of G_0 , which is the SG of the nonmagnetic symmetry of the magnetic primitive cell. It is shown that most SSGs concentrate in crystal systems with relatively lower symmetry, i.e., monoclinic, orthorhombic, and tetragonal (89% in total). In Table II,

TABLE I. Nontrivial SSGs for different crystal systems and different magnetic configurations. “Collinear only” indicates nontrivial SSGs that support only collinear magnetic orders, i.e., $G^s = 1$ and $\bar{1}$. Similarly, “Noncoplanar only” requires that G^s is a polyhedral PG (T , T_d , T_h , O , and O_h). “Coplanar” contains nontrivial SSGs that support coplanar magnetic orders.

Crystal system	Collinear		Noncoplanar		Total
	only	Coplanar	only	Total	
Triclinic (2)	5	55	0	60	
Monoclinic (13)	78	3540	0	3618	
Orthorhombic (59)	503	53 734	0	54 237	
Tetragonal (68)	502	31 185	0	31 687	
Trigonal (25)	83	2331	62	2476	
Hexagonal (27)	137	7149	111	7397	
Cubic (36)	113	840	184	1137	
Total (230)	1421	98 834	357	100 612	

TABLE II. The PG G^s in spin space for all SSGs with the cell expansion limited to $i_k \leq 8$. The H-M symbol stands for Hermann-Mauguin symbol.

H-M symbol	Point group
n	1, 2, 3, 4, 5, 6, 7, 8, 9, 10, 12, 14, 15, 16, 18, 20, 21, 24, 28, 30, 42
nm	$3m$, $5m$, $7m$, $9m$, $(15)m$, $(21)m$
nmm	$mm2$, $4mm$, $6mm$, $8mm$, $(10)mm$, $(12)mm$, $(14)mm$, $(16)mm$, $(18)mm$, $(20)mm$, $(24)mm$, $(28)mm$, $(30)mm$, $(42)mm$
$-n$	-1 , m , -3 , -4 , -5 , -6 , -7 , -8 , -9 , -10 , -12 , -14 , -15 , -16 , -18 , -20 , -21 , -24 , -28 , -30 , -42
n/m	$2/m$, $4/m$, $6/m$, $8/m$, $(10)/m$, $(12)/m$, $(14)/m$, $(16)/m$
$n2$	32 , 52 , 72 , 92 , $(15)2$, $(21)2$
$n22$	222 , 422 , 622 , 822 , $(10)22$, $(12)22$, $(14)22$, $(16)22$, $(18)22$, $(20)22$, $(24)22$, $(28)22$, $(30)22$, $(42)22$
$-nm$	$-3m$, $-5m$, $-7m$, $-9m$, $(-15)m$, $(-21)m$
$-n2m$	$-42m$, $-62m$, $-82m$, $(-10)2m$, $(-12)2m$, $(-14)2m$, $(-16)2m$, $(-18)2m$, $(-20)2m$, $(-24)2m$, $(-28)2m$, $(-30)2m$, $(-42)2m$
n/mmm	mmm , $4/mmm$, $6/mmm$, $8/mmm$, $(10)/mmm$, $(12)/mmm$, $(14)/mmm$, $(16)/mmm$
Cubic	23 , 432 , $m - 3$, $-43m$, $m - 3m$

we show the 122 types of G^s in spin space for all SSGs with $i_k \leq 8$, 90 of which are not crystallographic PGs.

We next take a series of t -type nontrivial SSGs to illustrate the correspondence of the group construction and the realistic magnetic structure. For clarity, we use the international symbol to present group operations hereafter, where P and T are denoted by $\bar{1}$ in real space and spin space, respectively. Considering two SGs $L_0 = P2/c$ (No. 13) and $G_0 = Pcca$ (No. 54) fulfilling normal subgroup relationship, $G_0 = L_0 \cup \{2_{010}|0\ 0\ 1/2\}L_0$. One can define two different sublattices [marked by different colors in Fig. 2(a)] with the group elements of L_0 keeping the sublattice invariant. Thus, L_0 can be defined as the sublattice group. On the other hand, the coset elements $\{2_{010}|0\ 0\ 1/2\}L_0$ transform one sublattice to the other, as shown in Fig. 2(b). Therefore, there are three possibilities of G^s being isomorphic to Z_2 (G_0/L_0), i.e., $\bar{1}$, 2, and m , leading to three inequivalent mappings for the magnetic moments, as shown in Figs. 2(c)–2(e). Taking (13.54.1.1) as an example, the nontrivial SSG is constructed by mapping the $\bar{1}$ operator in spin space (i.e., T) to the representative element $\{2_{010}|0\ 0\ 1/2\}$, leading to $G_{NS} = \{E||L_0\} \cup \{\bar{1}||2_{010}|0\ 0\ 1/2\}L_0$.

While there is no multiplicity of different mappings for a specific order-two G^s , there is another inequivalent coset decomposition $G_0 = L_0 \cup \{2_{001}|1/2\ 0\ 0\}L_0$ for (L_0, G_0) , owing to the inequivalence between the a and c axes for SG $P2/c$. Consequently, there are another three nontrivial SSGs with a different choice of sublattices, as shown in

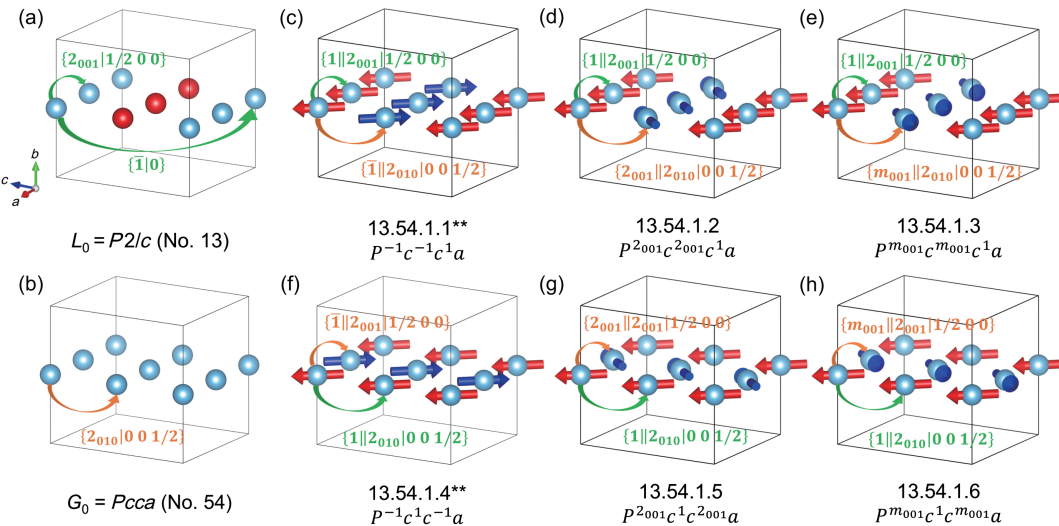


FIG. 2. Nontrivial SSGs generated from a t -type (L_0, G_0) subgroup pair and the corresponding magnetic configurations. In this case, the coordinate system xyz in spin space coincides with the coordinate system abc in real space. (a) Structure with sublattice group $L_0 = P2/c$ (No. 13). The group generators are indicated by green arrows. The balls with different colors denote different sublattices. (b) Structure with nonmagnetic group $G_0 = Pccca$ (No. 54). The group generators that connect different sublattices are indicated by orange arrows. (c)–(h) Magnetic configurations and the corresponding international notations for different nontrivial SSGs. Green and orange arrows indicate the generators connecting the same and the different sublattices, respectively. The double star denotes SSGs for collinear magnetic configurations. Note that when considering the spin-only group, the SSGs generated by $G^s = 2$ and m [e.g., panels (d) and (e); panels (g) and (h)] are equivalent.

Figs. 2(f)–2(h). Overall, there are six t -type nontrivial SSGs for the given (L_0, G_0) pair, with two supporting collinear magnetic structures ($G^s = \bar{1}$), and four of them supporting coplanar magnetic structures ($G^s = 2$ and m). However, we show later that when considering the spin-only group, the SSGs generated by $G^s = 2$ and m are indeed equivalent. The group constructions of the k -type and g -type nontrivial SSGs follow similar procedures, as exemplified by the SSGs of realistic materials CeAuAl₃ and CoNb₃S₆, respectively (see Secs. IVB and IVC).

C. International notation

International notation, also known as Hermann-Mauguin notation, is a widely used nomenclature for PGs, SGs, MPG, and MSGs. It is employed in the standard structural and symmetry reference, the International Tables for Crystallography [65], and is extensively utilized in various crystallography textbooks. Compared with Schoenflies notation, international notation is more favorable for presenting the directions of the symmetry axes and the translation symmetry elements in SGs.

We next develop the international notation for all SSGs. The international notation of an SG is denoted as $Bg_1g_2g_3$, where the first uppercase letter B describes the Bravais lattice, including the primitive (P), based-centered (A, B, C), body-centered (I), face-centered (F), and rhombohedral (R) lattice. The following three letters describe the representative symmetry operations, as defined in Appendix B Table VII. Since the translation operations in real space

could also couple a PG operation in spin space in SSGs, we first need to expand the $Bg_1g_2g_3$ notation to a more comprehensive one $Bg_1g_2g_3t_a t_b t_c b_1 b_2 b_3$. Here, $t_{a\sim c}$ present the integral translation of cell expansion, while for SGs we simply have $t_a = (1\ 0\ 0)$, $t_b = (0\ 1\ 0)$, $t_c = (0\ 0\ 1)$. $b_{1\sim 3}$ stand for the fractional translations for the specific Bravais centering type. The specific b_1, b_2 , and b_3 for each Bravais lattice can be found in Appendix C Table XVII (see more details on the international notation and operation symbols for SSG in Appendix B and Supplemental Material, Sec. I).

To construct an SSG, an SG $G_0 = Bg_1g_2g_3t_a t_b t_c b_1 b_2 b_3$ is decomposed into cosets with respect to one of its normal subgroups L_0 by Eq. (2), and then a PG G^s is mapped to the quotient group G_0/L_0 through an isomorphism relationship by Eq. (3). Consequently, each of the representative symmetry operations $g_{1\sim 3}$, Bravais centering-type fractional translation $b_{1\sim 3}$, and integral translation $t_{a\sim c}$ could combine with a spin PG operation under the basis of G_0 . Such a nomenclature is done for t -type and g -type SSGs. For k -type SSGs, we use a multicolor extension of the Belov-Neronova-Smirnova (BNS) convention of MSGs [66,67], yielding more convenience and simpler notations (see Appendix C 2).

Now we turn to the specific nomenclature of three types of SSGs. For t -type SSGs, $T(L_0) = T(G_0), P(L_0) \leq P(G_0)$. This implies that the group element of G^s (excluding the identity) in a t -type SSG can be combined only with nontrivial SG operations $\{R|0\}$ or $\{R|\tau\}$ with $R \neq E$, rather than pure translations $\{E|\tau\}$. As a result, the Bravais

TABLE III. Symmetry operations and general positions of SSG (13.54.1.1) $P^{-1}c^{-1}c^1a$. In this table, a , b , and c represent the coordinates of a general position using the lattice basis of the SSG; x , y , and z denote the corresponding components of the magnetic moment using Cartesian coordinates.

Operation	Coordinates	Operation	Coordinates
$\{1\ 1 0\}$	a, b, c, x, y, z	$\{-1\ 2_{100} 1/2 0 1/2\}$	$a + 1/2, -b, -c + 1/2, -x, -y, -z$
$\{1\ -1 0\}$	$-a, -b, -c, x, y, z$	$\{-1\ m_{100} 1/2 0 1/2\}$	$-a + 1/2, b, c + 1/2, -x, -y, -z$
$\{1\ 2_{001} 1/2 0 0\}$	$-a + 1/2, -b, c, x, y, z$	$\{-1\ 2_{010} 0 0 1/2\}$	$-a, b, -c + 1/2, -x, -y, -z$
$\{1\ m_{001} 1/2 0 0\}$	$a + 1/2, b, -c, x, y, z$	$\{-1\ m_{010} 0 0 1/2\}$	$a, -b, c + 1/2, -x, -y, -z$

fractional translation $b_{1\sim 3}$ and integral translation $t_{a\sim c}$ always combine with identity in spin space in a t -type SSG; thus, they can be omitted. In other words, a t -type SSG can be described following Litvin's notation on SPGs [18], i.e., $B^{g_{s_1}}g_1^{g_{s_2}}g_2^{g_{s_3}}g_3$ in the G_0 basis. The corresponding symmetry operations can be directly constructed by $\{g_{s_1}\|g_1\}$, $\{g_{s_2}\|g_2\}$, and $\{g_{s_3}\|g_3\}$. We still take SSG (13.54.1.1) as an example, where the symmetry operations and the resultant general positions are listed in Table III. Note that the Wyckoff positions and the corresponding magnetic configurations are constructed by using the site-symmetry groups of the SSG, with the details provided in Supplemental Material, Sec. II. It can be found that for $G_0 = Pcc\bar{a}$, the $\bar{1}$ operator in spin space is mapped to the glide reflections $\{m_{100}|1/2 0 1/2\}$ and $\{m_{010}|0 0 1/2\}$, leading to the international notation $P^{-1}c^{-1}c^1a$. Similarly, the international notations for (13.54.1.2) to (13.54.1.6) shown in Fig. 2 are $P^{2_{001}}c^{2_{001}}c^1a$, $P^{m_{001}}c^{m_{001}}c^1a$, $P^{-1}c^1c^{-1}a$, $P^{2_{001}}c^1c^{2_{001}}a$, and $P^{m_{001}}c^1c^{m_{001}}a$, respectively (see Appendix C for details).

For k -type SSGs, $T(L_0) < T(G_0)$, $P(L_0) = P(G_0)$. This indicates that a k -type SSG can be constructed directly using the sublattice SG $\{E\|L_0\}$ and an additional spin translation group $G_T^S = \{\{1\|1|0\}, \{g_{s_1}\|1|\tau_1\}, \dots, \{g_{s_{n-1}}\|1|\tau_{n-1}\}\}$ generated by $\{g_{s_1}\|1|\tau_1\}$, $\{g_{s_2}\|1|\tau_2\}$, and $\{g_{s_3}\|1|\tau_3\}$. Among them, $\tau_i = (a_i \ b_i \ c_i)$ denote the fractional translations after cell expansion along the three basis vectors of L_0 , and the product of the multiplicities of τ_{1-3} fulfills the imposed cutoff $i_k \leq 8$. Note that in k -type SSGs, L_0 and G_0 always belong to the same crystal systems, but not necessarily the same Bravais lattice. As a result, it is more convenient to denote a k -type SSG as $B^1g_1^1g_2^1g_3^{g_{s_1}}\tau_1^{g_{s_2}}\tau_2^{g_{s_3}}\tau_3$ in the L_0 basis, where $\tau_i = (a_i \ b_i \ c_i)$. In this sense, the symmetry operations of a k -type SSG can be directly constructed from the direct product of sublattice SG $\{E\|Bg_1g_2g_3\}$ and G_T^S . Indeed, such a nomenclature is a natural multicolor extension of the conventional BNS setting for type-IV MSGs [66,67]. Specifically, type-IV MSGs have the form $G + T\tau G$ ($i_k = 2$) and can thus be denoted by $B_Xg_1g_2g_3$, where X labels the black and white Bravais lattices. In comparison, the complexity of multicolor

Bravais lattices is incorporated by the notation of $g_{s_1}\tau_1^{g_{s_2}}\tau_2^{g_{s_3}}\tau_3$. We provide an example of a k -type SSG (99.107.4.1), whose international notation is written as $P^{141}m^1m^{4_{001}}(1/2 1/2 1/4)$ of a realistic material CeAuAl₃. A detailed explanation of this material example can be found in Sec. IV B and Appendix C.

Now we turn to the g -type SSGs with $T(L_0) < T(G_0)$ and $P(L_0) < P(G_0)$. The group element of G^S in spin space will combine with the representative symmetry operation $g_{1\sim 3}$, integral translation $t_{a\sim c}$, and Bravais fractional translation $b_{1\sim 3}$, no matter in the G_0 or L_0 basis. In g -type SSGs, L_0 and G_0 could belong to different crystal systems. Consequently, it is advantageous to write the international notation of the g -type SSGs in the G_0 basis, as the first letter B will reflect the information of the Bravais lattice of the magnetic cell (see Appendix C). Since each of the spatial operations is allowed to connect an independent rotation in spin space, the g -type SSGs are thus denoted as $B^{g_{s_1}}g_1^{g_{s_2}}g_2^{g_{s_3}}g_3|(g_{s_4}, g_{s_5}, g_{s_6}; g_{s_7}, g_{s_8}, g_{s_9})$ in the G_0 basis. Note that $g_{s_4}, g_{s_5}, g_{s_6}$ denote the spin rotation associated with t_a, t_b, t_c , while $g_{s_7}, g_{s_8}, g_{s_9}$ denote the spin rotation associated with b_1, b_2, b_3 (Appendix C Table XVII). Particularly, for the P Bravais lattice, $g_{s_7}, g_{s_8}, g_{s_9}$ can be simply omitted because all centering-type fractional translations b_1, b_2, b_3 are absent. We provide an example of a g -type SSG (4.182.4.2), whose international notation is written as $P^{3^2_{-11-1}}6_3^{m_{110}}2^{m_{011}}2|(2_{001}, 2_{100}, 1)$, of a realistic material CoNb₃S₆. A detailed explanation of this material example can be found in Sec. IV C and Appendix C.

Besides the examples mentioned above, we present more examples of various complicated cases of the three types of SSGs in Appendix C. In addition, the international notations of all the enumerated nontrivial SSGs are provided in our online program FINDSPINGROUP [59].

D. SSGs for different magnetic configurations

In Table I, we enumerate the nontrivial SSGs supporting collinear-only, noncoplanar-only, and coplanar magnetic configurations. We next implement spin-only group G_{SO} into G_{NS} to count all inequivalent SSGs for different magnetic configurations, including collinear, coplanar, and noncoplanar orders. We elucidate that G_{SO} plays a crucial role in finding equivalent collinear and coplanar

SSGs. Without the loss of generality, we assume that each sublattice contains only one type of magnetic ion. The enumeration process is based on different G^s , and is divided into the following classes:

Collinear SSGs. In collinear magnets, all local moments point toward the same or opposite direction (e.g., the z axis), and the corresponding SSG does not depend on the direction of the spins. The full SSG of a collinear magnet is written as $G_{\text{SS}} = G_{\text{NS}} \times Z_2^K \ltimes \text{SO}(2)$. The spin-only group $G_{\text{SO}}^I = Z_2^K \ltimes \text{SO}(2)$ (the international notation is ${}^\infty m 1$) of collinear SSG ensures that only time-reversal T needs to be considered for the spin space of G_{NS} , rendering only two possibilities, $G^s = 1$ and $\bar{1}$, corresponding to ferromagnets (ferrimagnets) and antiferromagnets, respectively. Therefore, collinear SSGs manifest one-by-one correspondence with the structure of MSGs, in which the magnetic sublattices with opposite directions of local moments can be regarded as black and white. Specifically, there are 230 SSGs for collinear ferromagnets or ferrimagnets with their nontrivial SSG $G_{\text{NS}} = \{E \parallel G_0\}$, where G_0 is one of the 230 SGs. These nontrivial t -type SSGs also have $G_0 = L_0$ and $G^s = 1$ corresponding to 230 type-I MSGs. For antiferromagnets, $G^s = \bar{1}$, the nontrivial SSG can thus be written as $\{E \parallel L_0\} \cup \{T \parallel AL_0\}$, where A denotes the symmetry operation connecting the sublattices with opposite spins. If A is a pure translation, i.e., $P(L_0) = P(G_0)$ and $i_k = 2$, the resulting SSGs correspond to 517 type-IV MSGs. On the other hand, if A is an inversion or rotation (proper or improper), the resulting SSGs with $T(L_0) = T(G_0)$ and $i_t = 2$ correspond to 674 type-III MSGs. Overall, there are 1421 inequivalent collinear SSGs in total, as marked by double stars in Supplemental Material [64].

Coplanar SSGs. For those SSGs describing coplanar magnetic configurations, the spin-only group is $G_{\text{SO}}^P = \{E, TU_n(\pi)\}$ (the international notation is ${}^m 1$). Thus, all the spin rotation axes of G^s should be either perpendicular or parallel to a specific axis n , implying that polyhedral PGs are excluded for G^s . In addition, due to the existence of the spin-only group G_{SO}^P , we can further limit G^s to unitary PGs, which do not contain T . To prove this, we consider an antiunitary nontrivial SSG $G_{\text{NS}}^{\text{AU}}$ with its maximal unitary subgroup $L_{\text{NS}}^{\text{MU}}$:

$$\begin{aligned} & G_{\text{NS}}^{\text{AU}} \times \{E, TU_n(\pi)\} \\ &= [L_{\text{NS}}^{\text{MU}} \cup (G_{\text{NS}}^{\text{AU}} \setminus L_{\text{NS}}^{\text{MU}})] \times \{E, TU_n(\pi)\} \\ &= [L_{\text{NS}}^{\text{MU}} \cup TU_n(\pi)(G_{\text{NS}}^{\text{AU}} \setminus L_{\text{NS}}^{\text{MU}})] \times \{E, TU_n(\pi)\} \\ &= G_{\text{NS}}^U \times \{E, TU_n(\pi)\}. \end{aligned} \quad (4)$$

Equation (4) suggests that for any antiunitary nontrivial SSG $G_{\text{NS}}^{\text{AU}}$, we can construct an equivalent unitary nontrivial SSG $G_{\text{NS}}^U = L_{\text{NS}}^{\text{MU}} \cup TU_n(\pi)(G_{\text{NS}}^{\text{AU}} \setminus L_{\text{NS}}^{\text{MU}})$ when taking G_{SO}^P into account. Therefore, to obtain all inequivalent coplanar SSGs from the full (L_0, G_0, i_k, m) SSG list, it is adequate to

add the condition $G^s \cong C_n$ or D_n . Note that for k subgroups and g subgroups, the C_n and D_n groups are not limited to crystallographic PGs (e.g., Z_5), resulting in 41 possibilities out of 122 G^s 's. Within the considered cell multiplicity $i_k \leq 8$, we find 16 383 inequivalent coplanar SSGs, which is a significantly reduced number compared with the number of G_{NS} that support coplanar magnetic configurations (98 834). We note two special portions of G_{NS} for coplanar configurations. The first one is $G^s = 2$ and m , for which G_{NS} supports both collinear and coplanar (but not noncoplanar) configurations. However, when they describe collinear configurations, they are exactly equivalent to the SSGs with $G^s = \bar{1}$ due to the existence of G_{SO}^I , so they do not contribute new entries to 1421 inequivalent collinear SSGs. On the other hand, when they describe coplanar configurations, they are equivalent to each other because of Eq. (4), contributing 1191 inequivalent coplanar SSGs. Therefore, there are 1191 entries with $G^s = m$ rendering equivalent SSGs when considering the G_{SO} part. Specifically, as for our example, (13.54.1.2) and (13.54.1.3) [Figs. 2(d) and 2(e)] are equivalent coplanar SSGs. The second case is $G^s = 2/m$, for which the G_{NS} supports coplanar configurations only. However, considering G_{SO}^P , the SSGs generated by antiunitary $2/m$ is equivalent to those generated from $G^s = 222$ according to Eq. (4). Therefore, there are 9501 entries with $G^s = 2/m$ rendering equivalent SSGs when considering the G_{SO} part.

Noncoplanar SSGs. The spin-only group for noncoplanar SSGs is simply an identity group. When G^s is a polyhedral PG (T , T_d , T_h , O , and O_h), there are 357 SSGs in total supporting only noncoplanar magnetic configurations. On the other hand, when taking other G^s except 1, $\bar{1}$, 2, m , $2/m$, and polyhedral PGs, the corresponding G_{NS} (86 951 entries) support both coplanar and noncoplanar configurations. Since $G_{\text{SS}} = G_{\text{NS}}$, all of these SSGs for noncoplanar configurations are inequivalent. Finally, there are 87 308 inequivalent noncoplanar SSGs in total.

We show in Fig. 3 the summary of the inequivalent SSGs for different magnetic configurations, indicating that the spin-only groups serve as another factor for equivalent SSGs. For example, the nontrivial SSGs supporting coplanar magnetic configurations indeed form a small subset of inequivalent coplanar SSGs (98 834).

III. REPRESENTATION OF SPIN SPACE GROUPS

Representation theory is the key to encoding the information of symmetry to quantum-mechanics wave functions, which determine the elementary excitations, geometric phases, selection rules, etc. In this section, we explore the general rep theory of SSGs, i.e., obtain the projective coirreps of the little group G^k , which consists of all symmetry operations that leave k invariant. In the following, we separately consider the SSGs supporting noncollinear (coplanar and noncoplanar) and collinear magnetic

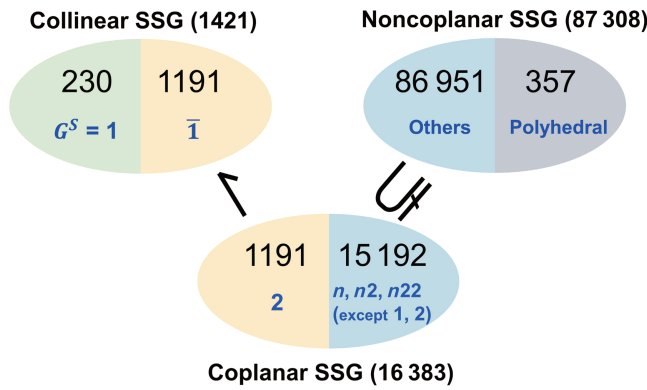


FIG. 3. Summary of inequivalent SSGs for collinear, coplanar, and noncoplanar magnetic configurations when considering their spin-only groups. The blue fonts denote the corresponding G^s . “Polyhedral” indicates polyhedral PGs, i.e., T , T_d , T_h , O , and O_h . “Others” indicates other G^s except 1, $\bar{1}$, 2, m , $2/m$, and polyhedral PGs. “—” means that when considering collinear spin-only group G'_{SO} , $G^s = \bar{1}$ and 2 yield equivalent collinear SSGs. “ \subseteq ” means that when considering coplanar spin-only group G''_{SO} , the 86 951 nontrivial SSGs (supporting both coplanar and noncoplanar magnetic configurations) is reduced to 15 192 inequivalent coplanar SSGs.

configurations, because the latter possess infinite symmetry operations owing to the spin-only group $\infty\text{m}1$.

For a noncollinear unitary SSG, we examine its regular projective reps, which are reducible reps containing all the possible irreducible representations (irreps). We then apply an approach that utilizes the eigenvalues and eigenvectors of a complete set of commuting operators (CSCOs) to decompose the regular projective rep to obtain all irreps of the unitary SSG [68,69]. Finally, we apply a modified Dimmock and Wheeler character sum rule to derive the coirreps of antiunitary SSGs. To illustrate the procedure, we derive the coirreps of the little groups for two materials, i.e., CeAuAl_3 and CoNb_3S_6 . The comparison of coirreps under SSG and MSG shows that the coirreps in SSG may have higher dimensions.

The 1421 collinear SSGs have one-by-one correspondence to types-I, -III, and -IV MSGs. However, we show that the coirreps of collinear SSGs can be obtained by considering the single-valued coirreps of type-II MSGs plus the extra degeneracies that originated from some critical spin symmetries. To illustrate this, we compare the dimensions of the coirreps under SSG and MSG for a collinear antiferromagnet RuO_2 in Sec. IV A.

A. Basics of representation theory For SGs and MSGs

We first briefly review the traditional approach to obtain the irreps of little group $G^k = \{R_1|\tau_1\}\mathbb{T} + \{R_2|\tau_2\}\mathbb{T} + \dots + \{R_n|\tau_n\}\mathbb{T}$ (\mathbb{T} denotes the crystallographic translation group; R_i and τ_i denote the real-space PG operation and fractional translation, respectively) in SGs and MSGs, with

more details provided in Appendix A. In SGs, the complexity of reps comes from the fractional translations. Specifically, the group of rep matrices covers the corresponding little cogroup $\check{G}^k = \{R_1, R_2, \dots, R_n\}$ multiple times because one R_k could combine with multiple translations. To simplify the problem, the theory of the projective rep is used to “mod” the influence of fractional translations and get all irreps of $\check{G}^k = G^k/\mathbb{T} = \{\{R_1|\tau_1\}, \{R_2|\tau_2\}, \dots, \{R_n|\tau_n\}\}$. In SGs, a projective irrep $M_k^l(\{R_i|\tau_i\})$ of a little group G^k leaves the complexity of fractional translation to the factor system, i.e., $d_k^l(\{R_i|\tau_i\}) = \exp(-ik\tau_i)M_k^l(\{R_i|\tau_i\})$, where $d_k^l(\{R_i|\tau_i\})$ denotes the l th irrep of \check{G}^k . On the other hand, $M_k^l(\{R_i|\tau_i\})$ can be obtained by looking for the reps of an extended group constructed by \check{G}^k and a cyclic group formed by the factor system $\exp(-iK_i\tau_i)$, which is also known as a central extension ($K_i = R_i^{-1}k - k$). This means that to obtain all the irreps of a SG, it is only necessary to find the reps of a few cyclic groups in addition to those of PGs (\check{G}^k) that are already known [2].

For MSGs, the incorporation of antiunitary operations gives rise to coirreps, which can be obtained in two steps. Since the little group G_{MS}^k for a given MSG could contain antiunitary operations, the first step is to get the irreps of the maximal unitary subgroup of G_{MS}^k ; they are calculated following the procedure of an SG discussed above. The second step is to take into account the antiunitary elements of G_{MS}^k , leading to three types of coirreps according to the famous Dimmock and Wheeler sum rule. The theory of coirreps is useful for analyzing extra degeneracies caused by antiunitary operations and the corresponding degenerate states [2]. The details of projective rep, central extension, and Dimmock and Wheeler’s sum rule are introduced in Appendix A.

B. Representation of coplanar and noncoplanar (nontrivial) SSGs

The rep theory of the SSG developed here combines the theory of projective reps in SG and a modified version of Dimmock and Wheeler’s sum rule in MSG. In the projective reps, the effect of unitary spin rotation is absorbed into the factor system. However, the little group of an SSG may contain some “spin nonsymmorphic symmetries” $\{g_s||E|\tau\}$, i.e., combined operations of spin operation g_s and fractional translation τ , rendering the central extension method rather complicated. Instead, we focus on the regular projective reps that contain all the irreps. These regular projective reps are decomposed into projective irreps using CSCCO method.

Unlike SGs, a single lattice operation R_i in SSGs may correspond to multiple nonsymmorphic translations $\tau_i^{(a)}$ for the case of $i_k > 1$, as well as spin operations $g_{s_i}^{(a)}$, where a labels different translations and spin operations

accompanied with one R_i . In addition, the factor system can also absorb an additional phase of spin rotation $g_{s_i}^{(a)}$, where the rotation of 2π picks up a phase of -1 . Considering $d_k^l(\{g_{s_i}^{(a)} \| R_i | \tau_i^{(a)}\})$ an irrep of a unitary little SSG G_{SS}^k , we have

$$d_k^l\left(\left\{g_{s_i}^{(a)} \| R_i | \tau_i^{(a)}\right\}\right) = \exp\left(-ik\tau_i^{(a)}\right) M_k^l\left(\left\{g_{s_i}^{(a)} \| R_i | \tau_i^{(a)}\right\}\right). \quad (5)$$

Here, $0 \leq \phi(g_{s_i}^{(a)}) < 2\pi$, in which $\phi(g_{s_i}^{(a)})$ is the rotation angle of $g_{s_i}^{(a)}$. We note that projective reps M_k^l do not distinguish translation operations that differ by integer multiples of lattice vectors, i.e., $M_k^l(\{g_{s_i}^{(a)} \| R_i | \tau_i^{(a)} + t_i\}) = M_k^l(\{g_{s_i}^{(a)} \| R_i | \tau_i^{(a)} + t_j\})$ for $t_i, t_j \in T(L_0)$. That is to say, $M_k^l(\{g_{s_i}^{(a)} \| R_i | \tau_i^{(a)}\})$ is a matrix-valued function on the elements $\{g_{s_i}^{(a)} \| R_i | \tau_i^{(a)}\}$ of the finite quotient group $\tilde{G}_{\text{SS}}^k = G_{\text{SS}}^k / T(L_0)$. According to the multiplication of reps d_k^l , for the projective reps of elements $\{g_{s_i}^{(a)} \| R_i | \tau_i^{(a)}\}$, $\{g_{s_j}^{(a)} \| R_j | \tau_j^{(a)}\} \in \tilde{G}_{\text{SS}}^k [0 \leq \phi(g_{s_i}^{(a)}), \phi(g_{s_j}^{(a)}) < 2\pi]$, we have

$$\begin{aligned} & M_k^l\left(\left\{g_{s_i}^{(a)} \| R_i | \tau_i^{(a)}\right\}\right) M_k^l\left(\left\{g_{s_j}^{(a)} \| R_j | \tau_j^{(a)}\right\}\right) \\ &= (-1)^{\xi(g_{s_i}^{(a)}, g_{s_j}^{(a)})} \exp(-iK_i\tau_j^{(a)}) M_k^l\left(\left\{g_{s_l}^{(a)} \| R_l | \tau_l^{(a)}\right\}\right). \end{aligned} \quad (6)$$

Here, $\{g_{s_l}^{(a)} \| R_l | \tau_l^{(a)}\} = \{g_{s_i}^{(a)} g_{s_j}^{(a)} \| R_i R_j | \tau_i^{(a)} + R_j \tau_j^{(a)} \bmod T(L_0)\}$, $K_i = R_i^{-1}k - k$, $\xi(g_{s_i}^{(a)}, g_{s_j}^{(a)}) = 0$ for $0 \leq \phi(g_{s_i}^{(a)}, g_{s_j}^{(a)}) < 2\pi$, and $\xi(g_{s_i}^{(a)}, g_{s_j}^{(a)}) = 1$ for $2\pi \leq \phi(g_{s_i}^{(a)}, g_{s_j}^{(a)}) < 4\pi$. Therefore, it is only necessary to find out all projective irreps of \tilde{G}_{SS}^k . For simplicity, we use $g_i^{(a)}$ to represent $\{g_{s_i}^{(a)} \| R_i | \tau_i^{(a)}\}$ hereafter.

Next, the CSCO method is employed to obtain projective irreps by decomposing the regular projective reps [68,69]. In quantum mechanics, a set of commuting operators (J^2, J_z) form the CSCO of the Hilbert space of angular momentum. The corresponding quantum numbers j and m_j are sufficient to diagonalize the Hamiltonian and label all the resulting eigenstates. Similarly, the basic idea of the CSCO approach used here is to decompose the projective reps of \tilde{G}_{SS}^k into blocks to distinguish all the irreps of \tilde{G}_{SS}^k . This is done by constructing a series of class operators analogous to the set of (J^2, J_z) , which commute with each other and commute with every group element. The specific procedure is described in Appendix D.

For any antiunitary little group G_{SS}^k , one can first decompose it with respect to its maximal unitary subgroups

L_{SS}^k , i.e., $G_{\text{SS}}^k = L_{\text{SS}}^k \cup TAL_{\text{SS}}^k$, where TA is the antiunitary coset representative element. The projective irreps $M_k^l(g_i^{(a)})$ and the corresponding irreps $d_k^l(g_i^{(a)})$ with $g_i^{(a)} \in \tilde{L}_{\text{SS}}^k = L_{\text{SS}}^k / \mathbb{T}$ can certainly be treated by using the CSCO method. Assuming that the basis set of $d_k^l(g_i^{(a)})$ is $|\psi\rangle = |\psi_1, \psi_2, \dots, \psi_{n_l}\rangle$, then for the coset the basis set can be adopted as $|\phi\rangle = |\phi_1, \phi_2, \dots, \phi_{n_l}\rangle = TA|\psi_1, \psi_2, \dots, \psi_{n_l}\rangle$. Consequently, the coreps for the full basis set $|\psi, \phi\rangle$ are

$$\begin{aligned} D_k^l(g_i^{(a)}) &= \begin{bmatrix} d_k^l(g_i^{(a)}) & 0 \\ 0 & d_k^{l*}(A^{-1}g_i^{(a)}A) \end{bmatrix}, \\ D_k^l(TA g_i^{(a)}) &= \begin{bmatrix} 0 & d_k^l(TA g_i^{(a)} TA) \\ d_k^{l*}(g_i^{(a)}) & 0 \end{bmatrix}. \end{aligned} \quad (7)$$

Then we can prove the following modified Dimmock and Wheeler character sum rule (see Supplemental Material, Sec. III), which helps to identify whether the coreps are irreducible or not:

$$\sum_{g_i^{(a)} \in TA \tilde{L}_{\text{SS}}^k} \chi^l((g_i^{(a)})^2) = \begin{cases} +|\tilde{L}_{\text{SS}}^k| & (\text{a}), \\ -|\tilde{L}_{\text{SS}}^k| & (\text{b}), \\ 0 & (\text{c}). \end{cases} \quad (8)$$

For Eq. (8a), the corep matrices D_k^l in Eq. (7) are reducible and have the same dimension as the irrep d_k^l . For Eqs. (8b) and (8c), the dimension of D_k^l is doubled compared with that of d_k^l . Following the approach presented here, we can obtain the projective coirreps of any arbitrary k -point for all finite SSGs.

The abovementioned procedure of obtaining the coirreps is exemplified by two realistic materials, i.e., CeAuAl₃ and CoNb₃S₆, as shown in Supplemental Material, Secs. V and VI. The corresponding electronic band structures and additional exotic properties of these two materials are discussed in Sec. IV.

C. Representation of collinear SSGs

The CSCO method cannot be applied to collinear SSGs because the SO(2) spin rotation symmetry renders the SSG a continuously infinite group. Interestingly, the incorporation of spin-only group $G_{\text{SO}}^l = Z_2^K \rtimes \text{SO}(2)$ ensures that the coirreps of collinear SSGs can be obtained by considering the single-valued coirreps of 230 type-II MSGs plus the extra degeneracies in spin space originated from some crucial symmetries beyond MSGs. We next discuss collinear SSGs in two categories, i.e., those describing ferromagnets and antiferromagnets.

For SSGs describing collinear ferromagnets and ferrimagnets, it is straightforward that $G_0 = L_0$, $G^s = 1$, and $G_{\text{SO}}^l = Z_2^K \ltimes \text{SO}(2)$. The corresponding SSG can be written as

$$G_{\text{SS}} = \{E \parallel L_0\} \times Z_2^K \ltimes \text{SO}(2). \quad (9)$$

While $Z_2^K \ltimes \text{SO}(2)$ itself cannot contribute extra degeneracy in spin space (see Appendix D 3), the conjugate symmetry operator K can combine two conjugated single-valued irreps in real space. Therefore, the coirreps of this type of SSG (230 in total) are the same as spinless gray SGs ($L_0 \times Z_2^K$), or single-valued coirreps of type-II MSGs.

For SSGs describing collinear antiferromagnets, L_0 is the sublattice group, which is an index-two normal subgroup of G_0 . In addition, we have $G^s = \bar{1}$ and a real-space operation A connecting the two sublattices with opposite magnetic moments. The corresponding SSG can be expressed as

$$G_{\text{SS}} = (\{E \parallel L_0\} \cup \{T \parallel AL_0\}) \times Z_2^K \ltimes \text{SO}(2). \quad (10)$$

The critical symmetries beyond MSGs include spin $\text{SO}(2)$, $\{T \parallel A\}$, and $\{U_n(\pi) \parallel A\}$. Among these, the $\text{SO}(2)$ group provides conjugated one-dimensional (1D) irreps $\Gamma_{+1/2}^S$ and $\Gamma_{-1/2}^S$ in spin space, leading to the following degeneracy doubling mechanisms: If the little group of k has $\{U_n(\pi) \parallel A\}$ or $\{T \parallel A\}$ symmetry, the combination of $\text{SO}(2)$ and $\{U_n(\pi) \parallel A\}$ or $\{T \parallel A\}$ pairs $\Gamma_{+1/2}^S$ and $\Gamma_{-1/2}^S$ into a two-dimensional (2D) irrep or coirrep, respectively (see Appendix D 3).

Overall, the general procedure to obtain coirreps of collinear SSGs can be summarized as the coirreps of the single-valued coirreps of the type-II MSG $L_0 \times Z_2^K$ (real space) plus additional double degeneracy caused by $\{U_n(\pi) \parallel A\}$ or $\{T \parallel A\}$ symmetry (spin space). As an example, we perform calculations of the coirreps for a collinear antiferromagnet RuO_2 , as shown in Supplemental Material, Sec. IV. The corresponding electronic band structures and the extra degeneracies in SSG are discussed in Sec. IV.

IV. REALISTIC MATERIALS

While SOC ultimately exists in realistic magnetic systems, under the circumstances when the SOC effect is weak or when considering the SOC-induced effects (e.g., orbital polarization) [70], it is useful to analyze the wavefunction properties of an SOC-free Hamiltonian [19]. SSGs provide a comprehensive symmetry description of such Hamiltonians. Given a realistic material with specific atomic positions and local moments, a practical need is to identify its SSG with all possible symmetry operations. We develop an online program FINDSPINGROUP for identifying the SSG symmetries of a magnetic crystal,

given the lattice parameters, the atomic positions, and the local moments in a magnetic cell [59]. The required input is a .mcif or .cif file (with magnetic moments). The corresponding outputs are the details of the SSG, including L_0 , G_0 , i_t , i_k , G^s , type of the magnetic configuration, the international notation, standard magnetic cell, and all the symmetry operations written based on the lattice vectors of the standard magnetic cell. We provide in Appendix E the specific procedure for identifying the SSG. Furthermore, we also identify the SSGs for the 2001 experimentally reported magnetic structures provided in the MAGNDATA database on the Bilbao Crystallographic Server. The results are listed on FINDSPINGROUP [59].

We then perform density-functional-theory (DFT) calculations on several material candidates to exemplify their SSG symmetries, the electronic band degeneracies, spin textures, geometric Hall effects, and the distinctions from MSG (see Appendix F for DFT methods). Importantly, we show that the spin space part and real space part of an SSG directly lead to the features of spin polarization and the geometric Hall effect, respectively. Our representative examples include the candidate altermagnet RuO_2 (t -type SSG), spiral antiferromagnet CeAuAl_3 (k -type SSG) with coplanar configuration, and noncoplanar antiferromagnet CoNb_3S_6 (g -type SSG).

A. Extra band degeneracies in altermagnet RuO_2

RuO_2 is a candidate altermagnet with a spin-polarized Fermi surface and thus holds great potential to realize various spintronic effects, including spin-polarized current, giant magnetoresistance, and spin-splitting torque [35–43]. It has a rutile structure with an out-of-plane collinear antiferromagnetic order, with Ru and O ions occupying $2a$ and $4f$ Wyckoff positions, respectively [Fig. 4(a)]. The resulting nonmagnetic SG and MSG are $P4_2/mnm$ (No. 136) and $P4'_2/mnm'$ (136.499), respectively. To elucidate its SSG, we first determine its sublattice SG L_0 by considering the subgroup of SG that preserves the moment of Ru, i.e., $L_0 = Cmmm$ (No. 65). It is a t -type normal subgroup of $G_0 = P4_2/mnm$, with the subgroup indices $i_t = 2$, $i_k = 1$. The coset representative element, which is the symmetry connecting the sublattices with opposite magnetic moments, is a nonsymmorphic fourfold rotation $\{4_{001}^1 | 1/2 1/2 1/2\}$, and the coupled spin space PG is $G^s = \bar{1} = \{E, T\}$. Consequently, the nontrivial SSG has the form $G_{\text{NS}} = \{E \parallel L_0\} \cup \{\bar{1} \parallel 4_{001}^1 | 1/2 1/2 1/2\}L_0$ labeled as (65.136.1.1); the corresponding international notation is written as $P^{-1}4_2/1m^{-1}n^1m$. The full SSG G_{SS} taking into account the spin-only group is $P^{-1}4_2/1m^{-1}n^1m^{\infty}1$, which is a continuously infinite group.

Figure 4(c) shows the band structure of RuO_2 calculated by DFT (see Appendix F). It can be found that the bands along several high-symmetry lines, such as Γ - X - M , Γ - Z - R - A , have twofold band degeneracies, while

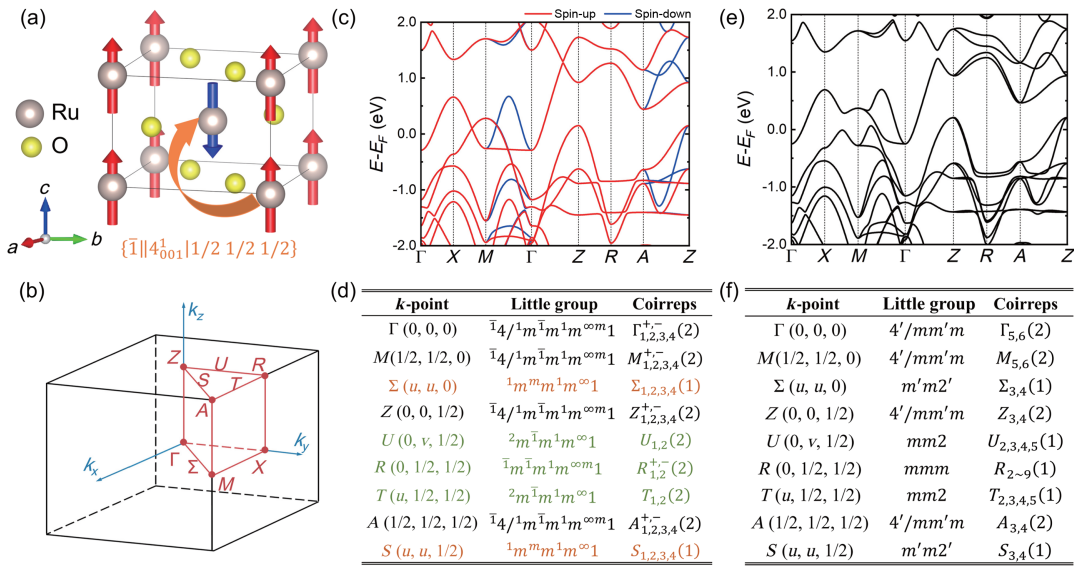


FIG. 4. Spin space group of altermagnet RuO_2 . (a) Crystal structure. The symmetry connecting different sublattices is indicated. The coordinate system xyz in spin space coincides with the coordinate system abc in real space. (b) Brillouin zone in momentum space. (c) SOC-free band structure with the projection of the spin components. (d) Little groups and the corresponding projective coirreps for different k -points within the regime of SSG. Brown fonts denote the k -points manifesting spin splitting; green fonts denote the k -points manifesting extra degeneracies compared with the band structure with SOC. (e) Same as (c) but with SOC. (f) Same as (d) but within the regime of MSG.

significant spin splitting occur along Γ - M and A - Z . The dimensions of the projective coirreps for these wave vectors are shown in Fig. 4(d), demonstrating that the rep theory successfully reproduces the calculated band degeneracies. In comparison, we also plot in Fig. 4(e) the band structure with the SOC, where the coirreps of MSG dictate the band degeneracy [Fig. 4(f)]. It is shown that the high-symmetric line Z - R - A manifests band splitting with the SOC, which is consistent with the MSG coirreps. While in MSG, the little groups of k along Z - R - A ($mm2$ or mmm) support only 1D coirreps, in SSG the little groups of these k -points have the operation $\{\bar{1}|m_{010}|1/2 1/2 1/2\}$, which can stick two conjugate 1D irreps of $\text{SO}(2)$ ($\Gamma_{+1/2}^S$ and $\Gamma_{-1/2}^S$) forming extra degeneracies. The details of the derivation of coirreps in SSG and the comparison of coirreps in SSG and MSG are provided in Supplemental Material, Sec. IV. Similar extra degeneracies protected by SSG have also been discussed in CoNb_3S_6 with collinear order [49,50], and Mn_3Sn with coplanar magnetic order [19]. On the other hand, in SSG, the little group $1m^m m^1 m^{\infty}$ at the Σ and S lines does not support 2D coirreps, thus leading to spin splitting even without SOC.

B. Spiral spin polarization in helimagnet CeAuAl_3

Spiral magnets, or helimagnets, present a type of magnetic ordering where the neighboring magnetic moments are arranged in a spiral pattern, with a characteristic turn angle between 0° and 180° . Such magnetic orders generally originated from the competition between ferromagnetic and antiferromagnetic exchange interactions.

Spiral magnets usually manifest combined spin rotation and fractional translation symmetry operations, which are not allowed within the MSG framework. However, for commensurate magnetic configurations, they serve as a nice platform to illustrate k -type and g -type SSGs. CeAuAl_3 has a tetragonal crystal structure with in-plane coplanar antiferromagnetic order [71], with a magnetic Ce ion occupying $4a$ Wyckoff positions [Fig. 5(a)]. The spin of the Ce layer rotates $\pi/2$ when moving to its neighboring Ce layer, resulting in a spiral configuration with a fourfold cell expansion. While its nonmagnetic SG is $I4mm$ (No. 107), the MSG is degraded to P_c4_1 (76.10), with only eight symmetry operations left.

Within the regime of SSG, its sublattice group is $L_0 = P4mm$ (No. 99), a k -type normal subgroup of $G_0 = I4mm$, with the subgroup indices $i_t = 1$, $i_k = 4$. The coset representative element connecting the neighboring sublattices (Ce layers) is a fractional translation $\{1|1/2 1/2 1/4\}$. Therefore, there are two possibilities of G^s being isomorphic to G_0/L_0 i.e., 4 and $\bar{4}$, resulting in two different nontrivial SSGs (99.107.4.1) and (99.107.4.2). CeAuAl_3 adopts the former one (99.107.4.1), which is constructed by mapping the element 4^1_{001} in spin space to $\{1|1/2 1/2 1/4\}$, i.e., $G_{NS} = L_0 \cup \{4^1_{001}|1|1/2 1/2 1/4\}L_0 \cup \{2_{001}|1|0 0 1/2\}L_0 \cup \{4^3_{001}|1|1/2 1/23/4\}L_0$. Specifically, it has a screw axis in spin space; i.e., $\{4^1_{001}|1|1/2 1/2 1/4\}$, serves as the generator of the spin translation group G_T^S isomorphic to 4 (a PG). Thus, the corresponding international notation is written as $P^14^1m^1m^4_{001}(1/2 1/2 1/4)$ (Appendix C).

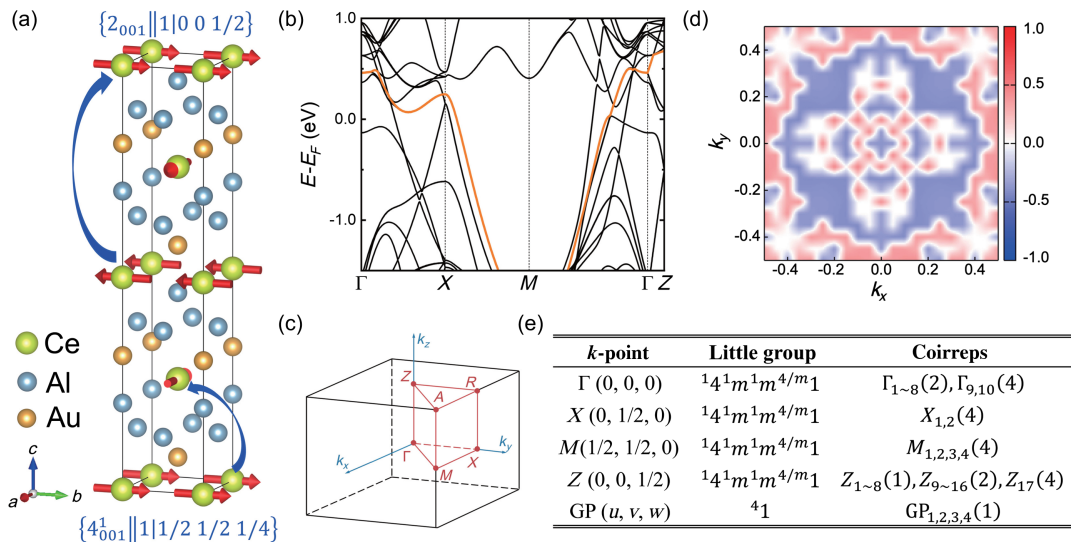


FIG. 5. Spin space group of spiral antiferromagnet CeAuAl_3 . (a) Crystal structure. The symmetry connecting different sublattices is indicated. The coordinate system xyz in spin space coincides with the coordinate system abc in real space. (b) SOC-free electronic band structure. (c) Brillouin zone in momentum space. (d) Spin polarization S_z at the $k_z = \pi/2$ plane for the band marked in panel (b). (e) Little groups and the corresponding projective coirreps for different k -points.

The full SSG is written as $G_{\text{SS}} = G_{\text{NS}} \times Z_2^K = P^1 4^1 m^1 m^{4^1_{001}} (1/2 1/2 1/4)^{m1}$, which has 64 symmetry operations. A similar procedure applies to (99.107.4.2) except that the coset representative of the nontrivial SSG is $\{\bar{4}^3_{001}\parallel 1|1/2 1/2 1/4\}$.

The DFT-calculated local moment for each Ce ion is $0.98\mu_B$, which is close to the experimental value ($1.05\mu_B$ [71]). Figure 5(b) exhibits the DFT-calculated band structure of CeAuAl_3 . We find that all the bands along the $X-M$ line are fourfold degenerate, and some of these bands split into two branches of doubly degenerate bands along the $\Gamma-X$ line. For the Γ and Z points, both Dirac and Weyl nodes exist. These node features are well explained by our CSCO projective rep theory, as comprehensively shown in Supplemental Material, Sec. V. As shown in Fig. 5(e), while the $X-M$ line supports only 4D coirreps, the Γ and Z points also allow 2D coirreps. Note that while the full SSG is isomorphic to the type-II MSG $I4mm1'$, the spin translation group generated by $\{4^1_{001}\parallel 1|1/2 1/2 1/4\}$ contributes to the factor system of projective reps, resulting in the emergence of 4D coirreps. In comparison, the type-II MSG $I4mm1'$ supports only 1D and 2D coirreps. Importantly, while it is believed that the existence of “ $U7$ ” symmetry (here it is $\{2_{001}\parallel 1|0 0 1/2\}$) protects spin degeneracy throughout the Brillouin zone [32,72], in noncollinear magnet CeAuAl_3 there is spin splitting along $\Gamma-Z$, indicating 1D coirreps for the corresponding little groups with $\{U_n(\pi)\parallel E|\tau\}$. Our results demonstrate that spin degeneracy enforced by $\{U_n(\pi)\parallel E|\tau\}$ symmetry is indeed present in collinear antiferromagnets, as $\{U_n(\pi)\parallel E|\tau\}$ sticks two conjugate 1D irreps of $\text{SO}(2)$.

More remarkably, such spiral magnets exhibit a new type of spiral spin polarization, for which the spin component

aligns the spiral axis, which is perpendicular to the direction of local moments. Figure 5(d) shows the spin texture of CeAuAl_3 at the $k_z = \pi/2$ plane for the band marked in Fig. 5(b). While all local moments are in plane, the S_x and S_y components of the extended Bloch states are enforced to be zero, leaving significant and continuous S_z distribution along the spiral direction (k_z). Such a spiral spin polarization is in sharp contrast to the conventional Rashba and Dresselhaus spin polarization (along the k -dependent effective magnetic field) in nonmagnetic materials and Zeeman spin polarization (along the direction of local moments) in ferromagnetic materials. To explain this, we note that the spin little group at an arbitrary k -point is 4, indicating that the spin texture has only an S_z component while the SSG-allowed operation 14 ensures fourfold symmetric pattern, consistent with our calculation shown in Fig. 5(d). Therefore, while such a spin polarization can survive with moderate SOC, its physical mechanism is apparently beyond the scenario of MSG.

C. Geometric Hall effect in nonplanar CoNb_3S_6

CoNb_3S_6 has attracted great interest due to its surprisingly large anomalous Hall effect and controversial magnetic configurations [50,73–77]. While its magnetic order was historically determined as a collinear antiferromagnet by neutron-diffraction measurements [78], a recent study reported an all-in-all-out noncoplanar antiferromagnetic order and accompanied topological Hall effect [77]. Here, we discuss the SSG symmetry of CoNb_3S_6 with the all-in-all-out antiferromagnetic order and conclude that such a noncoplanar order generates an anomalous Hall effect even without the assistance of SOC. As shown in Fig. 6(a), CoNb_3S_6 has a hexagonal crystal structure (nonmagnetic

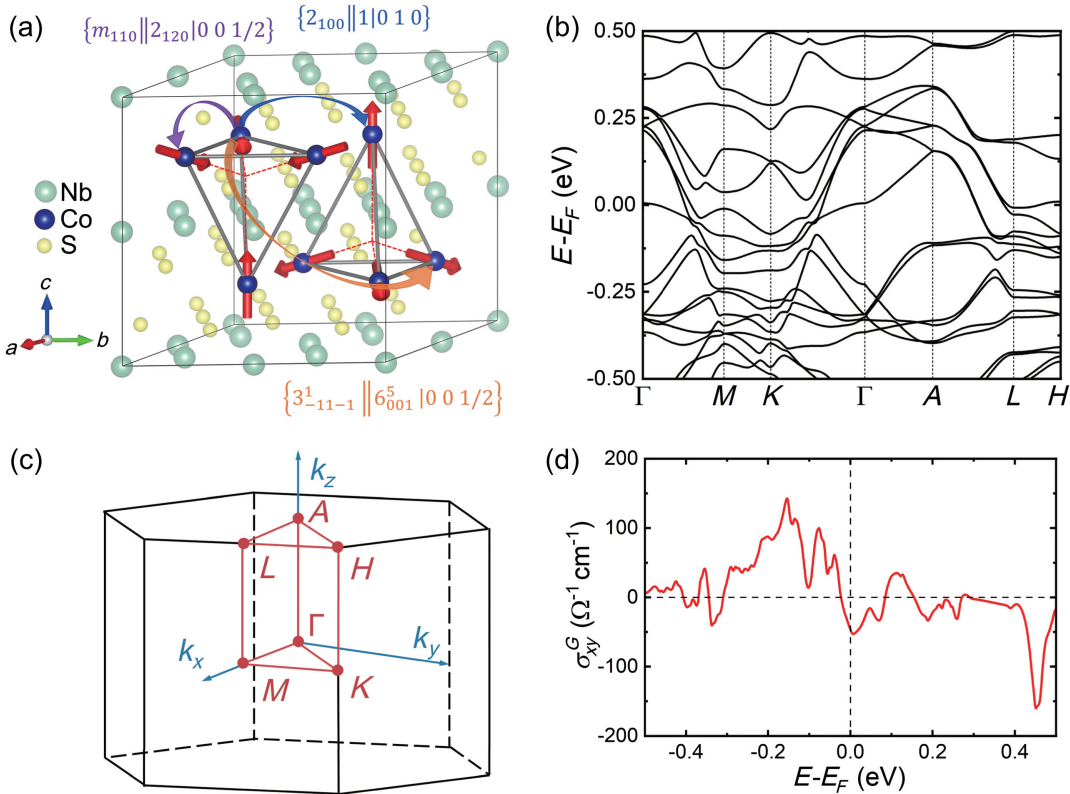


FIG. 6. Spin space group of noncoplanar antiferromagnet CoNb_3S_6 . (a) Crystal structure. The symmetry connecting different sublattices is indicated. The cubic structure in spin space is illustrated by the two tetrahedrons. The relationship between the xyz coordinate system in spin space and the abc coordinate system in real space can be expressed as follows: $a = -x - y$, $b = y + z$, and $c = -x + y - z$. (b) Electronic band structure. (c) Brillouin zone in momentum space. (d) Geometric Hall conductivity as a function of energy. SOC is excluded in the calculations.

SG is No. 182, $P6_322$) with magnetic Co ion occupying $2d$ Wyckoff positions. Interestingly, its all-in-all-out antiferromagnetic order forms a cubic structure in spin space, i.e., $G^s = \bar{4}3m$. However, the corresponding MSG is $P32'$ with only six symmetry elements because within the MSG framework, the spin rotation must compromise the spatial rotation, implying that the cubic nature of spin symmetry is lost.

With $G_0 = P6_322$, the sublattice group $L_0 = P2_1$ (No. 4) forms a g -type normal subgroup with the subgroup indices $i_t = 6$ and $i_k = 2 \times 2 \times 1 = 4$, the latter of which corresponds to twofold cell expansions along the x and y directions, i.e., $\{1|1\ 0\ 0\}$ and $\{1|0\ 1\ 0\}$. In addition, the threefold rotation $\{3_{001}^1|0\}$ and twofold rotation $\{2_{110}|0\}$ also belong to G_0/L_0 . Overall, there are two possibilities of 24-element G^s being isomorphic to G_0/L_0 , i.e., 432 and $\bar{4}3m$, with each corresponding to one inequivalent mapping. Therefore, there are two nontrivial SSGs in total labeled by (4.182.4.1) and (4.182.4.2), respectively. In the case of CoNb_3S_6 , real-space $\{2_{100}|0\}$ operation couples spin space m_{110} operation, rendering $G^s = \bar{4}3m$ and thus a nontrivial SSG (4.182.4.2). It can be generated using $\{3_{-11-1}^2||6_{001}^1|0\ 0\ 1/2\}$, $\{m_{110}|2_{100}|0\}$,

$\{m_{011}|2_{210}|0\ 0\ 1/2\}$, and generators of spin translation group G_T^S , i.e., $\{2_{001}|1|1\ 0\ 0\}$ and $\{2_{100}|1|0\ 1\ 0\}$. We note that the PG part of G_T^S forms a D_2 group in spin space. Therefore, the corresponding international notation is written as $P_{-11-1}^3 6_3 m_{110} 2 m_{011} 2 |(2_{001}, 2_{100}, 1)$ (Appendix C). Since G_{SO} is the identity group, the full SSG has 48 symmetry operations. Interestingly, such SSGs contain real-space and spin space symmetries from totally incompatible crystal systems, a scenario that is impossible within the scope of MSG.

Figure 6(b) shows the band structure of CoNb_3S_6 calculated using DFT. Notably, while PT is absent, the bands exhibit double degeneracy throughout the Brillouin zone. Such a new form of spin degeneracy appears only in the framework of SSG, attributed to the double-valued 2D coirreps of the little cogroup D_2 in spin space (the elements in G_T^S leave k invariant) at any arbitrary k -point. Furthermore, the three perpendicular twofold spin rotation axes enforce any spin-polarization components to be zero. Therefore, the spin degeneracy or spin splitting induced by magnetic order in noncollinear magnetic structures extends beyond the scope of MSGs, as only $T\tau$ symmetry in the spin translation group can be maintained when considering

the MSGs. Consequently, we summarize the complete criteria of spin splitting for noncollinear antiferromagnetic orders, i.e., (i) the absence of PT , and (ii) the spin space PG of the spin translation group does not contain D_n . This further highlights the importance of the enumeration and representation theory of SSGs.

The noncoplanar magnetic order could lead to responses without the assistance of SOC. For example, the anomalous Hall effect has long been attributed as a consequence of SOC under time-reversal breaking [79]. On the other hand, the exchange field induced by noncoplanar order could also induce an anomalous Hall effect without SOC. Instead of the topological Hall effect, we use the terminology of geometric Hall effect to emphasize the sole origin of magnetic geometry. While the characteristic quantities of noncoplanar magnets, e.g., scalar spin chirality [80] or band-resolved Berry curvature [81], cannot fully describe the existence of the geometric Hall effect, we note that due to the absence of SOC, the geometric Hall conductivity tensor can be fully determined by SSG. For collinear and coplanar orders, the spin-only symmetry $TU_n(\pi)$ behaves similarly to T , which enforces the geometric Hall conductivity σ_{xy}^G to be zero when integrating the Berry curvature over the Brillouin zone. Therefore, the anomalous Hall effect in collinear or coplanar magnets (even for ferromagnets) must be an SOC effect. However, for noncoplanar CoNb_3S_6 , the PG symmetries of the real-space part of the SSG (62'2') leave the z component of the magnetization invariant. Thus, an orbital magnetization along the z direction is allowed, leading to nonzero σ_{xy}^G . As shown in Fig. 6(d), our DFT calculation obtains nonzero geometric Hall conductivity throughout the energy window, consistent with our symmetry analysis. Remarkably, σ_{xy}^G reaches $47 \Omega^{-1} \text{cm}^{-1}$ at the Fermi level, which is comparable to the largest anomalous Hall conductivities in antiferromagnets with the assistance of SOC [82].

V. SUMMARY

To conclude, we present a systematic study of the enumeration and the representation theory of SSG applied to describe different magnetic configurations. By using a group extension approach, our enumeration constructs a collection of over 100 000 nontrivial SSGs named by a four-index nomenclature. The international notation system for SSGs is also developed. Furthermore, we derive the irreducible projective corepresentations of the little groups of the wave vectors within the SSG framework, which is the foundation for understanding the symmetry-enforced degeneracies in band spectra. To facilitate the search for SSG symmetries, we develop an online program FINDSPINGROUP [59] that can identify the SSG symmetries of any given magnetic crystal. The SSG identification for the 2001 experimentally reported magnetic structures provided in the MAGNDATA database is also

provided. We then show representative material examples, including altermagnet RuO_2 , helimagnets CeAuAl_3 , and noncoplanar antiferromagnet CoNb_3S_6 to illustrate their SSG symmetries and the emergent properties beyond the MSG framework. Our work further develops the group theory in describing materials with magnetic order, thereby unlocking possibilities for future exploration into exotic phenomena within magnetic materials. A recent example is the comprehensive diagnosis of quantum geometry nonlinear transports induced by magnetic geometry [83].

LIST OF SYMBOLS AND ABBREVIATIONS

PG,	point group
SG,	space group
MPG,	magnetic point group
MSG,	magnetic space group
SPG,	spin point group
SSG,	spin space group
SOC,	spin-orbit coupling
rep,	representation
irrep,	irreducible representation
corep,	corepresentation
coirrep,	irreducible corepresentation
HM,	Hermann-Mauguin Notation, international notation
CSCO,	complete set of commuting operators
DFT,	density-functional theory
G_0 ,	supergroup of L_0
L_0 ,	normal subgroup of G_0
g_s ,	operations in spin space
g_l ,	operations in real space
R ,	PG part of g_l
τ ,	fractional translation part of g_l
\mathbb{T} ,	translation group
P ,	space inversion
T ,	time reversal
$U_\alpha(\theta)$,	spin rotation of θ degree along the α axis
$C_\beta(\theta)$,	spatial rotation of θ degree along the β axis
$T(G)$,	translation subgroup of SG G
$P(G)$,	quotient group of G with respect to the $T(G)$
t ,	integral translation operation in translation group \mathbb{T} or $T(G)$
$ G $,	order of group G
i_t ,	PG index of $ P(G_0) / P(L_0) $
i_k ,	supercell index of $ T(G_0) / T(L_0) $
G^s ,	mapped PG in spin space
G_{SG} ,	SG
G_{MS}	MSG

G_{SS} ,	SSG
G_{SO} ,	spin-only group
G_{NS} ,	nontrivial SSG
L ,	maximal unitary subgroup of G
G^k ,	little group of G at the k -point
\tilde{G}^k ,	the quotient group of G^k with respect to translation group \mathbb{T}
\check{G}^k ,	little cogroup of G at the k -point
$\check{G}^{k,*}$,	central extension group of \check{G}^k
Z_g ,	cyclic group of integers
\tilde{G}^k ,	intrinsic group of \tilde{G}^k
M_k ,	projective irrep of the little group G^k
d_k ,	irrep of \tilde{G}^k
D_k ,	rep matrix of corep
G_R ,	SG of input structure without magnetic configurations
G_S ,	the quotient group of the PG of magnetic moment vectors with respect to the spin-only group
$\left\{ g_{s_i}^{(a)} \ R_i \tau_i^{(a)} \right\}$,	SSG symmetry with i labels the PG part R_i in real space, and (a) labels the corresponding translations and spin operations
$\phi(g_{s_i}^{(a)})$,	rotation angle of $g_{s_i}^{(a)}$
$N_G(L)$,	normalizer of L with respect to G
$N_{A^+}(L)$,	chirality-preserving affine normalizer of L
G_T^S ,	spin translation group
G^q ,	site-symmetry group at the q -point
M_T ,	transformation matrix

Note added. Recently, we became aware of related studies of the classification of spin space groups from Fang and co-workers [84] and Song and co-workers [85]. In addition, we also noticed recent studies of symmetry analysis and search of spin space groups [86,87], as well as the representations of spin point groups [88].

TABLE IV. Six types of operations in SGs, MSGs, and SSGs. For pure spin PG symmetry and spin nonsymmorphic symmetry in MSGs, g_s can be only time-reversal T ; for general symmorphic symmetry and general nonsymmorphic symmetry in MSGs, g_s can be only proper or improper spin rotations $U_n(\theta)$ or $TU_n(\theta)$ compatible with the spatial rotation $C_n(\theta)$.

	Notation	Spin PG	Spatial PG	Fractional translation
Spatial symmorphic symmetry	$\{C_n(\theta), IC_n(\theta) 0\}$		✓	
Spatial nonsymmorphic symmetry	$\{C_n(\theta), IC_n(\theta) \tau\}$		✓	✓
Pure spin symmetry	$\{g_s \ E 0\}$	✓		
Spin nonsymmorphic symmetry	$\{g_s \ E \tau\}$	✓		✓
General symmorphic symmetry	$\{g_s \ C_n(\theta), IC_n(\theta) 0\}$	✓	✓	
General nonsymmorphic symmetry	$\{g_s \ C_n(\theta), IC_n(\theta) \tau\}$	✓	✓	✓

ACKNOWLEDGMENTS

We thank Chen Fang and Zhi-Da Song for helpful discussions. This work was supported by National Key R&D Program of China under Grant No. 2020YFA0308900, the National Natural Science Foundation of China under Grant No. 12274194, Guangdong Provincial Key Laboratory for Computational Science and Material Design under Grant No. 2019B030301001, Shenzhen Science and Technology Program under Grant Nos. RCJC20221008092722009 and 20231117091158001, the Science, Technology and Innovation Commission of Shenzhen Municipality (Grant No. ZDSYS20190902092905285), Special Funds for the Cultivation of Guangdong College Students' Scientific and Technological Innovation (Grant No. pdjh2024c10202), China Postdoctoral Science Foundation under Grant No. 2023M741544, and the Center for Computational Science and Engineering of Southern University of Science and Technology.

APPENDIX A: SGs, MSGs, SSGs, AND THEIR REPRESENTATIONS

1. Types of symmetry operations

We first discuss SGs, MSGs, and SSGs in terms of their symmetry operations, as summarized in Table IV. SGs describe the geometry of a nonmagnetic material, or the Hamiltonian that does not contain the spin operator (nonmagnetic materials without SOC). Therefore, their symmetry operations include spatial symmorphic symmetry (pure spatial PG symmetry) $\{C_n(\theta), IC_n(\theta)|0\}$ and spatial nonsymmorphic symmetry $\{C_n(\theta), IC_n(\theta)|\tau\}$, as shown in the first two rows of Table IV.

On the other hand, while MSGs and SSGs contain all the operations listed in Table IV, the specific manifestations of each row for the two types of groups are quite different. If no additional symmetry operations are introduced compared to ordinary SGs, the MSGs are often regarded as type-I MSGs (colorless group). If an MSG contains pure spin PG symmetry $\{g_s \| E | 0\}$ where no spatial rotations or fractional translations τ are involved, g_s can be only time-reversal T ,

corresponding to a type-II MSG (gray group). If an MSG contains general symmetry $\{g_s||C_n(\theta), IC_n(\theta)|\tau\}$, g_s can be only proper or improper spin rotations $U_n(\theta)$ or $TU_n(\theta)$ compatible with the spatial rotation $C_n(\theta)$ corresponding to a type-III MSG (colored point group). If an MSG contains spin nonsymmorphic symmetry $\{g_s||E|\tau\}$ where a spin operation is combined with a fractional translation τ , again, g_s can be only time-reversal T corresponding to a type-IV MSG (colored lattice). In comparison, SSGs allow separated spatial and spin rotations, leading to much more symmetry operations that are not allowed by MSGs. Specifically, pure spin PG symmetries in SSGs form the spin-only group G_{SO}^p , including $G_{SO}^p = \{E, TU_n(\pi)\} = Z_2^K$ for coplanar configurations and $G_{SO}^l = Z_2^K \ltimes SO(2)$ for collinear configurations. In addition, spin nonsymmorphic symmetry widely exists in spiral magnetic configurations with a -type SSG. For example, the k -type SSG with $i_k = 4$ has spin nonsymmorphic symmetry $\{U_z(\pi/2)||E|\tau_{1/4}\}$.

For general symmetric symmetry and general nonsymmetric symmetry, MSG requires that g_s can be only proper or improper spin rotations $U_n(\theta)$ or $TU_n(\theta)$ compatible with the spatial rotation $C_n(\theta)$. In comparison, within the framework of SSG, g_s can be $U_m(\phi)$ or $TU_m(\phi)$ with the rotational angle and axis not necessarily compatible with those of the spatial rotation.

2. Construction of SSGs by finding inequivalent coset decompositions and inequivalent mappings

This part is devoted to explaining the mathematical procedure of finding inequivalent coset decompositions and inequivalent mappings between the quotient group G_0/L_0 and the spin space PG G^s , which is an essential step to eliminate equivalent SSGs in the enumeration process. Before getting into the details of the mathematical procedure, we first introduce some necessary concepts.

Chirality-preserving operations are symmetry operations that preserve the chirality of the object. Specifically, in 3D Euclidean space \mathbb{R}^3 , the orthogonal linear transformations form a 3D orthogonal group $O(3) = SO(3) \cup PSO(3)$, where P represents space inversion. Elements of $SO(3)$ are regarded as chirality-preserving operations because their transformation matrices have a determinant of 1. Therefore, the chirality-preserving Euclidean mappings in \mathbb{R}^3 include all translations, proper rotations, and screw rotations, yet excluding reflections, inversions, rotoinversions, and glide reflections.

Affine transformation, or affine mapping, is a linear mapping method that preserves points, straight lines, and planes. After an affine transformation, although the Euclidean lengths and angles may change, sets of parallel lines remain parallel.

Normalizer. For a group G and its subgroup L , the normalizer of L with respect to G denotes the set of elements $g \in G$ that leave the subgroup L unchanged by conjugation:

$$N_G(L) = \{g|g^{-1}Lg = L, g \in G\}. \quad (\text{A1})$$

Let us review the establishment of SG briefly. In the enumeration of SG, the group G_0 and G'_0 belong to the same affine space-group type if an affine transformation $a \in T(\mathbb{R}^3) \rtimes GL(3, R)$ exists, for which

$$G'_0 = a^{-1}G_0a \quad (\text{A2})$$

holds. Here, $T(\mathbb{R}^3)$ contains all translations in \mathbb{R}^3 , and $GL(3, R)$ denotes the 3D general linear group whose entries of matrices are real numbers. However, there are only 219 affine space-group types in total as the rotation part of an affine transformation a may have a negative determinant. In other words, it means that a does not preserve the chirality of G_0 . Only when the affine transformation a is required to be chirality preserving during the mapping process, can we distinguish 11 pairs of enantiomorph SGs (left-handed versus right-handed structures), as shown in Table V, and $230 = 219 + 11$ crystallographic SG types are obtained [65].

To construct an SSG, the first step is to decompose an SG G_0 into its subgroups L_0 ,

$$G_0 = L_0 \cup g_1L_0 \cup \dots \cup g_{n-1}L_0. \quad (\text{A3})$$

For two pairs (G_0, L_0) and (G'_0, L'_0) , it is obvious that if G_0 and G'_0 belong to different SGs, as well as L_0 and L'_0 , the coset decompositions and thus the resulting SSGs are different. On the other hand, even if both (G_0, L_0) and (G'_0, L'_0) cannot be distinguished just by their SGs, the coset decompositions of the two pairs may still be different. To provide a differentiation, one can first transform L_0 and L'_0 to the default setting of SGs so that they are identical ($L_0 = L'_0$). Then the chirality-preserving affine normalizer of L_0 , $N_{A^+}(L_0)$ and acted to G_0 to judge the equivalency of the two pairs following the process described below.

Overall, the chirality-preserving affine normalizer $N_{A^+}(L_0)$ was employed to find all inequivalent coset decompositions [65]. All affine mappings in \mathbb{R}^3 that

TABLE V. Eleven pairs of enantiomorph SGs.

$P4_1$ (No.76)	$P4_3$ (No.78)
$P4_122$ (No.91)	$P4_322$ (No.95)
$P4_12_2$ (No.92)	$P4_32_2$ (No.96)
$P3_1$ (No.144)	$P3_2$ (No.145)
$P3_12$ (No.151)	$P3_212$ (No.153)
$P3_121$ (No.152)	$P3_221$ (No.154)
$P6_1$ (No.169)	$P6_5$ (No.170)
$P6_2$ (No.171)	$P6_4$ (No.172)
$P6_122$ (No.178)	$P6_522$ (No.179)
$P6_222$ (No.180)	$P6_422$ (No.181)
$P4_132$ (No.213)	$P4_332$ (No.212)

map L_0 onto itself by conjugation and preserve its chirality form the chirality-preserving affine normalizer of L_0 :

$$N_{A^+}(L_0) = \{a | a^{-1}L_0a = L_0, a \in T(\mathbb{R}^3) \rtimes \text{SL}(3, \mathbb{Z})\} \quad (\text{A4})$$

Here, $\text{SL}(3, \mathbb{Z})$ denotes the 3D linear group whose entries of matrices are integers and the determinant is of 1. Thus, two pairs (G_0, L_0) and (G'_0, L_0) are equivalent if their supergroups are conjugated under $a \in N_{A^+}(L_0)$:

$$a^{-1}G'_0a = G_0, \quad \exists a \in N_{A^+}(L_0). \quad (\text{A5})$$

The conclusion can be directly extended when considering the inclusion of a spin part, i.e., nontrivial SSGs. Two nontrivial SSGs G'_{NS} and G_{NS} with equivalent (G_0, L_0) pairs are equivalent if they can be mapped onto each other by

$$\begin{aligned} a^{-1}G'_{\text{NS}}a &= G_{\text{NS}}, \\ \exists a &\in [N_{A^+}(L_0) \cap N_{A^+}(G_0)] \times N_{O(3)}(G^s), \end{aligned} \quad (\text{A6})$$

where $N_{A^+}(G_0)$ is the chirality-preserving affine normalizer of G_0 , and $N_{O(3)}(G^s)$ is the normalizer of G^s in orthogonal group $O(3)$.

The abovementioned mathematical procedure of identifying all inequivalent coset decompositions and inequivalent mappings for constructing SSGs using Eqs. (A4)–(A6) is performed by MAGMA, which is a large, well-supported software package designed for computations in abstract mathematical objects. It basically provides nearly all the significant algorithms for finite groups and finitely presented infinite groups.

3. Little group and little cogroup

The translation generators of an SG G determine its Bravais lattice and also its Brillouin zone (BZ). Points in the BZ are denoted by k in momentum space. The action of $g = \{R|\tau\} \in G$ on k is $gk = Rk$, where translation τ leaves k invariant. All elements in an SG G that keep a reciprocal vector k invariant form a group named the little group of k . Since we focus on the properties of Bloch states under band theory, where Bloch states are labeled by reciprocal vectors k , the little group of k is of great importance. The PG part of a little group is called a little cogroup. Such a concept is introduced because the theory of projective rep maps the derivation of the irreps of a little group to the derivation of projective irreps of the corresponding little cogroup, in which lattice translation is neglected, and the fractional translation is included in factor systems (the details will be discussed later).

4. Representation, irreducible representation, and regular representation

A representation of group G is formally defined as a homomorphism from G to the group form by general linear

transformations on a vector space V , i.e., the general linear group $\text{GL}(V)$. The matrix forms of those linear transformations are called representation matrices. In quantum physics, group rep is considered with a certain group of quantum states as a basis. Under this situation, a group rep can be simply understood as the matrix form of all symmetry operators. This method allows us to describe the symmetry of quantum systems with easily manipulated linear algebra. Generally, by basis transformation, a vector space can be separated into subspaces such that all vectors of one subspace are transformed only into each other. This allows us to block diagonalize the full rep matrices of all group elements simultaneously and view the full rep as the direct sum of reps on every subspace. Those reps which have rep matrices that cannot be block diagonalized by any basis transformation are called irreducible representations. In quantum physics, irreps describe the degeneracy of quantum states and encode basic symmetry information of quantum states, e.g., parity, angular momentum numbers, etc.

A regular representation is defined as the rep formed by using the group space as the rep space, where the group elements function as both the operators and as the basis for the space. It is a particularly interesting set of matrices that forms a reducible rep of the group G , which can be block diagonalized to give all irreps of the group. The matrices of the regular rep are constructed with the following relation:

$$D_{jk}^{\text{reg}}(R_i) = \begin{cases} 1 & \text{if } R_i R_k = R_j, \\ 0 & \text{otherwise.} \end{cases} \quad (\text{A7})$$

The multiplicity a_j of each irrep in the regular rep can be calculated to be equal to its dimension l_j :

$$a_j = \frac{1}{g} \sum_{R \in G} \chi_j(R)^* \chi^{\text{reg}}(R) = \chi_j(E)^* = l_j. \quad (\text{A8})$$

Namely,

$$X^{-1} D^{\text{reg}}(R) X = \bigoplus_j l_j D_j(R), \quad \chi(R) = \sum_j l_j \chi_j^{\text{reg}}(R), \quad (\text{A9})$$

where $\chi_j(R)$, $D_j(R)$ represent the character and the rep matrix for the irrep j of the group G , respectively, while $\chi^{\text{reg}}(R)$, $D^{\text{reg}}(R)$ represent the character and the rep matrix for the reducible rep of the regular rep, respectively. E , g , and X stand for the identity, the order of the group G , and the similarity transformation, respectively.

In summary, the regular rep contains each irrep a number of times equal to the dimensionality of the rep; i.e., the n -dimensional irreps appear n times in regular reps.

5. Projective representation in ordinary SGs

In SGs, the fractional translations usually bring complexities to the reps, leading to extra degeneracies that could

corresponds to emergent Dirac semimetal, hourglass semi-metal, symmetry enhanced spin-polarization, etc. The reps of any little group of k can be obtained by the projective reps of the corresponding little cogroup. To elaborate on this, we first consider a little group G^k with the coset form with respect to translation group \mathbb{T} to be

$$G^k = \{R_1|\tau_1\}\mathbb{T} \cup \{R_2|\tau_2\}\mathbb{T} \cup \dots \cup \{R_n|\tau_n\}\mathbb{T}. \quad (\text{A10})$$

The rep of \mathbb{T} with a basis of Bloch functions at momentum k is already known with the form $\exp(-ik\tau)$. Thus, to get a full list of irreps of G^k , all we need to do is to derive the irreps of the coset representatives $\tilde{G}^k = G^k/\mathbb{T} = (\{R_1|\tau_1\}, \{R_2|\tau_2\}, \dots, \{R_n|\tau_n\})$. One can naively think the rep of the coset representatives as the rep of the corresponding little cogroup $\check{G}^k = (R_1, R_2, \dots, R_n)$. However, they are not always the same because of the possible nonsymmorphic translation τ_i ; i.e., if we assume $R_i R_j = R_k$, the product of $\{R_i|\tau_i\}$ and $\{R_j|\tau_j\}$ may not be $\{R_k|\tau_k\}$, but follow the relation

$$\{R_i|\tau_i\}\{R_j|\tau_j\} = \{R_i R_j|\tau_i + R_i \tau_j\} = \{E|\tau_{ij}\}\{R_k|\tau_k\}, \quad (\text{A11})$$

where $\tau_{ij} = \tau_i + R_i \tau_j - \tau_k$. Therefore, the nonsymmorphic translation τ_i and τ_j could result in a lattice translation $\{E|\tau_{ij}\}$ beyond the $\{R_k|\tau_k\}$. Thus, the product relation of a rep d_k at the k -point should obey the following:

$$\begin{aligned} d_k(\{R_i|\tau_i\})d_k(\{R_j|\tau_j\}) &= d_k(\{E|\tau_{ij}\})d_k(\{R_k|\tau_k\}) \\ &= \exp(-ik\tau_{ij})d_k(\{R_k|\tau_k\}), \end{aligned} \quad (\text{A12})$$

which exhibit an additional phase factor $\exp(-ik\tau_{ij})$.

Strictly speaking, the group of rep matrices could be much larger than the group of coset representatives \tilde{G}^k , or the little cogroup \check{G}^k . These rep matrices should include all reps of $\{R_i R_j|\tau_i + R_i \tau_j\}$ in addition to those of $\{R_i|\tau_i\}$. In other words, the group of rep matrices could cover little cogroup \check{G}^k multiple times because one R_k could combine with different translations. To simplify the problem, we can use the theory of projective rep to “mod” the influence of nonsymmorphic translations and get all irreps of G^k by deriving the corresponding irreducible projective reps.

Projective representation is formally defined as follows: For a group H consisting of elements h_i , where i ranges from 1 to $|H|$, a nonsingular matrix function Δ on group H is a projective representation of H if it satisfies the following rule: For each group product $h_i h_j = h_k$, there exists a scalar function $\mu(h_i, h_j)$ on the group elements h_i, h_j , obeying that

$$\Delta(h_i)\Delta(h_j) = \mu(h_i, h_j)\Delta(h_k). \quad (\text{A13})$$

The function $\mu(h_i, h_j)$ is called a factor system for the projective rep Δ .

In the problem of multiple reps of $\{R_i R_j|\tau_i + R_i \tau_j\}$ discussed above, we can see that the product of rep d_k does not follow the rule of Eq. (A13) because $\tau_{ij} = \tau_i + R_i \tau_j - \tau_k$ is dependent on τ_k . To solve this, we define the projective rep corresponding to d_k to be M_k :

$$d_k(\{R|\tau\}) = \exp(-ik\tau)M_k(\{R|\tau\}). \quad (\text{A14})$$

Under this definition, one can show that

$$M_k(\{R_i|\tau_i\})M_k(\{R_j|\tau_j\}) = \exp(-iK_i \cdot \tau_j)M_k(\{R_k|\tau_k\}), \quad (\text{A15})$$

where $K_i = R_i^{-1}k - k$. The set of M_k together with a factor system $\mu(R_i, R_j) = \exp(-iK_i \tau_j)$ form a projective irrep of the little group G^k . The set M_k forms an irrep of the isomorphic PG, where the factor system $\mu(R_i, R_j) = \exp(-iK_i \tau_j)$ is completely dependent on $\{R_i|\tau_i\}$ and $\{R_j|\tau_j\}$. Consequently, to get all irreps d_k of \check{G}^k , one needs to derive all of the corresponding projective irreps M_k of \check{G}^k . In practice, M_k is obtained by the central extension method, which is introduced in the following.

6. Central extension

We now encounter two possibilities regarding the multiplier factor system. One case is the entire factor system $\mu(R_i, R_j) = 1$, and hence, the irreps of little group G^k and the little cogroup \check{G}^k coincide. If one of the following three conditions is reached, the factor system maps into unity: (1) G is a symmorphic SG; (2) G^k is a symmorphic group; (3) k lies inside the first Brillouin zone.

Another case is that the factor system $\mu(R_i, R_j)$ can take multiple values when G^k is a nonsymmorphic group and k lies on the Brillouin zone boundary. In such a situation, a typical treatment, called the central extension, to obtain the projective reps is to find the reps of a new abstract group $\check{G}_k^{*,*} = \check{G}^k \times Z_g$, where Z_g denotes the cyclic group of integers $(0, 1, \dots, g-1)$. Here, g comes from the factor system $\mu(R_i, R_j) = \exp[2\pi i a(R_i, R_j)/g]$ with the condition $0 \leq a(R_i, R_j) \leq g-1$. The multiplication table of the operations in \check{G}_k^* is determined by the following relationship:

$$(R_i, \alpha)(R_j, \beta) = [R_i R_j, a(R_i, R_j) + \alpha + \beta], \quad (\text{A16})$$

where (R_i, α) are group elements of the central extension of little cogroup $\check{G}_k^{*,*}$ and $\alpha \in \{0, 1, \dots, g-1\}$.

Following this approach, $\check{G}_k^{*,*}$ can be identified with one isomorphic abstract group and the irreps can be determined. Of all irreps, we focus only on the right irreps with $M_k(E, \alpha) = \exp(2\pi i \alpha/g)\mathbb{I}$, where \mathbb{I} is the identity matrix.

Following the above, we can construct the character table of the projective irreps of G^k . More details and specific examples can be found in Ref. [2].

7. Corepresentation

In magnetic materials, group description usually involves antiunitary operations that include time-reversal operator T . These operations contain a complex-conjugation operation that transforms any complex number into its complex conjugate. A well-known example of band degeneracy induced by antiunitary groups is the so-called Kramers degeneracy. However, a comprehensive understanding of the transformation of quantum states under antiunitary groups requires more than just knowledge of the Kramers degeneracy. To achieve this, we must first know the unitary rep matrices under antiunitary groups. Owing to the properties of antiunitary operations, the matrix representatives D do not obey the ordinary multiplication relations associated with unitary groups, but rather satisfy the following equations:

$$D(u_1)D(u_2)=D(u_1u_2), \quad D(u)D(a)=D(ua), \quad (\text{A17})$$

$$D(a)D^*(u)=D(au), \quad D(a_1)D^*(a_2)=D(a_1a_2), \quad (\text{A18})$$

where u, u_1, u_2 represent any unitary operation, a, a_1, a_2 represent any antiunitary operation of the same magnetic group, and D^* is the complex conjugate rep of D . This kind of rep is called a “corepresentation” by Wigner. The theory of corep is useful for analyzing extra degeneracies caused by antiunitary operations and the corresponding degenerate states.

8. Dimmock and Wheeler’s character sum rule

Following the above, the coirreps of MSGs are constructed. For any little group G_{MS}^k of an MSG G_{MS} : (1) If G_{MS}^k contains only unitary group elements, then the irreps of G_{MS}^k are given as those in SGs; (2) if G_{MS}^k contains antiunitary group elements, then G_{MS}^k can be written as $G_{\text{MS}}^k = L_{\text{MS}}^k \cup TAL_{\text{MS}}^k$, where L_{MS}^k is a unitary subgroup of index two in G_{MS}^k , and $TA \notin L_{\text{MS}}^k$ is an antiunitary group element of G_{MS}^k . Now we define the quotient group $\tilde{G}_{\text{MS}}^k = G_{\text{MS}}^k / \mathbb{T} = \tilde{L}_{\text{MS}}^k \cup TA\tilde{L}_{\text{MS}}^k$. Since the irreps of \tilde{L}_{MS}^k are already given in the SGs, we need only to classify the induced coirreps from the irreps of the maximal unitary subgroup \tilde{L}_{MS}^k using Dimmock and Wheeler’s sum rule as summarized in three cases.

- (a) The corep $D^{(i)}$ of \tilde{G}_{MS}^k corresponds to a single rep $d^{(i)}$ of \tilde{L}_{MS}^k and has the same dimension; in this case, no extra degeneracy is introduced.
- (b) The corep $D^{(i)}$ of \tilde{G}_{MS}^k corresponds to a single rep $d^{(i)}$ of \tilde{L}_{MS}^k but with the doubled dimension; in this case, the degeneracy is doubled.
- (c) The corep $D^{(i)}$ of \tilde{G}_{MS}^k corresponds to two inequivalent reps of \tilde{L}_{MS}^k , but these two can be stuck together under the antiunitary operators.

We summarize Dimmock and Wheeler’s sum rule as

$$\sum_{g \in T\tilde{A}\tilde{L}_{\text{MS}}^k} \chi(g^2) = \begin{cases} +|\tilde{L}_{\text{MS}}^k| & (\text{a}), \\ -|\tilde{L}_{\text{MS}}^k| & (\text{b}), \\ 0 & (\text{c}), \end{cases} \quad (\text{A19})$$

where χ is the character of d .

APPENDIX B: INTERNATIONAL NOTATION

In international notation, SGs are designated by a symbol $Bg_1g_2g_3$ that combines the SG symmetry with an uppercase letter describing the centering of the Bravais lattice. Specifically, B is denoted by P for primitive lattice, A, B, C for base-centered lattice, I for body-centered lattice, F for face-centered lattice, and R for rhombohedral lattice. The subsequent three symbols $g_1g_2g_3$ represent the representative symmetry operations when projected along one of the high-symmetry directions of the crystal. The high-symmetry directions of different crystal systems are shown in Table VI. Detailed Seitz symbols in real space and the extended one in spin space are given in Supplemental Materials, Secs. IA and IB. The complete list of SG $Bg_1g_2g_3$ with international notation and their corresponding Seitz symbols are also tabulated in Supplemental Materials, Tables S3–S9.

1. Viewing direction of SGs

For example, the four letters of $P3_212$ (153) represent a primitive lattice consisting of a threefold rotation along the [001] direction with a $2/3c$ translation, identity along the [100] direction, and a twofold rotation along the [210] direction.

2. International symbols of SGs

Here we list the international symbols and their corresponding symmetry operations used for SGs, such as

TABLE VI. The viewing direction of SGs in International notations.

Order	Triclinic	Monoclinic	Orthorhombic	Tetragonal	Trigonal	Hexagonal	Cubic
1		[010]	[100]	[001]	[001]	[001]	[100]
2			[010]	[100]	[100]	[100]	[111]
3			[001]	[110]	[210]	[210]	[110]

TABLE VII. Symbols of SG using international notation, including rotation axes, mirror planes, screw axes, and glide planes.

Name	Notation	Remark
Identity	1	
Inversion	-1	
Rotation	n	n -fold rotation
Rotation inversion	$-n$	n -fold rotation followed by an inversion
Mirror	m	Reflection in a plane
Mirror plane \perp to n -fold axes	n/m	
Screw	n_i	n -fold rotation followed by i/n fraction translation ($i = 1, 2, \dots, n-1$)
Glide mirror (combination of a mirror and a fraction translation)		
Axial glide	a	Translation of $a/2$
	b	Translation of $b/2$
	c	Translation of $c/2$
Diagonal glide	n	Translation of $(a+b)/2, (b+c)/2, (a+c)/2$
Diamond glide	d	Translation of $(a+b)/4, (b+c)/4, (a+c)/4$
Two \perp glides ^a	e	

^aSGs with two perpendicular glides are attributed to the centering type and the glide with perpendicular direction. For instance, the SG *Aem*2 (39) has a mirror parallel to a with a translation of $b/2$ and a centering fraction translation of $(b+c)/2$, resulting in the mirror parallel to a with a translation of $c/2$. As a consequence, *Aem*2 can be referred as *Abm*2 and *Acm*2 simultaneously. Therefore, the symbol “ e ” is employed for such planes. Similar situations can be found in *Aea*2 (41), *Cmce* (64), *Cmme* (67) and *Ccce* (68).

rotation, mirror, rotation inversion in the PG, as well as glide and screw in the SG.

APPENDIX C: THE NOMENCLATURE FOR t -TYPE, k -TYPE, AND g -TYPE SSGs

Below, we give the guidance for constructing nontrivial SSG G_{NS} using the nomenclature of t -type, k -type, and g -type SSGs.

1. t -type SSG

The t -type SSG $B^{g_{s_1}}g_1^{g_{s_2}}g_2^{g_{s_3}}g_3$ can be formed from $\{g_{s_1} \parallel g_1\}, \{g_{s_2} \parallel g_2\}, \{g_{s_3} \parallel g_3\}$.

a. 65.136.1.1

Following Table S6 [64], $P^{-1}4_2/1m^{-1}n^1m$ (65.136.1.1) can be generated using $\{-1\|4_0^1|1/2\ 1/2\ 1/2\}$, $\{1\|m_{001}|0\}$, $\{-1\|m_{100}|1/2\ 1/2\ 1/2\}$, and $\{1\|m_{110}|0\}$. All elements are listed below. Here, a , b , c and x , y , z coordination correspond to space coordination and the vector of magnetic moment, respectively, $\tau = (1/2\ 1/2\ 1/2)$.

As shown in Table VIII, we can conclude that the SSG with $G^s = -1$ supports only collinear magnetic structures,

TABLE VIII. General positions of $P^{-1}4_2/1m^{-1}n^1m$ (65.136.1.1).

Seitz	Coordination	Seitz	Coordination
$\{1\ 1 0\}$	$a, b, c,$ x, y, z	$\{-1\ 4_0^1 \tau\}$	$-b + 1/2, a + 1/2,$ $c + 1/2, -x, -y, -z$
$\{1\ 2_{001} 0\}$	$-a, -b, c,$ x, y, z	$\{-1\ 4_0^3 \tau\}$	$b + 1/2, -a + 1/2,$ $c + 1/2, -x, -y, -z$
$\{1\ 2_{110} 0\}$	$b, a, -c,$ x, y, z	$\{-1\ 2_{100} \tau\}$	$a + 1/2, -b + 1/2,$ $-c + 1/2, -x, -y,$ $-z$
$\{1\ 2_{1-10} 0\}$	$-b, -a, -c,$ x, y, z	$\{-1\ 2_{010} \tau\}$	$-a + 1/2, b + 1/2,$ $-c + 1/2, -x, -y,$ $-z$
$\{1\ -1 0\}$	$-a, -b, -c,$ x, y, z	$\{-1\ -4_0^1 \tau\}$	$b + 1/2, -a + 1/2,$ $-c + 1/2, -x, -y,$ $-z$
$\{1\ m_{001} 0\}$	$a, b, -c,$ x, y, z	$\{-1\ -4_0^3 \tau\}$	$-b + 1/2, a + 1/2,$ $-c + 1/2, -x, -y,$ $-z$
$\{1\ m_{110} 0\}$	$-b, -a, c,$ x, y, z	$\{-1\ m_{100} \tau\}$	$-a + 1/2, b + 1/2,$ $c + 1/2, -x, -y, -z$
$\{1\ m_{1-10} 0\}$	$b, a, c,$ x, y, z	$\{-1\ m_{010} \tau\}$	$a + 1/2, -b + 1/2,$ $c + 1/2, -x, -y, -z$

supposing that there is no inequivalent magnetic ion in the magnetic cell. Take the collinear antiferromagnet RuO₂ as an example, whose nontrivial SSG is $P^{-1}4_2/1m^{-1}n^1m$ (65.136.1.1). The spin-only part is $G_{\text{SO}}^l = Z_K^2 \ltimes \text{SO}(2)$, which is denoted as ${}^\infty m1$ in international notation. As a result, for collinear antiferromagnet RuO₂, its complete SSG is $P^{-1}4_2/1m^{-1}n^1m{}^\infty m1$.

b. 13.54.1.1–13.54.1.6

All general positions of 13.54.1.1–13.54.1.6 are also listed below in Tables IX–XIV. The international notations for 13.54.1.1–13.54.1.6 are $P^{-1}c^{-1}c^1a$, $P^{2_{001}}c^{2_{001}}c^1a$, $P^{m_{001}}c^{m_{001}}c^1a$, $P^{-1}c^1c^{-1}a$, $P^{2_{001}}c^1c^{2_{001}}$, and $P^{m_{001}}c^1c^{m_{001}}a$, respectively.

2. k -type SSG

In the BNS setting, MSGs are constructed from space group L_0 . This can be achieved by adding a “primed sublattice” generated by an operation that combines time inversion with a fractional translation to describe the “reversal” of spin between different nonmagnetic unit cells. The type-IV group is constructed by $M_{\text{IV}} = L_0 + T\tau L_0$, where τ is the mentioned translation. The k -type SSG can be seen as the multicolor extension of MSG. In this case, due to the decoupling of spin space and lattice space, a point group in spin space is used to describe the propagation vector in the enlarged magnetic unit cell. As a result, we use the nomenclature of $B^1g_1^1g_2^1g_3^{g_{s_1}}\tau_1^{g_{s_2}}\tau_2^{g_{s_3}}\tau_3$ for the k -type SSG under the L_0 basis. In this vein, the k -type SSG is directly constructed from the direct product of sublattice

TABLE IX. General positions of $P^{-1}c^{-1}c^1a$ (13.54.1.1).

Seitz	Coordination	Seitz	Coordination
$\{1 1 0\}$	a, b, c, x, y, z	$\{-1 2_{100} 1/2\ 0\ 1/2\}$	$a + 1/2, -b, -c + 1/2, -x, -y, -z$
$\{1 -1 0\}$	$-a, -b, -c, x, y, z$	$\{-1 m_{100} 1/2\ 0\ 1/2\}$	$-a + 1/2, b, c + 1/2, -x, -y, -z$
$\{1 2_{001} 1/2\ 0\ 0\}$	$-a + 1/2, -b, c, x, y, z$	$\{-1 2_{010} 0\ 0\ 1/2\}$	$-a, b, -c + 1/2, -x, -y, -z$
$\{1 m_{001} 1/2\ 0\ 0\}$	$a + 1/2, b, -c, x, y, z$	$\{-1 m_{010} 0\ 0\ 1/2\}$	$a, -b, c + 1/2, -x, -y, -z$

TABLE X. General positions of $P^{2_{001}}c^{2_{001}}c^1a$ (13.54.1.2).

Seitz	Coordination	Seitz	Coordination
$\{1 1 0\}$	a, b, c, x, y, z	$\{2_{001} 2_{100} 1/2\ 0\ 1/2\}$	$a + 1/2, -b, -c + 1/2, -x, -y, -z$
$\{1 -1 0\}$	$-a, -b, -c, x, y, z$	$\{2_{001} m_{100} 1/2\ 0\ 1/2\}$	$-a + 1/2, b, c + 1/2, -x, -y, z$
$\{1 2_{001} 1/2\ 0\ 0\}$	$-a + 1/2, -b, c, x, y, z$	$\{2_{001} 2_{010} 0\ 0\ 1/2\}$	$-a, b, -c + 1/2, -x, -y, z$
$\{1 m_{001} 1/2\ 0\ 0\}$	$a + 1/2, b, -c, x, y, z$	$\{2_{001} m_{010} 0\ 0\ 1/2\}$	$a, -b, c + 1/2, -x, -y, z$

TABLE XI. General positions of $P^{m_{001}}c^{m_{001}}c^1a$ (13.54.1.3).

Seitz	Coordination	Seitz	Coordination
$\{1 1 0\}$	a, b, c, x, y, z	$\{m_{001} 2_{100} 1/2\ 0\ 1/2\}$	$a + 1/2, -b, -c + 1/2, x, y, -z$
$\{1 -1 0\}$	$-a, -b, -c, x, y, z$	$\{m_{001} m_{100} 1/2\ 0\ 1/2\}$	$-a + 1/2, b, c + 1/2, x, y, -z$
$\{1 m_{001} 1/2\ 0\ 0\}$	$a + 1/2, b, -c, x, y, z$	$\{m_{001} m_{010} 0\ 0\ 1/2\}$	$a, -b, c + 1/2, x, y, -z$
$\{1 2_{001} 1/2\ 0\ 0\}$	$-a + 1/2, -b, c, x, y, z$	$\{m_{001} 2_{010} 0\ 0\ 1/2\}$	$-a, b, -c + 1/2, x, y, -z$

TABLE XII. General positions of $P^{-1}c^1c^{-1}a$ (13.54.1.4).

Seitz	Coordination	Seitz	Coordination
$\{1 1 0\}$	a, b, c, x, y, z	$\{-1 2_{100} 1/2\ 0\ 1/2\}$	$a + 1/2, -b, -c + 1/2, -x, -y, -z$
$\{1 -1 0\}$	$-a, -b, -c, x, y, z$	$\{-1 m_{100} 1/2\ 0\ 1/2\}$	$-a + 1/2, b, c + 1/2, -x, -y, -z$
$\{1 m_{010} 0\ 0\ 1/2\}$	$a, -b, c + 1/2, x, y, z$	$\{-1 m_{001} 1/2\ 0\ 0\}$	$a + 1/2, b, -c, -x, -y, -z$
$\{1 2_{010} 0\ 0\ 1/2\}$	$-a, b, -c + 1/2, x, y, z$	$\{-1 2_{001} 1/2\ 0\ 0\}$	$-a + 1/2, -b, c, -x, -y, -z$

TABLE XIII. General positions of $P^{2_{001}}c^1c^{2_{001}}a$ (13.54.1.5).

Seitz	Coordination	Seitz	Coordination
$\{1 1 0\}$	a, b, c, x, y, z	$\{2_{001} 2_{100} 1/2\ 0\ 1/2\}$	$a + 1/2, -b, -c + 1/2, -x, -y, -z$
$\{1 -1 0\}$	$-a, -b, -c, x, y, z$	$\{2_{001} m_{100} 1/2\ 0\ 1/2\}$	$-a + 1/2, b, c + 1/2, -x, -y, z$
$\{1 2_{010} 0\ 0\ 1/2\}$	$-a, b, -c + 1/2, x, y, z$	$\{2_{001} 2_{001} 1/2\ 0\ 0\}$	$-a + 1/2, -b, c, -x, -y, z$
$\{1 m_{010} 0\ 0\ 1/2\}$	$a, -b, c + 1/2, x, y, z$	$\{2_{001} m_{001} 1/2\ 0\ 0\}$	$a + 1/2, b, -c, -x, -y, z$

TABLE XIV. General positions of $P^{m_{001}}c^1c^{m_{001}}a$ (13.54.1.6).

Seitz	Coordination	Seitz	Coordination
$\{1 1 0\}$	a, b, c, x, y, z	$\{m_{001} 2_{100} 1/2\ 0\ 1/2\}$	$a + 1/2, -b, -c + 1/2, x, y, -z$
$\{1 -1 0\}$	$-a, -b, -c, x, y, z$	$\{m_{001} m_{100} 1/2\ 0\ 1/2\}$	$-a + 1/2, b, c + 1/2, x, y, -z$
$\{1 2_{010} 0\ 0\ 1/2\}$	$-a, b, -c + 1/2, x, y, z$	$\{m_{001} 2_{001} 1/2\ 0\ 0\}$	$-a + 1/2, -b, c, x, y, -z$
$\{1 m_{010} 0\ 0\ 1/2\}$	$a, -b, c + 1/2, x, y, z$	$\{m_{001} m_{001} 1/2\ 0\ 0\}$	$a + 1/2, b, -c, x, y, -z$

SG $\{E\|Bg_1g_2g_3\}$ and additional spin translation group G_T^S , where G_T^S can be generated by $\{g_{s_1}\|\tau_1\}$, $\{g_{s_2}\|\tau_2\}$, and $\{g_{s_3}\|\tau_3\}$. Note that the integer translation of L_0 is always $t_a = (1\ 0\ 0)$, $t_b = (0\ 1\ 0)$, $t_c = (0\ 0\ 1)$.

a. 99.107.4.1

$P^{14}1m^1m^{4^1_{001}}(1/2\ 1/2\ 1/4)$ (99.107.4.1) can be constructed using $\{E\|P4mm\}$ and $G_T^S = \{\{1\|1|0\}, \{4^1_{001}\|1\ 1/2\ 1/2\ 1/4\}, \{2_{001}\|1|0\ 0\ 1/2\}, \{4^3_{001}\|1|1/2\ 1/2\ 3/4\}\}$. All general positions are listed in Table XV.

Similarly, $P^{14}1m^1m^{-4^3_{001}}(1/2\ 1/2\ 1/4)$ (99.107.4.2) can be constructed by $G_T^S = \{\{1\|1|0\}, \{-4^3_{001}\|1|1/2\ 1/2\ 1/4\}, \{2_{001}\|1|0\ 0\ 1/2\}, \{-4^1_{001}\|1|1/2\ 1/2\ 3/4\}\}$, and $\{E\|P4mm\}$.

TABLE XV. General positions of $P^{14}1m^1m^{4^1_{001}}(1/2\ 1/2\ 1/4)$ (99.107.4.1).

Seitz	Coordination
$\{1\ 1 0\}$	a, b, c, x, y, z
$\{1\ 2_{001} 0\}$	$-a, -b, c, x, y, z$
$\{1\ 4^1_{001} 0\}$	$-b, a, c, x, y, z$
$\{1\ 4^3_{001} 0\}$	$b, -a, c, x, y, z$
$\{1\ m_{010} 0\}$	$a, -b, c, x, y, z$
$\{1\ m_{100} 0\}$	$-a, b, c, x, y, z$
$\{1\ m_{110} 0\}$	$-b, -a, c, x, y, z$
$\{1\ m_{1-10} 0\}$	b, a, c, x, y, z
$\{4^1_{001}\ 1 1/2\ 1/2\ 1/4\}$	$a + 1/2, b + 1/2, c + 1/4, -y, x, z$
$\{4^1_{001}\ 2_{001}\ 1/2\ 1/2\ 1/4\}$	$-a + 1/2, -b + 1/2, c + 1/4, -y, x, z$
$\{4^1_{001}\ 4^1_{001}\ 1/2\ 1/2\ 1/4\}$	$-b + 1/2, a + 1/2, c + 1/4, -y, x, z$
$\{4^1_{001}\ 4^3_{001}\ 1/2\ 1/2\ 1/4\}$	$b + 1/2, -a + 1/2, c + 1/4, -y, x, z$
$\{4^1_{001}\ m_{010}\ 1/2\ 1/2\ 1/4\}$	$a + 1/2, b + 1/2, c + 1/2, -y, x, z$
$\{4^1_{001}\ m_{100}\ 1/2\ 1/2\ 1/4\}$	$-a + 1/2, b + 1/2, c + 1/4, -y, x, z$
$\{4^1_{001}\ m_{110}\ 1/2\ 1/2\ 1/4\}$	$-b + 1/2, -a + 1/2, c + 1/4, -y, x, z$
$\{4^1_{001}\ m_{1-10}\ 1/2\ 1/2\ 1/4\}$	$b + 1/2, a + 1/2, c + 1/4, -y, x, z$
$\{2_{001}\ 1 0\ 0\ 1/2\}$	$a, b, c + 1/2, -x, -y, z$
$\{2_{001}\ 2_{001}\ 0\ 0\ 1/2\}$	$-a, -b, c + 1/2, -x, -y, z$
$\{2_{001}\ 4^1_{001}\ 0\ 0\ 1/2\}$	$-b, a, c + 1/2, -x, -y, z$
$\{2_{001}\ 4^3_{001}\ 0\ 0\ 1/2\}$	$b, -a, c + 1/2, -x, -y, z$
$\{2_{001}\ m_{010}\ 0\ 0\ 1/2\}$	$a, -b, c + 1/2, -x, -y, z$
$\{2_{001}\ m_{100}\ 0\ 0\ 1/2\}$	$-a, b, c + 1/2, -x, -y, z$
$\{2_{001}\ m_{110}\ 0\ 0\ 1/2\}$	$-b, -a, c + 1/2, -x, -y, z$
$\{2_{001}\ m_{1-10}\ 0\ 0\ 1/2\}$	$b, a, c + 1/2, -x, -y, z$
$\{4^3_{001}\ 1 1/2\ 1/2\ 1/4\}$	$a + 1/2, b + 1/2, c + 3/4, y, -x, z$
$\{4^3_{001}\ 2_{001}\ 1/2\ 1/2\ 1/4\}$	$-a + 1/2, -b + 1/2, c + 3/4, y, -x, z$
$\{4^3_{001}\ 4^1_{001}\ 1/2\ 1/2\ 1/4\}$	$-b + 1/2, a + 1/2, c + 3/4, y, -x, z$
$\{4^3_{001}\ 4^3_{001}\ 1/2\ 1/2\ 1/4\}$	$b + 1/2, -a + 1/2, c + 3/4, y, -x, z$
$\{4^3_{001}\ m_{010}\ 1/2\ 1/2\ 1/4\}$	$a + 1/2, b + 1/2, c + 3/4, y, -x, z$
$\{4^3_{001}\ m_{100}\ 1/2\ 1/2\ 1/4\}$	$-a + 1/2, b + 1/2, c + 3/4, y, -x, z$
$\{4^3_{001}\ m_{110}\ 1/2\ 1/2\ 1/4\}$	$-b + 1/2, -a + 1/2, c + 3/4, y, -x, z$
$\{4^3_{001}\ m_{1-10}\ 1/2\ 1/2\ 1/4\}$	$b + 1/2, a + 1/2, c + 3/4, y, -x, z$

b. 174.174.3.1

Now we show why we use the L_0 basis rather than the G_0 basis for the k -type SSG. The L_0 basis depicts the magnetic primitive cell, while the G_0 basis sometimes gives a larger primitive cell. Now we take $P^1 - 6^{3^1_{001}}(2/3\ 1/3\ 0)$ (174.174.3.1) as an example.

Under the L_0 basis, the sublattice SG is $L_0 = P - 6$, and the spin translation group is $G_T^S = \{\{1\|1|0\}, \{3^1_{001}\|1|2/3\ 1/3\ 0\}, \{3^2_{001}\|1|1/3\ 2/3\ 0\}\}$. All general positions are listed in Table XVI.

Using the transformation matrix

$$M_T = \begin{pmatrix} 1 & 1 & 0 & 0 \\ -1 & 2 & 0 & 0 \\ 0 & 0 & 1 & 0 \end{pmatrix},$$

which transforms from the L_0 basis to G_0 basis, the three spin translation operations are transformed into $\{1\|1|0\}$, $\{3^1_{001}\|1|1\ 0\ 0\}$, $\{3^2_{001}\|1|1\ 1\ 0\}$, and the full G_T^S is

$$G_T^S = \left\{ \begin{array}{l} \{1\|1|0\}, \{1\|1|1\ 2\ 0\}, \{1\|1|2\ 1\ 0\}, \\ \{3^1_{001}\|1|1\ 0\ 0\}, \{3^2_{001}\|1|1\ 1\ 0\}, \{3^1_{001}\|1|0\ 1\ 0\}, \\ \{3^2_{001}\|1|2\ 0\ 0\}, \{3^2_{001}\|1|0\ 2\ 0\}, \{3^1_{001}\|1|2\ 2\ 0\}. \end{array} \right\} \quad (C1)$$

It is clear that the magnetic cell under the G_0 basis is 3 times larger than the L_0 basis as shown in Fig. 7. In other words, the magnetic cell under the L_0 basis is also the minimum periodic unit cell, while the magnetic cell under the G_0 basis is sometimes larger than the previous one, depending on the transformation matrix.

3. g-type SSG

For the g -type SSG with $B^{g_{s_1}}g_1^{g_{s_2}}g_2^{g_{s_3}}g_3|(g_{s_4}, g_{s_5}, g_{s_6}; g_{s_7}, g_{s_8}, g_{s_9})$ in the G_0 basis, $g_{s_4}, g_{s_5}, g_{s_6}$ are combined with the three-integer translation t_a, t_b, t_c , while $g_{s_7}, g_{s_8}, g_{s_9}$ are combined with the centering-type fractional translation b_1, b_2, b_3 . The spin translation group can be constructed from $\{g_{s_4}\|t_a\}$, $\{g_{s_5}\|t_b\}$, $\{g_{s_5}\|t_c\}$, $\{g_{s_7}\|b_1\}$, $\{g_{s_8}\|b_2\}$, and $\{g_{s_9}\|b_3\}$. The sequence of b_1, b_2, b_3 for different Bravais lattices is given in Table XVII. When $B = P$ for a primitive lattice, $g_{s_7}, g_{s_8}, g_{s_9}$ are omitted. Below we show several examples of a g -type SSG.

a. 4.182.4.2

The first is $P^{3^2_{-11-1}}6_3^{m_{110}}2^{m_{011}2}|(2_{001}, 2_{100}, 1)$ (4.182.4.2) of CoNb_3S_6 . It can be generated using $\{3^2_{-11-1}\|6^1_{001}\|0\ 0\ 1/2\}$, $\{m_{110}\|2_{100}\|0\}$, $\{m_{011}\|2_{210}\|0\ 0\ 1/2\}$, and the spin translation group $G_T^S = \{\{1\|1|0\}, \{2_{001}\|1|1\ 0\ 0\}, \{2_{100}\|1|0\ 1\ 0\}, \{2_{010}\|1|1\ 1\ 0\}\}$. All general positions are listed in Table XVIII.

TABLE XVI. General positions of $P^1 - 6^{3_{001}}(2/3\ 1/3\ 0)$ (174.174.3.1).

Seitz	Coordination
$\{1 1 0\}$	a, b, c, x, y, z
$\{1 3_{001}^1 0\}$	$-b, a-b, c, x, y, z$
$\{1 3_{001}^2 0\}$	$-a+b, -a, c, x, y, z$
$\{1 m_{001} 0\}$	$a, b, -c, x, y, z$
$\{1 -6_{001}^5 0\}$	$-b, a-b, -c, x, y, z$
$\{1 -6_{001}^1 0\}$	$-a+b, -a, -c, x, y, z$
$\{3_{001}^1\ 1 2/3\ 1/3\ 0\}$	$a+2/3, b+1/3, c, -(x+\sqrt{3}y)/2, (\sqrt{3}x-y)/2, z$
$\{3_{001}^1\ 3_{001}^1 2/3\ 1/3\ 0\}$	$-b+2/3, a-b+1/3, c, -(x+\sqrt{3}y)/2, (\sqrt{3}x-y)/2, z$
$\{3_{001}^1\ 3_{001}^2 2/3\ 1/3\ 0\}$	$-a+b+2/3, -a+1/3, c, -(x+\sqrt{3}y)/2, (\sqrt{3}x-y)/2, z$
$\{3_{001}^1\ m_{001} 2/3\ 1/3\ 0\}$	$a+2/3, b+1/3, -c, -(x+\sqrt{3}y)/2, (\sqrt{3}x-y)/2, z$
$\{3_{001}^1\ -6_{001}^5 2/3\ 1/3\ 0\}$	$-b+2/3, a-b+1/3, -c, -(x+\sqrt{3}y)/2, (\sqrt{3}x-y)/2, z$
$\{3_{001}^1\ -6_{001}^1 2/3\ 1/3\ 0\}$	$-a+b+2/3, -a+1/3, -c, -(x+\sqrt{3}y)/2, (\sqrt{3}x-y)/2, z$
$\{3_{001}^2\ 1 1/3\ 2/3\ 0\}$	$a+1/3, b+2/3, c, (-x+\sqrt{3}y)/2, -(\sqrt{3}x+y)/2, z$
$\{3_{001}^2\ 3_{001}^1 1/3\ 2/3\ 0\}$	$-b+1/3, a-b+2/3, c, (-x+\sqrt{3}y)/2, -(\sqrt{3}x+y)/2, z$
$\{3_{001}^2\ 3_{001}^2 1/3\ 2/3\ 0\}$	$-a+b+1/3, -a+2/3, c, (-x+\sqrt{3}y)/2, -(\sqrt{3}x+y)/2, z$
$\{3_{001}^2\ m_{001} 1/3\ 2/3\ 0\}$	$a+1/3, b+2/3, -c, (-x+\sqrt{3}y)/2, -(\sqrt{3}x+y)/2, z$
$\{3_{001}^2\ -6_{001}^5 1/3\ 2/3\ 0\}$	$-b+1/3, a-b+2/3, -c, (-x+\sqrt{3}y)/2, -(\sqrt{3}x+y)/2, z$
$\{3_{001}^2\ -6_{001}^1 1/3\ 2/3\ 0\}$	$-a+b+1/3, -a+2/3, -c, (-x+\sqrt{3}y)/2, -(\sqrt{3}x+y)/2, z$

b. 3.22.8.1

In the G_0 basis, the Bravais-centering fractional translation $b_1 b_2 b_3$ can also combine with nontrivial spin operation. Below, we show how to construct the full SSG from the nomenclature of $F^{m_{010}} 2^{m_{010}} 2^{1/2} | (1, 1, 2_{001}; m_{001}, 4_{001}^1, -4_{001}^3) \quad (3.22.8.1)$.

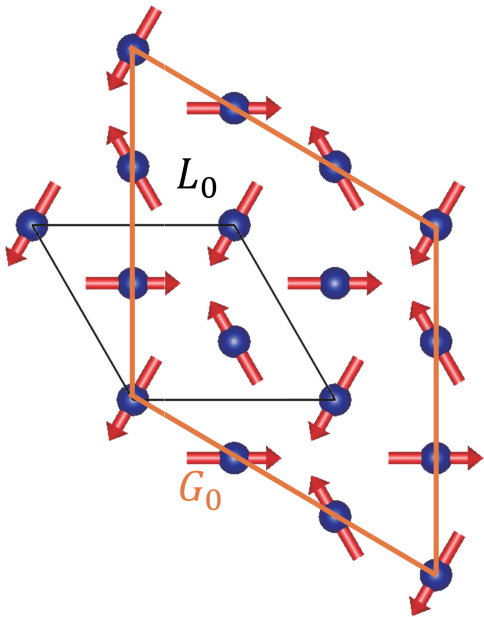


FIG. 7. Magnetic primitive cell of $P^1 - 6^{3_{001}}(2/3\ 1/3\ 0)$ (174.174.3.1) under L_0 basis (black line) and under G_0 basis (orange line).

The spin translation group G_T^S for 3.22.8.1 can be constructed from $\{2_{001}\|1|0\ 0\ 1\}$, $\{m_{001}\|1|1/2\ 1/2\ 0\}$, $\{4_{001}^1\|1|1/2\ 0\ 1/2\}$, $\{-4_{001}^3\|1|0\ 1/2\ 1/2\}$, and the full G_T^S is

$$G_T^S = \left\{ \begin{array}{l} \{1|1|0\}, \{-1|1|1/2\ 1/2\ 1\}, \\ \{-4_{001}^3\|1|0\ 1/2\ 1/2\}, \{-4_{001}^1\|1|0\ 1/2\ 3/2\}, \\ \{2_{001}\|1|0\ 0\ 1\}, \{m_{001}\|1|1/2\ 1/2\ 0\}, \\ \{4_{001}^1\|1|1/2\ 0\ 1/2\}, \{4_{001}^3\|1|1/2\ 0\ 3/2\}. \end{array} \right\} \quad (C2)$$

The integral translations along the three basis vectors of G_0 for 3.22.8.1 are $\{1|1|1\ 0\ 0\}$, $\{1|1|0\ 1\ 0\}$, and $\{1|1|0\ 0\ 2\}$, respectively. Then we add $\{m_{010}\|2_{100}|0\}$,

TABLE XVII. The centering-type fractional translation b_1, b_2, b_3 for SG in different Bravais lattices, which is used as a default sequence in g-type SSG.

Bravais lattice	b_1	b_2	b_3
P			
F	$\{1 1/2\ 1/2\ 0\}$	$\{1 1/2\ 0\ 1/2\}$	$\{1 0\ 1/2\ 1/2\}$
I	$\{1 1/2\ 1/2\ 1/2\}$		
A	$\{1 0\ 1/2\ 1/2\}$		
C	$\{1 1/2\ 1/2\ 0\}$		
R	$\{1 2/3\ 1/3\ 1/3\}$	$\{1 1/3\ 2/3\ 2/3\}$	

TABLE XVIII. General positions of $P^{3^2_{-11-1}6_3m_{110}2^{m_{011}2}}(2_{001}, 2_{100}, 1)$ (4.182.4.2).

Seitz	Coordination
$\{1\ 1 0\}$	a, b, c, x, y, z
$\{3^1_{-11-1}\ 3^1_{001} 0\}$	$-b, a - b, c, z, -x, -y$
$\{3^2_{-11-1}\ 3^2_{001} 0\}$	$-a + b, -a, c, -y, -z, x$
$\{1\ 2_{001} 0\ 0\ 1/2\}$	$-a, -b, c + 1/2, x, y, z$
$\{3^1_{-11-1}\ 6^5_{001} 0\ 0\ 1/2\}$	$b, -a + b, c + 1/2, z, -x, -y$
$\{3^2_{-11-1}\ 6^1_{001} 0\ 0\ 1/2\}$	$a - b, a, c + 1/2, -y, -z, x$
$\{m - 101\ 2_{110} 0\}$	$b, a, -c, z, y, x$
$\{m_{110}\ 2_{100} 0\}$	$a - b, -b, -c, -y, -x, z$
$\{m_{011}\ 2_{010} 0\}$	$-a, -a + b, -c, x, -z, -y$
$\{m_{-101}\ 2_{1-10} 0\ 0\ 1/2\}$	$-b, -a, -c + 1/2, z, y, x$
$\{m_{110}\ 2_{120} 0\ 0\ 1/2\}$	$-a + b, b, -c + 1/2, -y, -x, z$
$\{m_{011}\ 2_{210} 0\ 0\ 1/2\}$	$a, a - b, -c + 1/2, x, -z, -y$
$\{2_{001}\ 1 1\ 0\ 0\}$	$1 + a, b, c, -x, -y, z$
$\{3^1_{-1-11}\ 3^1_{001} 1\ 0\ 0\}$	$1 - b, a - b, c, -z, x, -y$
$\{3^2_{111}\ 3^2_{001} 1\ 0\ 0\}$	$1 - a + b, -a, c, y, z, x$
$\{2_{001}\ 2_{001} 1\ 0\ 1/2\}$	$1 - a, -b, c + 1/2, -x, -y, z$
$\{3^1_{-1-11}\ 6^5_{001} 1\ 0\ 1/2\}$	$1 + b, -a + b, c + 1/2, -z, x, -y$
$\{3^2_{111}\ 6^1_{001} 1\ 0\ 1/2\}$	$1 + a - b, a, c + 1/2, y, z, x$
$\{-4^1_{010}\ 2_{110} 1\ 0\ 0\}$	$1 + b, a, -c, -z, -y, x$
$\{m_{1-10}\ 2_{100} 1\ 0\ 0\}$	$1 + a - b, -b, -c, y, x, z$
$\{-4^1_{100}\ 2_{010} 1\ 0\ 0\}$	$1 - a, -a + b, -c, -x, z, -y$
$\{-4^1_{010}\ 2_{1-10} 1\ 0\ 1/2\}$	$1 - b, -a, -c + 1/2, -z, -y, x$
$\{m_{1-10}\ 2_{120} 1\ 0\ 1/2\}$	$1 - a + b, b, -c + 1/2, y, x, z$
$\{-4^1_{100}\ 2_{210} 1\ 0\ 1/2\}$	$1 + a, a - b, -c + 1/2, -x, z, -y$
$\{2_{100}\ 1 0\ 1\ 0\}$	$a, 1 + b, c, x, -y, -z$
$\{3^1_{111}\ 3^1_{001} 0\ 1\ 0\}$	$-b, 1 + a - b, c, z, x, y$
$\{3^2_{1-1-1}\ 3^2_{001} 0\ 1\ 0\}$	$-a + b, 1 - a, c, -y, z, -x$
$\{2_{100}\ 2_{001} 0\ 1\ 1/2\}$	$-a, 1 - b, c + 1/2, x, -y, -z$
$\{3^1_{111}\ 6^5_{001} 0\ 1\ 1/2\}$	$b, 1 - a + b, c + 1/2, z, x, y$
$\{3^2_{1-1-1}\ 6^1_{001} 0\ 1\ 1/2\}$	$a - b, 1 + a, c + 1/2, -y, z, -x$
$\{-4^3_{010}\ 2_{110} 0\ 1\ 0\}$	$b, 1 + a, -c, z, -y, -x$
$\{-4^3_{001}\ 2_{100} 0\ 1\ 0\}$	$a - b, 1 - b, -c, -y, x, -z$
$\{m_{01-1}\ 2_{010} 0\ 1\ 0\}$	$-a, 1 - a + b, -c, x, z, y$
$\{-4^3_{010}\ 2_{1-10} 0\ 1\ 1/2\}$	$-b, 1 - a, -c + 1/2, z, -y, -x$
$\{-4^3_{001}\ 2_{120} 0\ 1\ 1/2\}$	$-a + b, 1 + b, -c + 1/2, -y, x, -z$
$\{m_{01-1}\ 2_{210} 0\ 1\ 1/2\}$	$a, 1 + a - b, -c + 1/2, x, z, y$
$\{2_{010}\ 1 1\ 1\ 0\}$	$a, b, c, -x, y, -z$
$\{3^1_{1-1-1}\ 3^1_{001} 1\ 1\ 0\}$	$-b, a - b, c, -z, -x, y$
$\{3^2_{1-11}\ 3^2_{001} 1\ 1\ 0\}$	$-a + b, -a, c, y, -z, -x$
$\{2_{010}\ 2_{001} 1\ 1\ 1/2\}$	$-a, -b, c + 1/2, -x, y, -z$
$\{3^1_{1-1-1}\ 6^5_{001} 1\ 1\ 1/2\}$	$b, -a + b, c + 1/2, -z, -x, y$
$\{3^2_{1-11}\ 6^1_{001} 1\ 1\ 1/2\}$	$a - b, a, c + 1/2, y, -z, -x$
$\{m_{101}\ 2_{110} 1\ 1\ 0\}$	$b, a, -c, -z, y, -x$
$\{-4^1_{001}\ 2_{100} 1\ 1\ 0\}$	$a - b, -b, -c, y, -x, -z$
$\{-4^3_{100}\ 2_{010} 1\ 1\ 0\}$	$-a, -a + b, -c, -x, -z, y$
$\{m_{101}\ 2_{1-10} 1\ 1\ 1/2\}$	$-b, -a, -c + 1/2, -z, y, -x$
$\{-4^1_{001}\ 2_{120} 1\ 1\ 1/2\}$	$-a + b, b, -c + 1/2, y, -x, -z$
$\{-4^3_{100}\ 2_{210} 1\ 1\ 1/2\}$	$a, a - b, -c + 1/2, -x, -z, y$

TABLE XIX. General positions of $F^{m_{010}2^{m_{010}2^1}2}(1, 1, 2_{001}; m_{001}, 4^1_{001}, -4^3_{001})$ (3.22.8.1).

Seitz	Coordination
$\{1\ 1 0\}$	a, b, c, x, y, z
$\{2_{001}\ 1 0\ 0\ 1\}$	$a, b, c + 1, -x, -y, z$
$\{4^1_{001}\ 1 1/2\ 0\ 1/2\}$	$a + 1/2, b, c + 1/2, -y, x, z$
$\{4^3_{001}\ 1 1/2\ 0\ 3/2\}$	$a + 1/2, b, c + 3/2, y, -x, z$
$\{-1\ 1 1/2\ 1/2\ 1\}$	$a + 1/2, b + 1/2, c + 1, -x, -y, -z$
$\{m_{001}\ 1 1/2\ 1/2\ 0\}$	$a + 1/2, b + 1/2, c, x, y, -z$
$\{-4^1_{001}\ 1 0\ 1/2\ 3/2\}$	$a, b + 1/2, c + 3/2, y, -x, -z$
$\{-4^3_{001}\ 1 0\ 1/2\ 1/2\}$	$a, b + 1/2, c + 1/2, -y, x, -z$
$\{1\ 2_{001} 0\}$	$-a, -b, c, x, y, z$
$\{2_{001}\ 2_{001} 0\ 0\ 1\}$	$-a, -b, c + 1, -x, -y, z$
$\{4^1_{001}\ 2_{001} 1/2\ 0\ 1/2\}$	$-a + 1/2, -b, c + 1/2, -y, x, z$
$\{4^3_{001}\ 2_{001} 1/2\ 0\ 3/2\}$	$-a + 1/2, -b, c + 3/2, y, -x, z$
$\{-1\ 2_{001} 1/2\ 1/2\ 1\}$	$-a + 1/2, -b + 1/2, c + 1, -x, -y, -z$
$\{m_{001}\ 2_{001} 1/2\ 1/2\ 0\}$	$-a + 1/2, -b + 1/2, c, x, y, -z$
$\{-4^1_{001}\ 2_{001} 0\ 1/2\ 3/2\}$	$-a, -b + 1/2, c + 3/2, y, -x, -z$
$\{-4^3_{001}\ 2_{001} 0\ 1/2\ 1/2\}$	$-a, -b + 1/2, c + 1/2, -y, x, -z$
$\{m_{010}\ 2_{010} 0\}$	$-a, b, -c, x, -y, z$
$\{m_{100}\ 2_{010} 0\ 0\ 1\}$	$-a, b, -c + 1, -x, y, z$
$\{m_{110}\ 2_{010} 1/2\ 0\ 1/2\}$	$-a + 1/2, b, -c + 1/2, -y, -x, z$
$\{m_{-10}\ 2_{010} 1/2\ 0\ 3/2\}$	$-a + 1/2, b, -c + 3/2, y, x, z$
$\{2_{010}\ 2_{010} 1/2\ 1/2\ 1\}$	$-a + 1/2, b + 1/2, -c + 1, -x, y, -z$
$\{2_{100}\ 2_{010} 1/2\ 1/2\ 0\}$	$-a + 1/2, b + 1/2, -c, x, -y, -z$
$\{2_{110}\ 2_{010} 0\ 1/2\ 3/2\}$	$-a, b + 1/2, -c + 3/2, y, x, -z$
$\{2_{-110}\ 2_{010} 0\ 1/2\ 1/2\}$	$-a, b + 1/2, -c + 1/2, -y, -x, -z$
$\{m_{010}\ 2_{100} 0\}$	$a, -b, -c, x, -y, z$
$\{m_{100}\ 2_{100} 0\ 0\ 1\}$	$a, -b, -c + 1, -x, y, z$
$\{m_{110}\ 2_{100} 1/2\ 0\ 1/2\}$	$-a + 1/2, b, -c + 1/2, -y, -x, z$
$\{m_{-110}\ 2_{100} 1/2\ 0\ 3/2\}$	$-a + 1/2, b, -c + 3/2, y, x, z$
$\{2_{010}\ 2_{100} 1/2\ 1/2\ 1\}$	$-a + 1/2, b + 1/2, -c + 1, -x, y, -z$
$\{2_{100}\ 2_{100} 1/2\ 1/2\ 0\}$	$-a + 1/2, b + 1/2, -c, x, -y, -z$
$\{2_{110}\ 2_{100} 0\ 1/2\ 3/2\}$	$-a, b + 1/2, -c + 3/2, y, x, -z$
$\{2_{-110}\ 2_{100} 0\ 1/2\ 1/2\}$	$-a, b + 1/2, -c + 1/2, -y, -x, -z$
$\{m_{010}\ 2_{100} 0\}$	$a, -b, -c, x, -y, z$
$\{m_{100}\ 2_{100} 0\ 0\ 1\}$	$a, -b, -c + 1, -x, y, z$
$\{m_{110}\ 2_{100} 1/2\ 0\ 1/2\}$	$a + 1/2, -b, -c + 1/2, -y, -x, z$
$\{m_{-110}\ 2_{100} 1/2\ 0\ 3/2\}$	$a + 1/2, -b, -c + 3/2, y, x, z$
$\{2_{010}\ 2_{100} 1/2\ 1/2\ 1\}$	$a + 1/2, -b + 1/2, -c + 1, -x, y, -z$
$\{2_{100}\ 2_{100} 1/2\ 1/2\ 0\}$	$a + 1/2, -b + 1/2, -c, x, -y, -z$
$\{2_{110}\ 2_{100} 0\ 1/2\ 3/2\}$	$a, -b + 1/2, -c + 3/2, y, x, -z$
$\{2_{-110}\ 2_{100} 0\ 1/2\ 1/2\}$	$a, -b + 1/2, -c + 1/2, -y, -x, -z$

$\{m_{010}\|2_{010}|0\}$, $\{1\|2_{001}|0\}$, and all general positions of SSG are shown in Table XIX.

APPENDIX D: REPRESENTATION THEORY OF SSG

1. Projective representation for spin rotation

In SSG, the projective rep is similar to that of MSG, where spin rotation is included. Based on SG, in SSG we introduce spin operation here with the full group of spin operations being $\text{SO}(3) \times Z_2^T$. Since we focus on spin-1/2 systems, the full spin rotation group $\text{SO}(3)$ should be represented by an $\text{SU}(2)$ double-valued rep, which is also a projective rep. Specifically, for any two elements g_{s_i} and g_{s_j} in spin rotation group $\text{SO}(3)$, the multiplication of these

two elements could have rotation angle $\phi(g_{s_i}g_{s_j})$ between 0 and 2π or between 2π and 4π . We use d^l to represent a rotation of 2π . Then we have

$$g_{s_i}g_{s_j} = \begin{cases} g_{s_l}, & 0 \leq \phi(g_{s_i}g_{s_j}) < 2\pi, \\ d^l g_{s_l}, & 2\pi \leq \phi(g_{s_i}g_{s_j}) < 4\pi, \end{cases} \quad (\text{D1})$$

where $g_{s_l} \in \text{SO}(3)$.

Then, we define $\rho(g_{s_i})$ to be the SU(2) rep of SO(3) with rep matrices belonging to the SU(2) group. We define the rotation angle and rotation axis of $\rho(g_{s_i})$ in the SU(2) group to be the same as those of g_{s_i} in the SO(3) group. Accordingly, we will have $\rho(d^l) = -1$. Therefore, the product of any two rep matrices follows the relation

$$\rho(g_{s_i})\rho(g_{s_j}) = \begin{cases} \rho(g_{s_k}), & 0 \leq \phi(g_{s_i}g_{s_j}) < 2\pi, \\ -\rho(g_{s_k}), & 2\pi \leq \phi(g_{s_i}g_{s_j}) < 4\pi, \end{cases} \quad (\text{D2})$$

since the coefficients of the above product results in complete dependence on g_{s_i} and g_{s_j} . This SU(2) rep is naturally a projective rep of SO(3) with factor system ± 1 .

Then, for a spin-1/2 rep $d_k(\{g_s\|R|\tau\})$ of little group G_k of an SSG, the corresponding projective rep $M_k(\{g_s\|R|\tau\})$ has the same definition as that of an SG

$$d_k^l(\{g_s\|R|\tau\}) = \exp(-ik\tau)M_k^l(\{g_s\|R|\tau\}). \quad (\text{D3})$$

The product of the two projective rep matrices follows the relation

$$\begin{aligned} M_k^l(\{g_{s_i}\|R_i|\tau_i\})M_k^l(\{g_{s_j}\|R_j|\tau_j\}) \\ = (-1)^{\xi(g_{s_i}, g_{s_j})} \exp(-iK_i\tau_j)M_k^l(\{g_{s_l}\|R_l|\tau_l\}). \end{aligned} \quad (\text{D4})$$

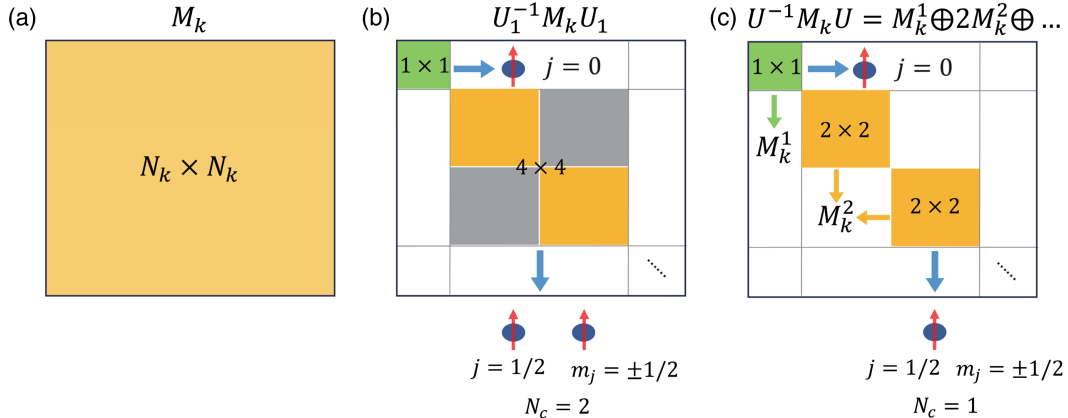


FIG. 8. The overall procedure of reducing left regular projective reps $M_k(g_i^{(a)})$. (a) The left regular projective reps are $N_k \times N_k$ rep matrices. (b) The transformation matrices U_1 formed by common eigenvectors of $(C, C(s))$ can partly diagonalize $M_k(g_i^{(a)})$ but fail to distinguish the same irreps. (c) the transformation matrices U formed by common eigenvectors of $(C, C(s), \bar{C}(s))$ can be used to completely lift the remaining degeneracy and find all inequivalent irreps.

Here, $\{g_{s_l}\|R_l|\tau_l\} = \{g_{s_i}g_{s_j}\|R_iR_j|\tau_i + R_j\tau_j \bmod T(L_0)\}$, $K_i = R_i^{-1}k - k$, $\xi(g_{s_i}, g_{s_j}) = 0$ for $0 \leq \phi(g_{s_i}g_{s_j}) < 2\pi$ and $\xi(g_{s_i}, g_{s_j}) = 1$ for $2\pi \leq \phi(g_{s_i}g_{s_j}) < 4\pi$.

2. Decomposition of regular projective representations using the CSCO method

In quantum mechanics, the commuting operators (J^2, J_z) form the CSCO of the Hilbert space of angular momentum, effectively characterizing the systems in terms of these observables. Note that J^2 is the invariant quantity (Casimir element) of $\text{SO}(3)$ and J_z is that of its subgroup $\text{SO}(2)$. Similarly, the projective irreps in a certain unitary group G can be identified through CSCO. The core principle of the CSCO method lies in the fact that every projective irrep reduced from the regular projective reps is labeled by eigenvalues of the CSCO. Consequently, all projective irreps can be extracted from the left regular projective reps.

The overall strategy to decompose the regular projective reps can be summarized as follows, with detailed explanations of some terminologies provided later:

- (1) Construct the left regular projective reps for a given factor system.
- (2) Construct the CSCO-I formed by the class operators of G to label the different rep spaces.
- (3) Construct the CSCO-II formed by the class operators of the canonical subgroup chain of the group G to distinguish each of the irreducible bases as the eigenvalues of CSCO-I are often degenerate [as shown in Fig. 8(b)].
- (4) Since the n -dimensional irreps appear n times in the regular reps, the next step is to construct the CSCO-III formed by the class operators of the canonical subgroup chain of the intrinsic group \bar{G} to distinguish the projective irreps that occur more than once [as shown in Fig. 8(c)].

- (5) Change the class and repeat above procedure until the projective irreps of all classes are obtained.

It is important to note that the character of a certain unitary group element is invariant under unitary transformation, and the character if each group element in a class is the same. Therefore, the CSCO method is applied to obtain the projective irreps of \tilde{L}_{SS}^k , which is the maximal unitary subgroup of the little group \tilde{G}_{SS}^k .

Several essential concepts of the projective reps are introduced in the following:

- (1) Left regular projective representation. In mathematics, the regular rep refers to a particular way of representing a group G as a set of linear transformations on a vector space V , whose basis vectors are nothing but the elements of G . In addition, the linear transformation for each group element that acts on each basis vector of V is defined as the group operation. The reason we use the regular projective rep to obtain the irreps of a unitary SSG is because a regular rep is a reducible rep that contains all the possible irreps. The left regular projective reps for a given factor system can be constructed using the group space as the rep space, where the group elements $g_i^{(a)} \in \tilde{L}_{\text{SS}}^k$ are also basis $|g_i^{(a)}\rangle$. The action of a group element $g_i^{(a)}$ on $|g_j^{(a)}\rangle$ is

$$g_i^{(a)}|g_j^{(a)}\rangle = (-1)^{\xi(\phi(g_{s_l}^{(a)}))} \exp(-iK_i \tau_j^{(a)}) |g_l^{(a)}\rangle, \quad (\text{D5})$$

the matrix element

$$\begin{aligned} M_k(g_i^{(a)})_{g_j^{(a)}} &= \langle g|g_i^{(a)}|g_j^{(a)}\rangle \\ &= (-1)^{\xi(\phi(g_{s_l}^{(a)}))} \exp(-iK_i \tau_j^{(a)}) \delta_{g_j^{(a)}}, \end{aligned} \quad (\text{D6})$$

where g_i has the form of $\{g_{s_i}^{(a)} \| R_i | \tau_i^{(a)}\}$, $K_i = R_i^{-1}k - k$, and the superscript (a) labels different translations and spin operations accompanied with one R_i . $(-1)^{\xi(\phi(g_{s_l}^{(a)}))}$ equals 1 or -1 when $0 \leq \phi(g_{s_l}^{(a)}) < 2\pi$ or $2\pi \leq \phi(g_{s_l}^{(a)}) < 4\pi$, respectively.

- (2) Class operator. For a regular projective rep of a certain finite group \tilde{L}_{SS}^k , the class operator is defined as

$$C_i^{(a)} = \sum_{g_j^{(a)} \in \tilde{L}_{\text{SS}}^k} M_k^{-1}(g_j^{(a)}) M_k(g_i^{(a)}) M_k(g_j^{(a)}), \quad (\text{D7})$$

where the class operator $C_i^{(a)}$ commutes with all the regular projective reps $M_k(g_j^{(a)})$.

- (3) Canonical subgroup chain. The canonical subgroup chain has a close relationship with the restricted reps. In the mathematical sense, an irrep d_k^l of the group \tilde{L}_k is certainly a rep of \tilde{L}_k 's subgroup \tilde{L}_{k1} denoted by $d_k^l \downarrow \tilde{L}_{k1}$. (\tilde{L}_k is the maximal unitary subgroup of \tilde{G}_k) In general, the restricted rep $d_k^l \downarrow \tilde{L}_{k1}$ is a reducible rep of \tilde{L}_{k1} , which can be reduced to a direct sum of the irreps of \tilde{L}_{k1} ,

$$d_k^l \downarrow \tilde{L}_{k1} = \bigoplus_v a_v^l d_{k1}^v, \quad (\text{D8})$$

where a_v^l is the multiplicity that irrep d_{k1}^v of \tilde{L}_{k1} occurs in the restricted rep $d_k^l \downarrow \tilde{L}_{k1}$. When $a_v^l \leq 1$ for all l and v , \tilde{L}_{k1} is said to be a canonical subgroup of \tilde{L}_k . A group chain $\tilde{L}_k > \tilde{L}_{k1} > \tilde{L}_{k2} > \dots > \tilde{L}_{kn}$ is a canonical subgroup chain if $\tilde{L}_{k(i+1)}$ is a canonical subgroup of \tilde{L}_{ki} for $i = 0, 1, \dots, n-1$ and \tilde{L}_{kn} is an Abelian group.

Although we do not know the irreps d_k^l of the group \tilde{L}_k in advance, we can still find the canonical subgroup by using certain empirical strategies in practical terms. Taking $\tilde{L}_k > \tilde{L}_{k1}$ as an example, \tilde{L}_{k1} contains all the translations and pure spin symmetries of \tilde{L}_k while the spatial PG part $P(\tilde{L}_{k1})$ is one of the maximal subgroups of the spatial PG part $P(\tilde{L}_k)$. In this way, \tilde{L}_{k1} usually serves as a canonical subgroup of \tilde{L}_k , and the canonical subgroup chain could be constructed.

- (4) Intrinsic group. The intrinsic group \bar{G} of a group G is the group of elements with multiplication on a basis defined as right multiplication. Specifically, for each element R of a group G , we can define a corresponding operator \bar{R} in the group rep space L_g through the right-multiplication rule with

$$\bar{R}S = SR \text{ for all } S \in L_g. \quad (\text{D9})$$

The group formed by the collection of operators \bar{R} is called the intrinsic group of \bar{G} .

- (5) Intrinsic regular projective reps. Each group element $g_i^{(a)} \in \tilde{L}_{\text{SS}}^k$ corresponds to an element $\bar{g}_i^{(a)}$ in the intrinsic group \bar{L}_{SS}^k , which obeys the right multiplication rule with $\bar{g}_i^{(a)} g_j^{(a)} = g_j^{(a)} \bar{g}_i^{(a)}$. Distinct from the typical right regular reps, \bar{L}_{SS}^k is anti-isomorphic to \tilde{L}_{SS}^k . Thus, one can define the intrinsic regular projective reps

$$\bar{g}_i^{(a)}|g_j^{(a)}\rangle = (-1)^{\xi[\phi(g_{s_m}^{(a)})]} \exp(-iK_j \tau_i^{(a)}) |g_m^{(a)}\rangle, \quad (\text{D10})$$

in which $g_m^{(a)} = \{g_{s_m}^{(a)} \| R_m | \tau_m^{(a)}\} = \{g_{s_j}^{(a)} g_{s_i}^{(a)} \| R_j R_i | \tau_j^{(a)} + R_j \tau_i^{(a)}\}$. Note that regular projective reps of \tilde{G}_{SS}^k commute with its intrinsic regular projective reps.

- (6) CSCO-I. The linear combination of class operators $C(\tilde{L}_{SS}^k) = \sum_i \lambda_i C_i^{(a)}$ form the CSCO-I of the left regular projective rep, where λ_i is any constant.
- (7) CSCO-II. For the canonical subgroup chain of \tilde{L}_{SS}^k , $\tilde{L}_{SS}^k(s) = \tilde{L}_{SS1}^k > \tilde{L}_{SS2}^k > \dots$, repeat the procedure in CSCO-I:

$$C_{i1}^{(a)} = \sum_{g_j^{(a)} \in \tilde{L}_{SS1}^k} M_k^{-1}(g_{j1}^{(a)}) M_k(g_{i1}^{(a)}) M_k(g_{j1}^{(a)}), \quad (D11)$$

where the linear combination of class operators $C(\tilde{L}_{SS1}^k) = \sum_i \lambda_i C_{i1}^{(a)}$ form CSCO-Is for the subgroup chain. The collection of the corresponding class operators $C(s) = (C(\tilde{L}_{SS1}^k), C(\tilde{L}_{SS2}^k), \dots)$ commute with the C , forming the operator set $(C, C(s))$, also known as CSCO-II.

- (8) CSCO-III. For the canonical subgroup chain of $\overline{\tilde{L}_{SS}^k}$, $\overline{\tilde{L}_{SS}^k}(s) = \overline{\tilde{L}_{SS1}^k} > \overline{\tilde{L}_{SS2}^k} > \dots$, repeat the procedure in CSCO-I:

$$\bar{C}_{i1}^{(a)} = \sum_{g_j^{(a)} \in \overline{\tilde{L}_{SS1}^k}} M_k^{-1}(\bar{g}_{j1}^{(a)}) M_k(\bar{g}_{i1}^{(a)}) M_k(\bar{g}_{j1}^{(a)}), \quad (D12)$$

where the linear combination of class operators $C(\overline{\tilde{L}_{SS1}^k}) = \sum_i \lambda_i \bar{C}_{i1}^{(a)}$ form CSCO-Is for the subgroup chain of the intrinsic group $\overline{\tilde{L}_{SS}^k}$. The collection of the corresponding class operators $\bar{C}(s) = (\bar{C}(\tilde{L}_{SS1}^k), \bar{C}(\tilde{L}_{SS2}^k), \dots)$ commute with C and $C(s)$. This complete set of class operators $(C, C(s), \bar{C}(s))$ is named CSCO-III.

Now we show the decomposition of the regular projective reps of the little group \tilde{G}_{SS}^k using the CSCO method.

- (1) The left regular projective reps $M_k(g_i^{(a)})$ are block diagonalized to obtain all the projective irreps, where the projective reps $M_k(g_i^{(a)})$ are $N_k \times N_k$ reducible matrices [shown in Fig. 8(a)].

We start from the unitary \tilde{L}_{SS}^k , in which the character χ_i^l of a projective irrep is a function of class operators $C_i^{(a)}$ as defined in Eq. (D7). The number of independent classes N_c equals the number of projective irreps, and an n_l -dimensional projective irrep will appear n_l times in $M_k(g_i^{(a)})$.

By constructing the linear combination of class operators $C = \sum_i k_i C_i^{(a)}$ (k_i is arbitrary constant numbers), we can decompose $M_k(g_i^{(a)})$ into N_c blocks. The number of eigenvalues of C is equal to the number N_c of inequivalent irreps. Analogous to quantum mechanics, we obtain the principal quantum number $|j\rangle$.

- (2) Generally, these principle quantum numbers are degenerate and cannot distinguish each of the irreducible bases. Therefore, the magnetic quantum number is introduced from the canonical subgroup chain of \tilde{L}_{SS}^k , $\tilde{L}_{SS}^k(s) = \tilde{L}_{SS1}^k > \tilde{L}_{SS2}^k > \dots$ [69,89]. The collection of corresponding class operators $C(s) = (C(\tilde{L}_{SS1}^k), C(\tilde{L}_{SS2}^k), \dots)$ commute with C , forming a CSCO-II set of $(C, C(s))$ together with C and provide the required magnetic quantum numbers m_j [shown in Fig. 8(b)]. Such a set helps us to distinguish the rows of an n_l -dimensional block of $M_k(g_i^{(a)})$. The CSCO-II can distinguish all the bases only if each irrep is one dimensional in the reduced regular rep.
- (3) However, in a left regular projective rep, an n_l -dimensional projective irrep occurs n_l times (see Appendix A 4). Therefore, we need another canonical subgroup chain of the intrinsic group $\overline{\tilde{L}_{SS}^k}$, $\overline{\tilde{L}_{SS}^k}(s) = \overline{\tilde{L}_{SS1}^k} > \overline{\tilde{L}_{SS2}^k} > \dots$ and the set of corresponding class operators $\bar{C}(s) = (\bar{C}(\tilde{L}_{SS1}^k), \bar{C}(\tilde{L}_{SS2}^k), \dots)$ to lift the remaining degeneracy. Finally, we have a CSCO set of $(C, C(s), \bar{C}(s))$ and a corresponding collection of eigenvalues, say, $|j, m_j, \bar{m}_j\rangle$, of group \tilde{L}_{SS}^k . By rearranging their eigenvectors, we can construct a transformation matrix to block diagonalize $M_k(g_i^{(a)})$ and get all projective irreps [shown in Fig. 8(c)].

The CSCO approach is applied to calculate the projective coirreps of any arbitrary k -points for all noncollinear SSGs. This approach is also applied to MSGs examples as given in Supplemental Material [64], Secs V and VI, yielding the same coirreps as those obtained in the Bilbao Crystallography Server [90,91].

3. Band representations in collinear SSGs

Now we turn to the derivation of coirreps in collinear SSGs. Considering the spin-only group $G_{SO}^l = Z_2^K \ltimes SO(2) = {}^\infty m 1$, the SSGs describing collinear ferromagnets and ferrimagnets with $G_0 = L_0, G^s = 1$ are expressed by

$$G_{SS} = \{E \| L_0\} \times Z_2^K \ltimes SO(2), \quad (D13)$$

while for SSGs describing collinear antiferromagnets, L_0 is an index-two normal subgroup of G_0 and $G^s = -1$, and they can be written by

$$G_{\text{SS}} = (\{E\|L_0\} \cup \{T\|AL_0\}) \times Z_2^K \ltimes \text{SO}(2). \quad (\text{D14})$$

Note that G_{SS} actually is the quotient group with respect to the translation group \mathbb{T} .

a. Double-valued representation

Since we are focusing on the SOC-free electronic band structure, the spinor rep or double-valued rep are necessary for constructing the coirreps of collinear SSGs. The spinor rep of rotations read

$$D(U_{\hat{n}}(\phi))$$

$$\begin{aligned} &= \exp\left(-i\sigma \frac{\hat{n}\phi}{2}\right) \\ &= \begin{pmatrix} \cos\left(\frac{\phi}{2}\right) - in_z \sin\left(\frac{\phi}{2}\right) & (-in_x - n_y) \sin\left(\frac{\phi}{2}\right) \\ (-in_x + n_y) \sin\left(\frac{\phi}{2}\right) & \cos\left(\frac{\phi}{2}\right) + in_z \sin\left(\frac{\phi}{2}\right) \end{pmatrix}, \end{aligned} \quad (\text{D15})$$

where $\hat{n} = (n_x, n_y, n_z)$ is the direction vector of the rotation axis \hat{n} , and ϕ is the rotation angle.

The character table of the double group $\text{SO}(2)$ is given in Table XX.

In collinear SSG, there are only nontrivial spin space symmetries T , $U_x(\pi)$, $U_z(\phi)$ and their combinations. (Here we define the spin principle axis and any axis perpendicular to the spin principle axis as the z and x direction, respectively). For electron systems with $m = \pm 1/2$,

$$D(U_z(\phi)) = \begin{pmatrix} e^{-i\frac{\phi}{2}} & 0 \\ 0 & e^{i\frac{\phi}{2}} \end{pmatrix}, \quad (\text{D16})$$

$$D(T) = \begin{pmatrix} 0 & 1 \\ -1 & 0 \end{pmatrix} K, \quad (\text{D17})$$

$$D(U_x(\pi)) = \begin{pmatrix} 0 & -i \\ -i & 0 \end{pmatrix}, \quad (\text{D18})$$

where K denotes complex conjugation.

TABLE XX. Character table of the double group of $\text{SO}(2)$ ($2m \in \mathbb{Z}, 0 < \phi < 2\pi$).

$\text{SO}(2)$	E	$U_z(\phi)$
Γ_0	1	1
Γ_m	1	$e^{-im\phi}$

In addition, we can find that

$$[U_x(\pi)]^2 = T^2 = -E, \quad (\text{D19})$$

$$[TU_x(\pi)]^2 = E, \quad (\text{D20})$$

$$[TU_x(\pi)U_z(\phi)]^2 = E, \quad (\text{D21})$$

$$[TU_z(\phi)]^2 = U_z(2\phi), \quad (\text{D22})$$

b. General rules for doubled degeneracy in SSGs

- (1) The combination of $\text{SO}(2)$ with $U_x(\pi)A$ symmetry pairs two conjugated one-dimensional irreps $\Gamma_{+1/2}^S(1)$ and $\Gamma_{-1/2}^S(1)$ into a two-dimensional irrep $\Gamma_{\pm 1/2}^S(2)$ as shown in Table XXI.
- (2) The combination of $\text{SO}(2)$ with TA symmetry pairs two conjugated one-dimensional irreps $\Gamma_{+1/2}^S(1)$ and $\Gamma_{-1/2}^S(1)$ into a two-dimensional coirrep $\Gamma_{\pm 1/2}^S(2)$ according to the Dimmock and Wheeler character sum rule ($L = \infty$):

$$\begin{aligned} \sum_{\beta \in TAL} \chi(\beta^2) &= \sum_{\phi} \chi((TAU_z(\phi))^2) \\ &= \sum_{\phi} \chi(U_z(2\phi)) \\ &= \sum_{\phi} \chi \begin{pmatrix} e^{-i\phi} & 0 \\ 0 & e^{i\phi} \end{pmatrix} \\ &= \int_0^{2\pi} 2 \cos(2\phi) = 0 \cdots (c). \end{aligned} \quad (\text{D23})$$

- (3) The combination of $\text{SO}(2)$ with $TU_x(\pi)$ symmetry cannot contribute to extra degeneracy in spin space according to the Dimmock and Wheeler character sum rule ($L = \infty$):

$$\begin{aligned} \sum_{\beta \in TU_x(\pi)L} \chi(\beta^2) &= \sum_{\phi} \chi((TU_x(\pi)U_z(\phi))^2) \\ &= \sum_{\phi} \chi(E) = g \cdots (a). \end{aligned} \quad (\text{D24})$$

- (4) $TU_x(\pi)$ can combine two conjugated single-valued irreps in real space, similar to that in SGs.

TABLE XXI. Character table of the double group of $\infty 2$ ($2m \in \mathbb{Z}, 0 < \phi < 2\pi$).

$\infty 2$	E	$U_z(\phi)$	$U_x(\pi)$
Γ_{0g}	1	1	1
Γ_{0u}	1	1	-1
Γ_m	2	$2 \cos(m\phi)$	0

TABLE XXII. Some typical little cogroups in collinear SSG.

Little cogroup	Sum rule	Type	Degeneracy in spin space
∞_1			
$^21\infty_1$			Double
$^{-1}2\infty_1$	$\sum_{\beta \in TAL} \chi(\beta^2) = 0$	(c) ^a	Double
$^{-1}-1\infty_1$	$\sum_{\beta \in TAL} \chi(\beta^2) = 0$	(c) ^a	Double
$^m1\infty_1$	$\sum_{\beta \in TAL} \chi(\beta^2) = g$	(a)	No
$^m-1\infty_1$	$\sum_{\beta \in TAL} \chi(\beta^2) = g$	(a)	No
$^{-1}-1^21\infty_1$	$\sum_{\beta \in TAL} \chi(\beta^2) = g$	(a)	Double ^a

^aThis double degeneracy in spin space arises from the unitary irrep of ∞_2 , rather than the extra degeneracy when introducing the antiunitary element.

(5) The concurrence of $SO(2)$ and $TU_x(\pi)$, $U_x(\pi)A$ (also TA) cannot contribute to quadruple degeneracy in spin space. The combination of $TU_x(\pi)$ and ∞_2 cannot pair the real two-dimensional irrep $\Gamma_{\pm 1/2}^S(2)$ of ∞_2 , as calculated from the character sum rule ($L = \infty_2$):

$$\begin{aligned} \sum_{\beta \in TU_x(\pi)L} \chi(\beta^2) &= \sum_{\phi} \{\chi((TU_z(\phi))^2) \\ &\quad + \chi((TU_x(\pi)U_z(\phi))^2)\} \\ &= 0 + g = g \cdots (a). \end{aligned} \quad (\text{D25})$$

Here we give some typical little cogroups in collinear SSG in Table **XXII**.

APPENDIX E: ONLINE PROGRAM IN SSG IDENTIFICATION

Here we provide the procedure for identifying the spin group symmetries from a given crystal and magnetic structure as schematic in Fig. 9, which is equipped on our online program [59]. On the website, the sentence “All experimentally determined magnetic structures available in the MAGNDATA database have been identified and provided here” presents the complete list of SSGs of magnetic

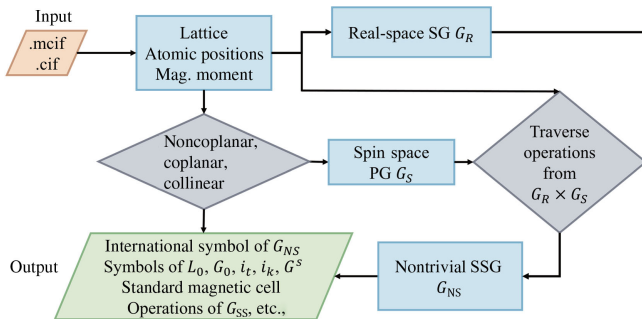


FIG. 9. Procedure of the identification of SSG from a given magnetic structure.

structures. This file includes the nontrivial SSG and spin-only group for all commensurate magnetic materials in MAGNDATA.

Step 1: Obtain the SG G_R of the input structure (without considering the magnetic moments) using the module SPGLIB [92], which is an open-source PYTHON package for searching crystal symmetries.

Step 2: Determine the type of magnetic moment, i.e., noncoplanar, coplanar, or collinear, by calculating the rank of all vectors of the magnetic moments.

Step 3: Extract all the magnetic moments and obtain the allowed PG G_S for spin space using PYMATGEN [93], which is an open-source PYTHON library for materials analysis. In order to construct the G_{NS} , the spin-only part in G_S should be excluded. For collinear magnetic configurations, set G_S to be $\{1, \bar{1}\}$; for coplanar magnetic configurations, add a constant small canting to each moment to exclude the mirror operation (Z_2^K) in G_S .

Step 4: Traverse all the symmetry operations of the direct product group $G_R \times G_S$ and apply them to the magnetic structure. The operations that keep the magnetic structure invariant form the nontrivial SSG G_{NS} of the given material.

Step 5: Within the symmetry operations of G_{NS} , all elements of real-space operations form G_0 by dropping the operations in spin space; all elements of G_0 that map the identity operation in spin space form the sublattice group L_0 ; all elements of spin space operations form PG G^s ; i_k , i_t , and the international notation of G_{NS} can also be obtained straightforwardly.

Step 6: Add the spin-only group to G_{NS} to obtain G_{SS} . For collinear configurations, we output the symmetry operations in G_{NS} because the spin-only group is continuously infinite; for coplanar configurations, we output the symmetry operations in $G_{SS} = G_{NS} \times Z_2^K$.

APPENDIX F: FIRST-PRINCIPLES METHODS

All DFT calculations herein are performed using projector augmented wave method, implemented in Vienna *ab initio* simulation package [94,95]. The generalized-gradient approximation of the Perdew-Burke-Ernzerhof-type exchange-correlation potential [96] is adopted. To include the effect of electron correlation, the DFT + U approach within the rotationally invariant formalism [97] are performed with $U_{\text{eff}} = 2.0$ eV for Ru 4d (RuO₂), $U_{\text{eff}} = 4.0$ eV for Ce 4f (CeAuAl₃), and $U_{\text{eff}} = 1.0$ eV for Co 3d (CoNb₃S₆). Tight-binding models are constructed from DFT bands using the WANNIER90 package [98,99]; the WANNIERTOOLS package is used for the calculations of anomalous Hall conductivity [100].

[1] M. S. Dresselhaus, G. Dresselhaus, and A. Jorio, *Group Theory: Application to the Physics of Condensed Matter* (Springer, New York, 2008).

- [2] C. J. Bradley and A. P. Cracknell, *The Mathematical Theory of Symmetry in Solids: Representation Theory for Point Groups and Space Groups* (Oxford University Press, New York, 1972).
- [3] J. O. Dimmock, *Use of symmetry in the determination of magnetic structures*, Phys. Rev. **130**, 1337 (1963).
- [4] H. M. Rietveld, *A profile refinement method for nuclear and magnetic structures*, J. Appl. Crystallogr. **2**, 65 (1969).
- [5] H. Grimmer, *Comments on tables of magnetic space groups*, Acta Crystallogr. Sect. A **65**, 145 (2009).
- [6] R.-J. Slager, A. Mesaros, V. Jurić, and J. Zaanen, *The space group classification of topological band-insulators*, Nat. Phys. **9**, 98 (2013).
- [7] J. Kruthoff, J. de Boer, J. van Wezel, C. L. Kane, and R.-J. Slager, *Topological classification of crystalline insulators through band structure combinatorics*, Phys. Rev. X **7**, 041069 (2017).
- [8] H. Watanabe, H. C. Po, and A. Vishwanath, *Structure and topology of band structures in the 1651 magnetic space groups*, Sci. Adv. **4**, eaat8685 (2018).
- [9] L. Elcoro, B. J. Wieder, Z. Song, Y. Xu, B. Bradlyn, and B. A. Bernevig, *Magnetic topological quantum chemistry*, Nat. Commun. **12**, 5965 (2021).
- [10] N. V. Belov and T. N. Tarkhova, *Color symmetry groups*, Sov. Phys. Crystallogr. **1**, 5 (1956).
- [11] V. E. Naish, *Magnetic structures of the metallic perovskites*, J. Magn. Magn. Mater. **24**, 299 (1981).
- [12] V. E. Naish, *On magnetic symmetry of crystals*, Proc. USSR Acad. Sci. **27**, 1496 (1963).
- [13] A. Kitz, *Über die Symmetriegruppen von Spinverteilungen Von*, Phys. Status Solidi (b) **10**, 455 (1965).
- [14] W. F. Brinkman and R. J. Elliott, *Theory of spin-space groups*, Proc. R. Soc. A **294**, 343 (1966).
- [15] W. Brinkman and R. J. Elliott, *Space group theory for spin waves*, J. Appl. Phys. **37**, 1457 (1966).
- [16] D. B. Litvin, *Spin translation groups and neutron diffraction analysis*, Acta Crystallogr. Sect. A **29**, 651 (1973).
- [17] D. B. Litvin and W. Opechowski, *Spin groups*, Physica (Utrecht) **76**, 538 (1974).
- [18] D. B. Litvin, *Spin point groups*, Acta Crystallogr. Sect. A **33**, 279 (1977).
- [19] P. Liu, J. Li, J. Han, X. Wan, and Q. Liu, *Spin-group symmetry in magnetic materials with negligible spin-orbit coupling*, Phys. Rev. X **12**, 021016 (2022).
- [20] A. Corticelli, R. Moessner, and P. A. McClarty, *Spin-space groups and magnon band topology*, Phys. Rev. B **105**, 064430 (2022).
- [21] L. Shekhtman, O. Entin-Wohlman, and A. Aharony, *Moriya's anisotropic superexchange interaction, frustration, and Dzyaloshinsky's weak ferromagnetism*, Phys. Rev. Lett. **69**, 836 (1992).
- [22] B. A. Bernevig, J. Orenstein, and S.-C. Zhang, *Exact SU(2) symmetry and persistent spin helix in a spin-orbit coupled system*, Phys. Rev. Lett. **97**, 236601 (2006).
- [23] J. Chaloupka and G. Khaliullin, *Hidden symmetries of the extended Kitaev-Heisenberg model: Implications for the honeycomb-lattice iridates A_2IrO_3* , Phys. Rev. B **92**, 024413 (2015).
- [24] T. Jungwirth, X. Marti, P. Wadley, and J. Wunderlich, *Antiferromagnetic spintronics*, Nat. Nanotechnol. **11**, 231 (2016).
- [25] V. Baltz, A. Manchon, M. Tsoi, T. Moriyama, T. Ono, and Y. Tserkovnyak, *Antiferromagnetic spintronics*, Rev. Mod. Phys. **90**, 015005 (2018).
- [26] L. Šmejkal, Y. Mokrousov, B. Yan, and A. H. MacDonald, *Topological antiferromagnetic spintronics*, Nat. Phys. **14**, 242 (2018).
- [27] S. Hayami, Y. Yanagi, and H. Kusunose, *Momentum-dependent spin splitting by collinear antiferromagnetic ordering*, J. Phys. Soc. Jpn. **88**, 123702 (2019).
- [28] M. Naka, S. Hayami, H. Kusunose, Y. Yanagi, Y. Motome, and H. Seo, *Spin current generation in organic antiferromagnets*, Nat. Commun. **10**, 4305 (2019).
- [29] L. Šmejkal, R. Gonzalez-Hernandez, T. Jungwirth, and J. Sinova, *Crystal time-reversal symmetry breaking and spontaneous Hall effect in collinear antiferromagnets*, Sci. Adv. **6**, eaaz8809 (2020).
- [30] S. Hayami, Y. Yanagi, and H. Kusunose, *Bottom-up design of spin-split and reshaped electronic band structures in antiferromagnets without spin-orbit coupling: Procedure on the basis of augmented multipoles*, Phys. Rev. B **102**, 144441 (2020).
- [31] I. I. Mazin, K. Koepernik, M. D. Johannes, R. Gonzalez-Hernandez, and L. Šmejkal, *Prediction of unconventional magnetism in doped FeSb_2* , Proc. Natl. Acad. Sci. U.S.A. **118**, e2108924118 (2021).
- [32] L.-D. Yuan, Z. Wang, J.-W. Luo, and A. Zunger, *Prediction of low-Z collinear and noncollinear antiferromagnetic compounds having momentum-dependent spin splitting even without spin-orbit coupling*, Phys. Rev. Mater. **5**, 014409 (2021).
- [33] H.-Y. Ma, M. Hu, N. Li, J. Liu, W. Yao, J.-F. Jia, and J. Liu, *Multifunctional antiferromagnetic materials with giant piezomagnetism and noncollinear spin current*, Nat. Commun. **12**, 2846 (2021).
- [34] R. González-Hernández, L. Šmejkal, K. Výborný, Y. Yahagi, J. Sinova, T. Jungwirth, and J. Železný, *Efficient electrical spin splitter based on nonrelativistic collinear antiferromagnetism*, Phys. Rev. Lett. **126**, 127701 (2021).
- [35] S. Karube, T. Tanaka, D. Sugawara, N. Kadoguchi, M. Kohda, and J. Nitta, *Observation of spin-splitter torque in collinear antiferromagnetic RuO_2* , Phys. Rev. Lett. **129**, 137201 (2022).
- [36] H. Bai, L. Han, X. Y. Feng, Y. J. Zhou, R. X. Su, Q. Wang, L. Y. Liao, W. X. Zhu, X. Z. Chen, F. Pan, X. L. Fan, and C. Song, *Observation of spin splitting torque in a collinear antiferromagnet RuO_2* , Phys. Rev. Lett. **128**, 197202 (2022).
- [37] L. Šmejkal, A. B. Hellenes, R. González-Hernández, J. Sinova, and T. Jungwirth, *Giant and tunneling magnetoresistance in unconventional collinear antiferromagnets with nonrelativistic spin-momentum coupling*, Phys. Rev. X **12**, 011028 (2022).
- [38] T. Berlijn, P. C. Snijders, O. Delaire, H. D. Zhou, T. A. Maier, H. B. Cao, S. X. Chi, M. Matsuda, Y. Wang, M. R. Koehler, P. R. C. Kent, and H. H. Weitering, *Itinerant antiferromagnetism in RuO_2* , Phys. Rev. Lett. **118**, 077201 (2017).

- [39] A. Bose, N. J. Schreiber, R. Jain, D.-F. Shao, H. P. Nair, J. Sun, X. S. Zhang, D. A. Muller, E. Y. Tsymbal, D. G. Schlom, and D. C. Ralph, *Tilted spin current generated by the collinear antiferromagnet ruthenium dioxide*, *Nat. Electron.* **5**, 267 (2022).
- [40] Z. Feng, X. Zhou, L. Šmejkal, L. Wu, Z. Zhu, H. Guo, R. González-Hernández, X. Wang, H. Yan, P. Qin, X. Zhang, H. Wu, H. Chen, Z. Meng, L. Liu, Z. Xia, J. Sinova, T. Jungwirth, and Z. Liu, *An anomalous Hall effect in altermagnetic ruthenium dioxide*, *Nat. Electron.* **5**, 735 (2022).
- [41] H. Bai, Y. C. Zhang, Y. J. Zhou, P. Chen, C. H. Wan, L. Han, W. X. Zhu, S. X. Liang, Y. C. Su, X. F. Han, F. Pan, and C. Song, *Efficient spin-to-charge conversion via altermagnetic spin splitting effect in antiferromagnet RuO₂*, *Phys. Rev. Lett.* **130**, 216701 (2023).
- [42] D.-F. Shao, Y.-Y. Jiang, J. Ding, S.-H. Zhang, Z.-A. Wang, R.-C. Xiao, G. Gurung, W. J. Lu, Y. P. Sun, and E. Y. Tsymbal, *Néel spin currents in antiferromagnets*, *Phys. Rev. Lett.* **130**, 216702 (2023).
- [43] D.-F. Shao, S.-H. Zhang, M. Li, C.-B. Eom, and E. Y. Tsymbal, *Spin-neutral currents for spintronics*, *Nat. Commun.* **12**, 7061 (2021).
- [44] Y.-P. Zhu *et al.*, *Observation of plaid-like spin splitting in a noncoplanar antiferromagnet*, *Nature (London)* **626**, 523 (2024).
- [45] L. Šmejkal, J. Sinova, and T. Jungwirth, *Emerging research landscape of altermagnetism*, *Phys. Rev. X* **12**, 040501 (2022).
- [46] L. Šmejkal, J. Sinova, and T. Jungwirth, *Beyond conventional ferromagnetism and antiferromagnetism: A phase with nonrelativistic spin and crystal rotation symmetry*, *Phys. Rev. X* **12**, 031042 (2022).
- [47] S. Lee, S. Lee, S. Jung, J. Jung, D. Kim, Y. Lee, B. Seok, J. Kim, B. G. Park, L. Šmejkal, C.-J. Kang, and C. Kim, *Broken Kramers degeneracy in altermagnetic MnTe*, *Phys. Rev. Lett.* **132**, 036702 (2024).
- [48] J. Krempasky *et al.*, *Altermagnetic lifting of Kramers spin degeneracy*, *Nature (London)* **626**, 517 (2024).
- [49] P. Liu, A. Zhang, J. Han, and Q. Liu, *Chiral Dirac-like fermion in spin-orbit-free antiferromagnetic semimetals*, *Innovation* **3**, 100343 (2022).
- [50] A. Zhang *et al.*, *Chiral Dirac fermion in a collinear antiferromagnet*, *Chin. Phys. Lett.* **40**, 126101 (2023).
- [51] Jian Yang, Zheng-Xin Liu, and C. Fang, *Symmetry invariants in magnetically ordered systems having weak spin-orbit coupling*, *arXiv:2105.12738*.
- [52] P.-J. Guo, Y.-W. Wei, K. Liu, Z.-X. Liu, and Z.-Y. Lu, *Eightfold degenerate fermions in two dimensions*, *Phys. Rev. Lett.* **127**, 176401 (2021).
- [53] L. M. Sandratskii, *Symmetry analysis of electronic states for crystals with spiral magnetic order. I. General properties*, *J. Phys. Condens. Matter* **3**, 8565 (1991).
- [54] L. M. Sandratskii, *Symmetry analysis of electronic states for crystals with spiral magnetic order. II. Connection with limiting cases*, *J. Phys. Condens. Matter* **3**, 8587 (1991).
- [55] N. Lazić, M. Milivojević, and M. Damjanović, *Spin line groups*, *Acta Crystallogr. Sect. A* **69**, 611 (2013).
- [56] R. Lifshitz, *Symmetry of magnetically ordered quasicrystals*, *Phys. Rev. Lett.* **80**, 2717 (1998).
- [57] R. Lifshitz and S. Even-Dar Mandel, *Magnetically ordered quasicrystals: Enumeration of spin groups and calculation of magnetic selection rules*, *Acta Crystallogr. Sect. A* **60**, 167 (2004).
- [58] S. Even-Dar Mandel and R. Lifshitz, *Symmetry of magnetically ordered three-dimensional octagonal quasicrystals*, *Acta Crystallogr. Sect. A* **60**, 179 (2004).
- [59] See <https://findspingroup.com> for the online program FINDSPINGROUP of SSG identification for any given magnetic structure, all the enumerated nontrivial SSGs and SSGs for all experimentally reported magnetic structures reported in MAGNDATA database.
- [60] S. V. Gallego, J. M. Perez-Mato, L. Elcoro, E. S. Tasci, R. M. Hanson, K. Momma, M. I. Aroyo, and G. Madariaga, *MAGNDATA: Towards a database of magnetic structures. I. The commensurate case*, *J. Appl. Crystallogr.* **49**, 1750 (2016).
- [61] H. Wondratschek, in *Symmetry Relations between Space Groups*, International Tables for Crystallography Vol. A1, edited by H. Wondratschek and U. Müller (Springer, Dordrecht, 2004).
- [62] S. Ivantchev, E. Kroumova, M. I. Aroyo, J. M. Perez-Mato, J. M. Igartua, G. Madariaga, and H. Wondratschek, *SUPERGROUPS—A computer program for the determination of the supergroups of the space groups*, *J. Appl. Crystallogr.* **35**, 511 (2002).
- [63] L. Elcoro, B. Bradlyn, Z. Wang, M. G. Vergniory, J. Cano, C. Felser, B. A. Bernevig, D. Orobengoa, G. de la Flor, and M. I. Aroyo, *Double crystallographic groups and their representations on the Bilbao Crystallographic Server*, *J. Appl. Crystallogr.* **50**, 1457 (2017).
- [64] See Supplemental Material at <http://link.aps.org/supplemental/10.1103/PhysRevX.14.031038> for Seitz symbols in SSG, the site-symmetry groups and Wyckoff positions of SSGs and the construction of a magnetic structure using site-symmetry groups, the modified Dimmock and Wheeler's character sum rule, the band reps of SSGs and the comparison of those between SSGs and MSGs for collinear RuO₂, coplanar CeAuAl₃, and noncoplanar CoNb₃S₆.
- [65] M. I. Aroyo, *International Tables for Crystallography* (Wiley, New York, 2013).
- [66] N. V. Belov, N. N. Neronova, and T. S. Smirnova, *Shubnikov groups*, *Sov. Phys. Crystallogr.* **2**, 311 (1957).
- [67] A. V. Shubnikov, N. V. Belov, and W. T. Holser, *Colored symmetry* (Pergamon Press, London, 1964).
- [68] J.-Q. Chen, M.-J. Gao, and G.-Q. Ma, *The representation group and its application to space-groups*, *Rev. Mod. Phys.* **57**, 211 (1985).
- [69] J.-Q. Chen, J. Ping, and F. Wang, *Group Representation Theory for Physicists* (World Scientific, Singapore, 2002).
- [70] J. Li, Q. Yao, L. Wu, Z. Hu, B. Gao, X. Wan, and Q. Liu, *Designing light-element materials with large effective spin-orbit coupling*, *Nat. Commun.* **13**, 919 (2022).
- [71] D. T. Adroja, C. de la Fuente, A. Fraile, A. D. Hillier, A. Daoud-Aladine, W. Kockelmann, J. W. Taylor, M. M. Koza, E. Burzurí, F. Luis, J. I. Arnaudas, and A. del Moral, *Muon spin rotation and neutron scattering study of the noncentrosymmetric tetragonal compound CeAuAl₃*, *Phys. Rev. B* **91**, 134425 (2015).

- [72] L.-D. Yuan, Z. Wang, J.-W. Luo, E. I. Rashba, and A. Zunger, *Giant momentum-dependent spin splitting in centrosymmetric low-Z antiferromagnets*, Phys. Rev. B **102**, 014422 (2020).
- [73] N. J. Ghimire, A. S. Botana, J. S. Jiang, J. Zhang, Y.-S. Chen, and J. F. Mitchell, *Large anomalous Hall effect in the chiral-lattice antiferromagnet CeAuAl₃*, Nat. Commun. **9**, 3280 (2018).
- [74] G. Tenasini, E. Martino, N. Ubrig, N. J. Ghimire, H. Berger, O. Zaharko, F. Wu, J. F. Mitchell, I. Martin, L. Forró, and A. F. Morpurgo, *Giant anomalous Hall effect in quasi-two-dimensional layered antiferromagnet Co_{1/3}NbS₂*, Phys. Rev. Res. **2**, 023051 (2020).
- [75] H. Tanaka, S. Okazaki, K. Kuroda, R. Noguchi, Y. Arai, S. Minami, S. Ideta, K. Tanaka, D. Lu, M. Hashimoto, V. Kandyba, M. Cattelan, A. Barinov, T. Muro, T. Sasagawa, and T. Kondo, *Large anomalous Hall effect induced by weak ferromagnetism in the noncentrosymmetric antiferromagnet CoNb₃S₆*, Phys. Rev. B **105**, L121102 (2022).
- [76] X. P. Yang, H. LaBollita, Z.-J. Cheng, H. Bhandari, T. A. Cochran, J.-X. Yin, M. S. Hossain, I. Belopolski, Q. Zhang, Y. Jiang, N. Shumiya, D. Multer, M. Liskevich, D. A. Usanov, Y. Dang, V. N. Strocov, A. V. Davydov, N. J. Ghimire, A. S. Botana, and M. Z. Hasan, *Visualizing the out-of-plane electronic dispersions in an intercalated transition metal dichalcogenide*, Phys. Rev. B **105**, L121107 (2022).
- [77] H. Takagi, R. Takagi, S. Minami, T. Nomoto, K. Ohishi, M.-T. Suzuki, Y. Yanagi, M. Hirayama, N. D. Khanh, K. Karube, H. Saito, D. Hashizume, R. Kiyanagi, Y. Tokura, R. Arita, T. Nakajima, and S. Seki, *Spontaneous topological Hall effect induced by non-coplanar antiferromagnetic order in intercalated van der Waals materials*, Nat. Phys. **19**, 961 (2023).
- [78] S. S. P. Parkin, E. A. Marseglia, and P. J. Brown, *Magnetic structure of Co_{1/3}NbS₂ and Co_{1/3}TaS₂*, J. Phys. C **16**, 2765 (1983).
- [79] N. Nagaosa, J. Sinova, S. Onoda, A. H. MacDonald, and N. P. Ong, *Anomalous Hall effect*, Rev. Mod. Phys. **82**, 1539 (2010).
- [80] R. Shindou and N. Nagaosa, *Orbital ferromagnetism and anomalous Hall effect in antiferromagnets on the distorted fcc lattice*, Phys. Rev. Lett. **87**, 116801 (2001).
- [81] M. Hirschberger, Y. Nomura, H. Mitamura, A. Miyake, T. Koretsune, Y. Kaneko, L. Spitz, Y. Taguchi, A. Matsuo, K. Kindo, R. Arita, M. Tokunaga, and Y. Tokura, *Geometrical Hall effect and momentum-space Berry curvature from spin-reversed band pairs*, Phys. Rev. B **103**, L041111 (2021).
- [82] L. Šmejkal, A. H. MacDonald, J. Sinova, S. Nakatsuji, and T. Jungwirth, *Anomalous Hall antiferromagnets*, Nat. Rev. Mater. **7**, 482 (2022).
- [83] H. Zhu, J. Li, X. Chen, Y. Yu, and Q. Liu, *Magnetic geometry to quantum geometry nonlinear transports*, arXiv:2406.03738.
- [84] Yi Jiang, Ziyin Song, Tiannian Zhu, Zhong Fang, Hongming Weng, Zheng-Xin Liu, Jian Yang, and C. Fang, following paper, *Enumeration of spin-space groups: Towards a complete description of symmetries of magnetic orders*, Phys. Rev. X **14**, 031039 (2024)..
- [85] Zhenyu Xiao, Jianzhou Zhao, Yanqi Li, Ryuichi Shindou, and Z.-D. Song, preceding paper, *Spin space groups: Full classification and applications*, Phys. Rev. X **14**, 031037 (2024).
- [86] K. Shinohara, A. Togo, H. Watanabe, T. Nomoto, I. Tanaka, and R. Arita, *Algorithm for spin symmetry operation search*, Acta Crystallogr. Sect. A **80**, 94 (2024).
- [87] H. Watanabe, K. Shinohara, T. Nomoto, A. Togo, and R. Arita, *Symmetry analysis with spin crystallographic groups: Disentangling effects free of spin-orbit coupling in emergent electromagnetism*, Phys. Rev. B **109**, 094438 (2024).
- [88] H. Schiff, A. Corticelli, A. Guerreiro, J. Romhányi, and P. McClarty, *The spin point groups and their representations*, arXiv:2307.12784.
- [89] J. Yang and Z.-X. Liu, *Irreducible projective representations and their physical applications*, J. Phys. A **51**, 025207 (2017).
- [90] M. I. Aroyo, J. M. Perez-Mato, C. Capillas, E. Kroumova, S. Ivantchev, G. Madariaga, A. Kirov, and H. Wondratschek, *Bilbao Crystallographic Server: I. Databases and crystallographic computing programs*, Z. Kristallogr. Crystallogr. Mater. **221**, 15 (2006).
- [91] Y. Xu, L. Elcoro, Z.-D. Song, B. J. Wieder, M. G. Vergniory, N. Regnault, Y. Chen, C. Felser, and B. A. Bernevig, *High-throughput calculations of magnetic topological materials*, Nature (London) **586**, 702 (2020).
- [92] A. Togo, K. Shinohara, and I. Tanaka, *SPGLIB: A software library for crystal symmetry search*, arXiv:1808.01590.
- [93] S. P. Ong, W. D. Richards, A. Jain, G. Hautier, M. Kocher, S. Cholia, D. Gunter, V. L. Chevrier, K. A. Persson, and G. Ceder, *PYTHON Materials Genomics (PYMATGEN): A robust, open-source PYTHON library for materials analysis*, Comput. Mater. Sci. **68**, 314 (2013).
- [94] G. Kresse and J. Furthmüller, *Efficient iterative schemes for ab initio total-energy calculations using a plane-wave basis set*, Phys. Rev. B **54**, 11169 (1996).
- [95] G. Kresse and D. Joubert, *From ultrasoft pseudopotentials to the projector augmented-wave method*, Phys. Rev. B **59**, 1758 (1999).
- [96] J. P. Perdew, K. Burke, and M. Ernzerhof, *Generalized gradient approximation made simple*, Phys. Rev. Lett. **77**, 3865 (1996).
- [97] S. L. Dudarev, G. A. Botton, S. Y. Savrasov, C. J. Humphreys, and A. P. Sutton, *Electron-energy-loss spectra and the structural stability of nickel oxide: An LSDA + U study*, Phys. Rev. B **57**, 1505 (1998).
- [98] A. A. Mostofi, J. R. Yates, Y.-S. Lee, I. Souza, D. Vanderbilt, and N. Marzari, *WANNIER90: A tool for obtaining maximally-localised Wannier functions*, Comput. Phys. Commun. **178**, 685 (2008).
- [99] N. Marzari, A. A. Mostofi, J. R. Yates, I. Souza, and D. Vanderbilt, *Maximally localized WANNIER functions: Theory and applications*, Rev. Mod. Phys. **84**, 1419 (2012).
- [100] Q. Wu, S. Zhang, H.-F. Song, M. Troyer, and A. A. Soluyanov, *WANNIERTOOLS: An open-source software package for novel topological materials*, Comput. Phys. Commun. **224**, 405 (2018).